Geometry of Phyllotactic Spiral Tilings

By

Takamichi Sushida

Doctoral Program in Applied Mathematics and Informatics

Graduate School of Science and Technology

Ryukoku University

2014

Geometry of Phyllotactic Spiral Tilings

By

Takamichi Sushida

A Dissertation Submitted In Partial Fulfillment of the Requirements

For the Degree of

DOCTOR of SCIENCE

The Dissertation of Takamichi Sushida is approved:

_____

Professor Hiroe Kokubu (Hiroe Oka)

_____

Professor Junta Matsukidaira

_____

Professor Shoji Yotsutani

_____

Professor Yoshihisa Morita

_____

Professor Waichiro Matsumoto

Graduate school of Science and Technology

Ryukoku University

2014

葉序的な螺旋タイリングの幾何学

T11D001 須志田 隆道

概要

植物の葉や種などの原基 (Primordia) の配置を葉序 (Phyllotaxis) という. ひまわりや松笠などの典型的な植物に現れる螺旋葉序の特徴は, 黄金比 $\tau = \frac{1+\sqrt{5}}{2}$ や Fibonacci 数 $1, 1, 2, 3, 5, 8, 13, \cdots$ で記述されることである. 葉序の数学的な理論の研究は, 19 世紀前半の Bravais 兄弟らによる円筒モデル (線形モデル) の研究から始められ, 物理学者 Vogel によって提案されたモデルを基盤とする円板モデル (非線形モデル) の研究が展開されている. 本論文の主題は, 円板モデルの問題であるボロノイ螺旋タイリングおよび三角形螺旋タイリングを包括的に記述することである.

はじめに, 円筒 $\mathbb{C}/\mathbb{Z}$ 上の螺旋格子 $\Lambda(\xi) = \xi\mathbb{Z} \pmod 1$, $\xi = x + \mathrm{i}y \in \mathbb{C}$, $y > 0$ を母点集合とするボロノイ図として得られるタイリングを考える. x を固定したとき, y の単調減少とともに変化する組合せ的構造の分岐過程は x の連分数近似によって説明される. その分岐図はボロノイ図が退化した長方形タイリングを作る複素数 ξ が属する円弧の和集合である. さらに, 分岐過程の各分岐点で得られる長方形タイリングのタイルの極限形状を考える. もし x が固定された二次無理数ならば, $y \to 0$ としたとき, 長方形タイルの縦横比の極限集合は二次無理数で記述される有限集合である. 葉序の分野では, 黄金比 τ に対等な無理数を noble number という. もし x が noble number ならば, 長方形タイルの形状は正方形に収束することが示される. 長方形タイルの極限形状に関する結論は, Rothen と Koch による the shape invariance under compression に数学的な拡張を与える.

複素指数函数 $\exp : \mathbb{C} \to \mathbb{C}\backslash\{0\}$ によって, 円筒 $\mathbb{C}/\mathbb{Z}$ の格子 $\Lambda(\xi)$ は一つの複素数 $\zeta = \mathrm{e}^{\xi}$ で生成される平面 $\mathbb{C}\backslash\{0\}$ の螺旋格子 $S = \{\zeta^j\}_{j\in\mathbb{Z}}$ に移る. 次に, 平面 $\mathbb{C}^*$ の螺旋格子 S を母点集合とするボロノイ螺旋タイリングを考える. $\mathrm{Arg}(\zeta)$ を固定したとき, $0 < r < 1$ の単調増加とともに変化する組合せ的構造の分岐過程は $\mathrm{Arg}(\zeta)/2\pi$ の連分数近似によって説明される. ここで, $-\pi < \mathrm{Arg}(z) \le \pi$ は $z \in \mathbb{C}\backslash\{0\}$ の偏角の主値を表す. 円筒 $\mathbb{C}/\mathbb{Z}$ のボロノイタイリングでは, 組合せ的構造の分岐図が円弧の和集合であったが, ボロノイ螺旋タイリングの組合せ的構造の分岐図は, $\mathrm{Arg}(\zeta)$ をパラメータとする実代数曲線の枝の和集合であり, 各枝に属する複素数 ζ は, ボロノイ図が退化した四角形タイリングを作る. さらに, 分岐過程の各分岐点で得られる四角形タイリングのタイルの極限形状を考える. $\mathrm{Arg}(\zeta)/2\pi$ を固定された二次無理数ならば, 縦横比が線形に近似され, 円筒 $\mathbb{C}/\mathbb{Z}$ のボロノイタイリングの場合と同様の結論が得られる.

最後に, 平面 $\mathbb{C}\backslash\{0\}$ の螺旋格子 S を頂点集合とする三角形螺旋タイリングを考える. 三角形螺旋タイリングは, 2005 年に日詰明男氏 (造形作家) によって, ひまわりの葉序がもつ数学的エッセンスを抽出した幾何学的造形物として考案された. 三角形螺旋タイリングには, $\mathrm{Arg}(\zeta)/2\pi$ の連分数近似によって説明される opposed parastichy pairs をもつタイリングとそうでないものがある. opposed parastichy pairs をもつ三角形螺旋タイリングを作る生成元 ζ の集合は $\mathrm{Arg}(\zeta)$ をパラメータとする実代数曲線の枝の和集合である. 一方, non-opposed parastichy pairs をもつ三角形螺旋タイリングを作る生成元 ζ の集合は $|\zeta|$ をパラメータとする実代数曲線の枝の和集合であり, それは単位円板 $\mathbb{D}$ の稠密部分集合を与える. さらに, opposed parastichy pairs をもつ三角形螺旋タイリングについて, 三角形タイルの極限形状を考える. ボロノイ螺旋タイリングの場合と同様に, $\mathrm{Arg}(\zeta)/2\pi$ が固定された二次無理数ならば, 三角形タイルの線分比は線形に近似され, 円筒 $\mathbb{C}/\mathbb{Z}$ のボロノイタイリングの場合と同様の結論が得られる. 特に, $\mathrm{Arg}(\zeta)/2\pi$ が noble number ならば, 極限集合は黄金比 τ で記述される.

本論文のボロノイ螺旋タイリングおよび三角形螺旋タイリングに関する各証明は, 平面 $\mathbb{C}\backslash\{0\}$ の被覆空間のタイリングとして定義される多重タイリングのもとで与えられる.

Geometry of Phyllotactic Spiral Tilings

T11D001 Takamichi Sushida

Abstract

Phyllotaxis is the regular arrangements of primordia of leaves and other organs of plants. Typical phyllotactic patterns form the spiral structures described by the golden section $\tau = \frac{1+\sqrt{5}}{2}$ and the Fibonacci numbers $1, 1, 2, 3, 5, 8, 13, \cdots$. In early half of the 19th century, the classical subject of geometrical phyllotactic patterns was started from the study of the cylindrical model (the linear model) by Bravais brothers. Moreover, it has studied as a multidisciplinary subject which contains the study of the disk model (the non-linear model) based on the mathematical model by Vogel. The main subject of the thesis is to describe comprehensively Voronoi spiral tilings and triangular spiral tilings.

First, we consider a tiling given as a Voronoi diagram with the spiral lattice $\Lambda(\xi) = \xi\mathbb{Z}(\mathrm{mod}\ 1)$, $\xi = x + \mathrm{i}y \in \mathbb{C}$, $y > 0$ of the cylinder $\mathbb{C}/\mathbb{Z}$. We show that a bifurcation process of combinatorial structures by monotone decreasing of $y > 0$ as x is fixed, is explained by the continued fraction of x. A bifurcation diagram of combinatorial structures is the union of arcs. A complex number ξ on each arc produces a rectangle tiling. Moreover, we consider limit sets of aspect ratios of rectangular tiles. If x is a fixed quadratic irrational, then the limit set given by $y \to 0$ is a finite set written by quadratic irrationals. In the phyllotaxis theory, an irrational number which is linearity equivalent of τ plays a vital role, and it is called the noble number. In particular, if x is a noble number, then the limit shape is the square. This is an extended result to the shape invariance under compression by Rothen and Koch.

By the complex exponential function $\exp : \mathbb{C} \to \mathbb{C}\backslash\{0\}$, $\Lambda(\xi)$ of $\mathbb{C}/\mathbb{Z}$ is mapped as the spiral lattice $S = \{\zeta^j\}_{j\in\mathbb{Z}}$ of the punctured plane $\mathbb{C}\backslash\{0\}$ generated by $\zeta = \mathrm{e}^{\xi}$. Second, we consider the Voronoi spiral tilings with S of $\mathbb{C}^*$. We show that a bifurcation process of combinatorial structures by monotone increasing of $0 < r < 1$ as $\mathrm{Arg}(\zeta)/2\pi$ is fixed, is explained by the continued fraction of $\mathrm{Arg}(\zeta)/2\pi$, where $-\pi < \mathrm{Arg}(z) \leq \pi$ denotes the principal argument of $z \in \mathbb{C}\backslash\{0\}$. A bifurcation diagram of combinatorial structures for Voronoi spiral tilings is the union of branches of real algebraic curves parameterized by $\mathrm{Arg}(\zeta)$. A complex number ζ on each branch produces a quadrilateral tiling. Moreover, we consider limit sets of aspect ratios of quadrilateral tiles. If $\mathrm{Arg}(\zeta)/2\pi$ is a fixed quadratic irrational, then the aspect ratios are written by the linear approximation, and we obtain the same results as Voronoi tilings on $\mathbb{C}/\mathbb{Z}$.

Finally, we consider the triangular spiral tilings with S of $\mathbb{C}\backslash\{0\}$. The triangular spiral tilings was devised as geometrical architectures with phyllotactic patterns by Akio Hizume. The set of generators ζ which produce triangular spiral tilings with opposed parastichy pairs, is the union of branches of real algebraic curves parameterized by $\mathrm{Arg}(\zeta)$. On the other hand, a set of generators ζ which produce triangular spiral tilings with non-opposed parastichy pairs, is the union of branches of real algebraic curves parameterized by $|\zeta|$, and it gives a dense subset of $\mathbb{D}$. Next we consider limit sets of line segment ratios of tiles for triangular spiral tilings with opposed parastichy pairs. In the same way as the Voronoi spiral tilings, if $\mathrm{Arg}(\zeta)/2\pi$ is a fixed quadratic irrational, then the line segment ratios are written by the linear approximation, and we obtain the same results as Voronoi tilings on $\mathbb{C}/\mathbb{Z}$. In particular, if $\mathrm{Arg}(\zeta)/2\pi$ is a noble number, then the limit set is written by τ.

Throughout the thesis, the proofs of the Voronoi spiral tilings and the triangular spiral tilings are given under multiple tilings defined as a tiling of a covering space of the punctured plane $\mathbb{C}^*$.

葉序的な螺旋タイリングの幾何学

T11D001 須志田 隆道

学位論文の要旨

植物の葉や種などの原基 (Primordia) の配置を葉序 (Phyllotaxis) という. ひまわりや松笠などの典型的な植物の葉序がもつ特徴は, 黄金比 $\tau = \frac{1+\sqrt{5}}{2}$ や Fibonacci 数 $1, 1, 2, 3, 5, 8, 13, \cdots$ で記述される螺旋構造を形成することである. 本論文の主題は, 円板上の問題であるボロノイ螺旋タイリングおよび三角形螺旋タイリングを包括的に記述することである.

研究の背景

葉序の数学的な理論の研究は, 19 世紀前半の Bravais brothers らの研究から始まった. 非常に複雑な構造をもつ葉序の数学的な構造を解明するために, 単純化された円筒上モデル (線形モデル) および円板モデル (非線形モデル) がそれぞれ研究された. 円筒モデルの研究では, 加法群が推移的に作用する点列を母点集合とするボロノイタイリングの組合せ的構造が回転角の連分数近似によって説明され, その分岐過程が力学系の観点から記述された. 一方, 円板モデルの研究では, 1979 年に物理学者 Vogel によって提案されたひまわりの頭状花にある筒状花の螺旋模様に対応する点列 $V = \{\phi_j(r)\mathrm{e}^{\mathrm{i}\cdot j\theta}\}_{j\in\mathbb{N}}$, $\phi_j(r) = r\sqrt{j}$, $r > 0$, $\theta \in \mathbb{R}$ を母点集合とするボロノイタイリングについて, 準結晶構造の観点からからその組合せ的構造を説明した研究がある. さらに, 葉序の幾何学モデルの研究に加え, 生物学的な根拠を考慮したモデル方程式の研究がある. 最近では, 生物学的な研究の進展により, 細胞間における植物ホルモン「オーキシン」の輸送が黄金比やフィボナッチ数で記述される生物学的機構の一つであることが発見され, 対応するモデル方程式が提案されている.

一方で, 造形作家 日詰明男氏によって考案されたひまわりの葉序の数学的エッセンスを抽出した幾何学的造形物がある. 1987 年に日詰氏は, フィボナッチ・タワーと呼ばれる幾何学的建築物を考案した. これは, 擬球面上にひまわりの頭状花にある筒状花の螺旋模様を模したものである. 日詰氏はさまざまなワークショップなどで竹を用いた巨大なフィボナッチ・タワーを建造した. 2005 年に日詰氏は, フィボナッチ・タワーの土台として, フィボナッチ・トルネードと呼ばれる三角形螺旋タイリングを考案した. これは, 原点を除いた平面 $\mathbb{C}^*$ において, 黄金比 τ で記述される相似変換群が推移的に作用するタイリングであり, 原点を除いた円板モデルとして捉えることができる. さらに, フィボナッチ・トルネードに関するもう一つの話題として, 折り紙による造形物がある. 日詰氏は折紙作家 布施知子氏によって考案されたねじれ多重塔と呼ばれる折り紙の作品を参考にして, 2005 年にフィボナッチ・トルネードを 1 枚の紙で製作することに成功した.

研究の内容

本論文では, 単位円板 $\mathbb{D}$ 内の一つの複素数 $\zeta = r\mathrm{e}^{\mathrm{i}\theta} \in \mathbb{D}\backslash\mathbb{R}$ で生成される平面 $\mathbb{C}^* := \mathbb{C}\backslash\{0\}$ の相似変換群 $S = \{\zeta^j\}_{j\in\mathbb{Z}}$ が推移的に作用するボロノイ螺旋タイリングおよび三角形螺旋タイリングを位相幾何学的な観点から考える.

本論文は次の 5 章から構成されている. 各章ごとに, 独立した記号を用いる.

第 1 章では, 研究の背景および論文の構成が述べられている.

第 2 章では, 円板上の問題を考えるための準備として, 葉序の分野でよく知られている円筒 $\mathbb{C}/\mathbb{Z}$ のボロノイ図として得られるタイリングの分岐構造を記述する. ここで, タイリングの理論に従い, 二次元多様体 X のタイリングは, topological disk $T_j \subset X$ の族 $\mathcal{T} = \{T_j\}_j$ であり, かつ $X = \bigcup_j T_j$ and $\mathrm{int}(T_j) \cap \mathrm{int}(T_k) = \emptyset$, $j \neq k$ を満たすものと定める. 平面 $\mathbb{C}$ 上の格子 $\Lambda(z) := z\mathbb{Z} + \mathbb{Z}$, $z \in \mathbb{C}$, $\mathrm{Im}(z) > 0$ を母点集合とするボロノイ図 $\mathcal{V}(z) := \{V(\lambda)\}_{\lambda\in\Lambda(z)}$,

$$V(\lambda) = V(\lambda; z) := \{\zeta \in \mathbb{C} : |\zeta - \lambda| \leq |\zeta - \lambda'|,\ \forall\lambda' \in \Lambda(z)\}$$

が $\mathbb{C}$ のタイリングであることは容易に示される. $\mathbb{C}$ のボロノイタイリング $\mathcal{V}(z)$ は, 射影 $\pi : \mathbb{C} \to \mathbb{C}/\mathbb{Z}$ によって, $\pi(z)$ で生成される加法群 $\pi(z\mathbb{Z} + \mathbb{Z}) = \pi(z)\mathbb{Z}$ が推移的に作用する族 $\mathcal{T}(z) := \{T(\lambda) := \pi(V(\lambda))\}_{\lambda\in\Lambda(z)}$,

$$T(\lambda) := \{\zeta \in \mathbb{C}/\mathbb{Z} : \mathrm{dist}(\zeta, \pi(\lambda)) \leq \mathrm{dist}(\zeta, \pi(\lambda')),\ \forall\lambda' \in \Lambda(z)\},\ \lambda \in \Lambda(z).$$

である. $E := \{z \in \mathbb{C} : |z - \frac{1}{2}| < \frac{1}{2}\}$, $\mathbb{H} := \{z \in \mathbb{C} : \mathrm{Im}(z) > 0\}$ とする. もし $z \notin \mathbb{Z} + \mathbb{H} \cap E$ ならば $\mathcal{T}(z)$ は円筒 $\mathbb{C}/\mathbb{Z}$ のタイリングでなく, もし $z \in \mathbb{Z} + \mathbb{H} \cap E$ ならば $\mathcal{T}(z)$ は円筒 $\mathbb{C}/\mathbb{Z}$ のタイリングである. 円筒 $\mathbb{C}/\mathbb{Z}$ 上のボロノイタイリング $\mathcal{T}(z)$ について, 以下が成り立つ.

- $\mathcal{T}(z)$ のタイル $T(\lambda)$ $(\lambda \in \Lambda(z))$ の形状は六角形もしくは長方形である.
- $\mathrm{Re}(z)$ を固定したとき, $\mathrm{Im}(z)$ の単調減少による $\mathcal{T}(z)$ の組合せ的構造の分岐過程は, $\mathrm{Re}(z)$ の連分数展開で説明される.
- 長方形タイリングを作る $z \in \mathbb{C}$ の集合は円弧の和集合である.
- 長方形タイルの形状パラメータ (縦横比) は $\mathrm{Re}(z)$ の連分数展開によって記述される. さらに, $\mathrm{Re}(z)$ が二次無理数とし, $\mathrm{Im}(z) \to 0$ とするとき, 長方形タイルにおける形状パラメータの極限集合は二次無理数で記述される有限集合であることが示される. 特に, $\mathrm{Re}(z)$ が黄金比 τ に対等な無理数ならば長方形タイルの極限形状は正方形であることが示される. 長方形タイルの極限形状に関する結論は, Rothen と Koch による the shape invariance under compression に数学的な拡張を与える.

第 3 章では, 平面 $\mathbb{C}^*$ の被覆空間である開リーマン面 M_v 上の $\zeta = re^{i\theta} \in M_v$, $0 < r < 1$ で生成される螺旋点列 $S = \{\zeta^j\}_{j\in\mathbb{Z}} \subset M_v$ を母点集合とするボロノイ螺旋多重タイリング $\mathcal{T} := \{T_j\}_{j\in\mathbb{Z}}$ を考える. ここで, $v \neq 0$ は整数である. M_v のボロノイ螺旋多重タイリング $\mathcal{T}$ について, 以下が成り立つ.

- $\mathcal{T}$ のタイル T_j $(j \in \mathbb{Z})$ の形状は六角形もしくは四角形である.
- $\theta/2\pi v$ を固定したとき, $0 < r < 1$ の単調増加による $\mathcal{T}$ の組合せ的構造の分岐過程は, $\theta/2\pi v$ の連分数展開で説明される.
- 四角形ボロノイ螺旋多重タイリングを作る $\zeta \in M_v$ の集合は, 単位円板 $\mathbb{D}$ 内において, θ をパラメータとする実代数曲線の枝の和集合 B_v である. さらに, 和集合 $\bigcup_{v>0} B_v$ は単位円板 $\mathbb{D}$ の稠密部分集合を与える.
- $\theta/2\pi v$ を固定された二次無理数とし, $r \to 1$ とするとき, 四角形タイルの形状パラメータ (縦横比) の近似式は $\theta/2\pi v$ の連分数展開によって記述され, その極限集合は二次無理数で記述される有限集合であることが示される. 特に, $\theta/2\pi v$ が黄金比 τ に対等な無理数ならば四角形タイルの極限形状は正方形であることが示される.

数学的な結論は円筒 $\mathbb{C}/\mathbb{Z}$ 上のボロノイタイリングに似ているが, ボロノイ螺旋多重タイリングは円板上の問題であるため, 数学的な議論の展開が複雑である.

第 4 章では, 螺旋点列 S を頂点集合とする三角形螺旋タイリングを考える. はじめに, 平面 $\mathbb{C}^*$ の被覆空間 $C_v = \mathbb{C}/2\pi v\mathrm{i}\mathbb{Z}$ のタイリングとして螺旋多重タイリングを定義する. ここで, $v \neq 0$ は整数である. 次に, $T_0 := \square(1, \zeta^m, \zeta^{m+n}, \zeta^n)$ がこの順番で頂点が並ぶ $\mathbb{C}^*$ の四角形であるならば, 四角形の族 $\mathcal{T} = \{T_j := \square(\zeta^j, \zeta^{j+m}, \zeta^{j+m+n}, \zeta^{j+n})\}_{j\in\mathbb{Z}}$ は, 多重度 $v := |n\mathrm{Arg}(\zeta^m) - m\mathrm{Arg}(\zeta^n)|$ をもつ平面 $\mathbb{C}^*$ の螺旋多重タイリングであることが示される. ここで, $-\pi < \mathrm{Arg}(z) \leq \pi$ は $z \in \mathbb{C}^*$ の偏角の主値を表す. 葉序の分野では, 四角形螺旋多重タイリング $\mathcal{T}$ の組合せ的指標 $\{m, n\}$ において, $\mathrm{Arg}(\zeta^m)\mathrm{Arg}(\zeta^n) < 0$ となるとき, $\{m, n\}$ を opposed parastichy pair といい, $\mathrm{Arg}(\zeta^m)\mathrm{Arg}(\zeta^n) > 0$ となるとき, $\{m, n\}$ を non-opposed parastichy pair という. 次に, 四角形螺旋多重タイリング $\mathcal{T}$ の opposed parastichy pair$\{m, n\}$ が $\theta/2\pi v$ の連分数展開における主近似分数およびその次の主近似分数までの中間近似分数の分母の対であることが示される.

四角形 $T_0 := \square(1, \zeta^m, \zeta^{m+n}, \zeta^n)$ の 4 頂点のうち 3 頂点が同一直線上にあるとき, 四角形螺旋多重タイリング $\mathcal{T}$ は三角形螺旋多重タイリングになる. 円筒 $\mathbb{C}/\mathbb{Z}$ 上のボロノイタイリングおよびボロノイ螺旋多重タイリングでは, ボロノイ図が退化した特殊な場合として non-opposed parastichy pairs をもつタイリングは得られないが, 三角形螺旋多重タイリングには, non-opposed parastichy pairs をもつタイリングが存在する. 三角形螺旋多重タイリングについて, 以下が成り立つ.

- 三角形タイルはすべて相似であるから, 三角形タイルの形状は２つの角度に依存する. 従って, 三角形タイルの形状の自由度は実二次元である. $I = (-\pi, \pi]$ とし, 三角形タイルの２つの角度に関するパラメータ空間を $\Delta := \{(\theta_1, \theta_2) \in I^2 : \ 0 < \theta_1 < \theta_2 + \pi < \pi\}$, $\Delta' := \{(\theta_1, \theta_2) \in I^2 : \ \theta_1, \theta_2 > 0, \theta_1 + \theta_2 < \pi\}$ とする. $v > 0$ を整数とし, parastichy pair$\{m, n\}$ をもつ多重度 v の螺旋多重タイリングを作る三角形の形状の集合 $\ell_{m,n,v}$ とする. このとき, 以下が成り立つ.

  (i) $L_v := \bigcup_{(m,n)\in R} \ell_{m,n,v}$ は $\Delta \cup \Delta'$ 内において全疎である. 位相空間 X の集合 A が全疎であるとは, A の閉包の内部が空集合である.

  (ii) $L := \bigcup_{v>0} L_v$ は $\Delta \cup \Delta'$ 内の稠密部分集合である.

- opposed parastichy pair$\{m, n\}$ をもつ多重度 v の三角形螺旋多重タイリングを生成する $\zeta \in \mathbb{D}\backslash\mathbb{R}$ の集合 $P_{m,n,v}$ は $\theta = \mathrm{Arg}(\zeta)$ をパラメータとする実代数曲線の枝である. さらに, 和集合 $\bigcup_{v>0} \bigcup_{(m,n)\in R} P_{m,n,v}$ は単位円板 $\mathbb{D}$ の稠密部分集合である.

- non-opposed parastichy pair$\{m, n\}$ をもつ多重度 v の三角形螺旋多重タイリングを生成する $\zeta \in \mathbb{D}\backslash\mathbb{R}$ の集合 $Q_{m,n,v}$ は絶対値 $r = |\zeta|$ をパラメータとする実代数曲線の枝であり, 和集合 $\bigcup_{(m,n)\in R} Q_{m,n,v}$ は単位円板 $\mathbb{D}$ の稠密部分集合である.

- $\theta/2\pi v$ を固定された二次無理数とし, $r \to 1$ とするとき, opposed parastichy pairs をもつ三角形螺旋多重タイリングの三角形タイルの形状パラメータ (線分比) の近似式は $\theta/2\pi v$ の連分数展開によって記述され, その極限集合は二次無理数で記述される有限集合であることが示される. 特に, $\theta/2\pi v$ が黄金比 τ に対等な無理数ならば形状パラメータの極限集合は黄金比 τ で記述されることが示される.

第 5 章では, 本論文のまとめおよび展望が述べられている.

Contents

Chapter 1

Introduction

The main subjects of the thesis are Voronoi spiral tilings [63] and triangular spiral tilings [59, 60, 61, 62] which admit a transitive action by the similarity transformation group $S = \{\zeta^j\}_{j\in\mathbb{Z}}$ of the punctured plane $\mathbb{C}^* := \mathbb{C}\backslash\{0\}$, which is generated by a single element $\zeta = re^{i\theta} \in \mathbb{D}\backslash\mathbb{R}$. The topology of spiral tilings is intimately related to the phyllotaxis theory. First, we recall several topics related to the subject of phyllotaxis. Second, we introduce phyllotactic architectures by Akio Hizume. Finally, we explain an outline of the thesis.

1.1 Background

1.1.1 Several topics related to the subject of phyllotaxis

One of the most beautiful features of plants is the regular arrangements of botanical units such as leaves and other organs, which are called *phyllotaxis* [35]. For example, phyllotactic patterns are observed in leaves on a stem, scales on a pine cone, a skin of a pineapple and florets in the head inflorescence of a daisy such as a sunflower.

In the subject of phyllotaxis, from the viewpoint of symmetry, the phyllotactic patterns are classified four broad categories which are called the *spiral phyllotaxis*, the *distichous phyllotaxis*, the *whorled phyllotaxis* and the *multijugate phyllotaxis*, respectively. In the spiral phyllotaxis, botanical units grow one by one at each node of a stem, and an angle between two successive botanical units is called the *divergence angle*. In the distichous phyllotaxis, botanical units grow one by one at each node of a stem, which is preserving the divergence angle π radians. This is a special case of the spiral phyllotaxis. In the whorled phyllotaxis, two or more botanical units grow at each node on a stem. Botanical units in a node are uniformly spread around the stem at a center between botanical units in the previous node. In the multijugate phyllotaxis, two or more botanical units grow at each node on the stem, and botanical units in a whorl grow uniformly around the stem. Moreover, each whorl preserves a constant divergence angle between the previous whorl.

It is well observed that most of phyllotactic patterns are the spiral phyllotaxis. The spiral phyllotaxis is classified as the *planar phyllotaxis* and the *cylindrical phyllotaxis*. As a remarkable feature of the planar phyllotaxis and the cylindrical phyllotaxis, it is well observed that combinatorial structures (the divergence angle and the number of visible spirals) of typical plants are described by the golden section $\tau = \frac{1+\sqrt{5}}{2}$ and the Fibonacci numbers $1, 2, 3, 5, 8, 13, \cdots$. For example, the divergence angle of the spiral phyllotactic patterns of typical plants such as a sunflower is written by the golden section, and a pair of the number of two parastichies (clockwise spirals or counterclockwise spirals) is a pair of two successive terms of the Fibonacci sequence. It is often called the *Fibonacci phyllotaxis*. In addition to the Fibonacci phyllotaxis, there are spiral phyllotactic patterns described by the Lucas numbers $1, 3, 4, 7, 11, 18, \cdots$. It is often called the *Lucas phyllotaxis*, and its divergence angle is written by the irrational number $\frac{5+\sqrt{5}}{10}$, where

$\frac{5+\sqrt{5}}{10}$ is an irrational number which is linearity equivalent of the golden section τ. According to the investigation by Jean [35, pp.21], the Fibonacci phyllotaxis arises more than 92% and the Lucas phyllotaxis arises about 2%. That is, the Lucas phyllotaxis is the minority compared with the Fibonacci phyllotaxis. In addition to the both phyllotactic patterns, there are spiral phyllotactic patterns described by the Fibonacci-like sequences such that $1, 4, 5, 9, 14, 23, \cdots$ and $1, 5, 6, 11, 17, 28, \cdots$ etc. These phyllotactic patterns are the minority compared with the Fibonacci phyllotaxis. In the study of phyllotaxis, the following problem is the central problem. *What are physical, chemical or biological mechanisms that most of spiral phyllotactic patterns are described by the golden section and the Fibonacci numbers ?* In order to elucidate the above central problem, phyllotactic patterns have studied as an interdisciplinary subject related to mathematics, physics, chemical and biology, from the ancient times. See the historical review [1].

The mathematical study of phyllotaxis has continued from early half of the 19th century. In 1837, Bravais brothers derived a cylindrical representation of phyllotaxis and studied the relationship between the continued fraction approximations of the divergence angles and the lattice structures. By subsequent studies [12, 35, 2] about the cylindrical model of phyllotaxis, its mathematical formulation was rewritten by scientists Coxeter [10], Adler [2], Erickson [12, Chapter 3], Jean [35]. In 1989, Rothen and Koch studied the shape invariance under compression in the Voronoi tilings with the cylindrical lattices on the cylinder [49]. Recently, the bifurcation processes of the combinatorial structures in the Voronoi tilings with the cylindrical lattices on the cylinder was described from the viewpoint of dynamical systems [3]. In addition to the cylindrical model, Vogel [72] proposed the simplest disk model for a phyllotactic pattern of a sunflower as the sequence in 1979. Its sequence is given by the complex sequence $V = \{\phi_j(r)\mathrm{e}^{\mathrm{i}\cdot j\theta}\}_{j\in\mathbb{N}}$, $\phi_j(r) = r\sqrt{j}$, where $r > 0$ and $\theta \in \mathbb{R}$ are constants. In the disk model, combinatorial structures in the Voronoi tiling with the site set V are studied from the viewpoint of crystallography [45, 46, 47]. In addition to the cylindrical model and the disk model, there are studies about the conical model [5] and the curvature model [48]. In the geometrical approach, there is a tendency which deals with a model suitable for the problem. Under any geometrical models, the continued fractions [22, 68] and the lattice structures [9] play important roles.

On the other hand, there are studies about self-organized processes of phyllotactic patterns from the viewpoint of mathematical biology. In the phyllotaxis theory, it was considered that a botanical unit which is generated together with the growth of a plant grow while generating a diffusible inhibitor. That is, it implies that each botanical unit is generated at a place with the least influential of inhibitor which compared to the previous one. In 1970s, corresponding two dimensional diffusion equations were proposed [70, 71, 74]. In 1996, Douady and Couder [14, 15, 16] did an artificial experiment of the disk model of phyllotaxis and they showed the bifurcation diagram of combinatorial structures. Recently, there are new proposals of the reaction diffusion equation [52, 69].

Moreover, by the progress of the biological study of phyllotaxis, it is known that one of reason which the divergence angle is the golden angle, is an auxin transportation [44, 7, 38] between cells in a plant. Recently, several model equations (non-linearity partial differential equations) which is considering an auxin fluctuation concentration, are proposed [53, 8, 40].

1.1.2 Phyllotactic architectures by Akio Hizume

In addition to studies of the classical subject of phyllotaxis, several phyllotactic architectures were devised by Akio Hizume who is inspired by the golden section and the Fibonacci numbers. In 1987, he devised an architecture which extracted a mathematical essence of the Fibonacci phyllotaxis of a sunflower. It was named the *sunflower tower* [24], and he manufactured it as a giant architecture by using bamboos (See Figure 1.1). In 2005, he devised triangular spiral tilings named the *Fibonacci tornado* [25], as a foundation of the sunflower towers (See Figure 1.2 and Figure 4.4). The remarkable feature of the Fibonacci tornado is admitting no rotational

(a)  (b) 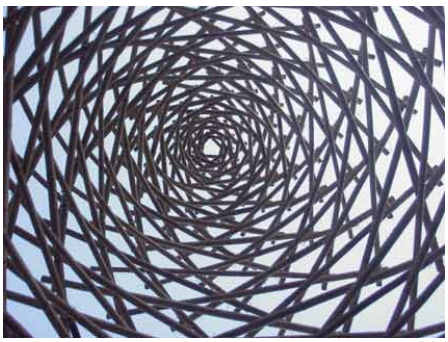

Figure 1.1: The sunflower tower manufactured by bamboos. There are two pictures in Hizume's web page (http://www.starcage.org). (a) Side view of the sunflower tower. (b) Bottom-up view of the sunflower tower.

(a) 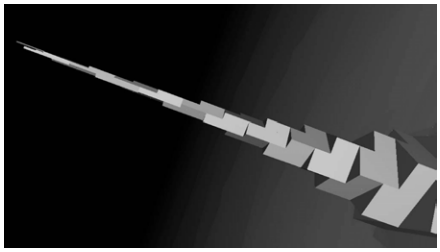 (b) 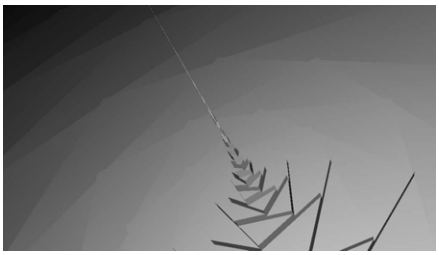

Figure 1.2: The Fibonacci tornado designed as a tower. There are two pictures in Hizume's web page. (a) Side view of the top. (b) Top-down view.

symmetry and involving a transitive action by a similarity transformation written by the golden angle. That is, in the Fibonacci tornado, any two triangles are not congruence. In the tiling theory [20, 65, 21], tilings which admit an action by a similarity symmetry group are well-known. However, there are not studies of triangular spiral tilings such as the Fibonacci tornado.

The Fibonacci tornado is a tiling of the plane $\mathbb{R}^2$ given by the following theorem, where a tiling of the plane $\mathbb{R}^2$ conforms to the definition in the tiling theory (See Definition 2.1).

Theorem 1.1 ([25]). *Let* $\mathrm{A}_j := (r^j \cos 2\pi\tau j, r^j \sin 2\pi\tau j) \in \mathbb{R}^2$ *with* $0 < r < 1$, *where* $\tau = \frac{1+\sqrt{5}}{2}$ *is the golden section. Let* $F_n := \{f_n\}_{n\geq 1}$ *be the Fibonacci sequence determined by* $f_1 = 2$, $f_2 = 3$, $f_{n+2} = f_{n+1} + f_n$, $n \geq 1$. *Then, for each* $n \geq 1$, *there exists* $0 < r < 1$ *uniquely such that the family of triangles* $\mathcal{T} = \{\triangle(\mathrm{A}_j, \mathrm{A}_{j+f_n}, \mathrm{A}_{j+f_{n+1}})\}_{j\in\mathbb{Z}}$ *gives a tiling of* $\mathbb{R}^2$.

In 2008, he succeeded to progress the theory of triangular spiral tilings by applying the continued fraction theory, and they are named the *real tornado* [29]. In 2009, Akio Hizume and Yoshikazu Yamagishi showed a mathematical description between triangular spiral tilings and the continued fractions of the divergence angles [30, 31]. In these studies, it was observed that there are triangular spiral tilings without the relation with the continued fraction expansions of the divergence angles.

As an another background about the Fibonacci tornado, there is its origami development. Its origin is an origami art by Fuse Tomoko, a Japanese origami artist. In 1994, she devised origami towers named the *twisted multiple towers* [17, 18] based on her origami lampshades. Their top-down views are spiral sequences of concentric regular polygons. Exactly, these patterns are tilings by congruence polygons which are well-known in the tiling theory. Recently, these origami designs are applied into a clothing by Issey Miyake and Jun Mitani [1] In addition to the twisted multiple

[1] Issey Miyake and Reality Lab Project Team, '132.5 ISSEY MIYAKE', in: REALITY LAB: rebirth and regeneration, exhibition, (directors: Issey Miyake and Katsumi Asaba), 21_21 DESIGN SIGHT, Tokyo, 16 November to 26 December 2010.

towers, there are also Chris Palmer's flower towers [51]. In 2005, Akio Hizume was influenced by the twisted multiple towers and he succeeded to make the Fibonacci tornado as an origami development by one sheet of paper [26] (See Figure 4.5).

At almost the same time, Taketoshi Nojima devised an origami development with phyllotactic patterns, called *Nojima's pine cone* [54]. In his studies, there are origami developments manufactured by metals [41, 42]. In the study of the rigid origami [67] manufactured by metals etc, *Miura ori* [39] applied solar panels of satellites and the Stanford bunny by Tomohiro Tachi [66] are famous rigid origami architectures. It is the remarkable fact that these rigid origami architectures are folded in one sheet of paper. There is a comprehensive text about origami foldability [43]. Recently, there are new proposals of origami developments and these engineering applications [33, 34].

1.2 Outline of the thesis

The thesis consists of three parts. The aim of Part I is to give an extended results for the shape invariance under compression by Rothen and Koch [49] in the helical Voronoi tilings on the cylinder [64]. The aim of Part II and Part III is to construct theoretical frameworks about the Voronoi spiral tilings [63] and the triangular spiral tilings [59, 60, 61, 62], which are not known in the tiling theory.

1.2.1 Helical Voronoi tilings

Part I gives a mathematical description of the helical Voronoi tilings on the cylinder. In this part, we consider the Voronoi tiling $\mathcal{V}(z) := \{V(\lambda)\}_{\lambda\in\Lambda(z)}$,

$$V(\lambda) = V(\lambda; z) := \{\zeta \in \mathbb{C} : |\zeta - \lambda| \le |\zeta - \lambda'|,\ \forall\lambda' \in \Lambda(z)\}.$$

of the plane $\mathbb{C}$ with the site set $\Lambda(z) := z\mathbb{Z} + \mathbb{Z}$, where $z = x + \mathrm{i}y \in \mathbb{C}\backslash\mathbb{R}$, $x, y \in \mathbb{R}$. In the phyllotaxis theory, $x = \mathrm{Re}(z)$ is called the *divergence* and $\mathrm{e}^y = \mathrm{e}^{\mathrm{Im}(z)} = |\mathrm{e}^{-\mathrm{i}z}|$ is called the *plastochrone ratio*. By the conical projection $\pi : \mathbb{C} \to \mathbb{C}/\mathbb{Z}$, the plane $\mathbb{C}$ is a covering space of the cylinder $\mathbb{C}/\mathbb{Z}$. Thus, the family $\mathcal{T}(z) := \{T(\lambda)\}_{\lambda\in\Lambda(z)}$,

$$T(\lambda) := \{\zeta \in \mathbb{C}/\mathbb{Z} : \mathrm{dist}(\zeta, \pi(\lambda)) \le \mathrm{dist}(\zeta, \pi(\lambda')),\ \forall\lambda' \in \Lambda(z)\},\ \lambda \in \Lambda(z).$$

of the cylinder $\mathbb{C}/\mathbb{Z}$ admits a transitive action by an additive group of translations $\pi(z\mathbb{Z} + \mathbb{Z}) = \pi(z)\mathbb{Z}$ generated by a single element $\pi(z)$.

Two distinct tiles $T_1, T_2 \in \mathcal{T}(z)$ are *adjacent* if $T_1 \cap T_2$ contains at least two points. Let $E = \{z \in \mathbb{C} : |z - \frac{1}{2}| \le \frac{1}{2}\}$. If $z \notin \mathbb{Z} + E$, then the two tiles $V(0)$, $V(1) \in \mathcal{V}(z)$ are adjacent to each other, and hence the Voronoi region $T(0) = T(1)$ in the cylinder is not simply connected. If $z \in \mathbb{Z} + E \setminus \mathbb{R}$, then $T(\lambda)$, $\lambda \in \Lambda(z)$, are simply connected, and $\mathcal{T}(z)$ is a tiling of the cylinder by convex polygons. It is called the *helical Voronoi tiling* generated by z.

In Section 2.1, it is shown in Lemma 2.4 that tiles of helical Voronoi tilings $\mathcal{T}(z)$ are hexagons or rectangles.

In the phyllotaxis theory, the pair $\{m, n\}$ of positive integers is called an *opposed parastichy pair* if $V(0)$ is adjacent to $V(mz - a), V(nz - b)$, and $\mathrm{Re}(nz - b) \cdot \mathrm{Re}(mz - a) < 0$, for some $a, b \in \mathbb{Z}$. It is shown in Lemma 2.4 that helical Voronoi tilings $\mathcal{T}(z)$ have opposed parastichy pairs.

If a helical Voronoi tiling becomes a rectangular tiling with an opposed parastichy pair $\{m, n\}$, then the four points 0, λ, $\lambda + \lambda'$ and λ' lie on a same circle in this order of vertices, where $\lambda = mz - a$, $\lambda' = nz - b$. In Section 2.2, we describe the set (Figure 2.1) of generators z which produce rectangular tilings for each opposed parastichy pair $\{m, n\}$. it is shown in Lemma 2.5 that there are generators z which produce hexagonal tilings for every opposed parastichy pairs, by its bifurcation diagram.

In Section 2.3, we show a relationship between the continued fraction expansions of the divergence and opposed parastichy pairs of the helical Voronoi tilings.

In Section 2.4, we consider the shape convergence property of the rectangular helical Voronoi tilings. We address the following question:

- *What are limit shapes of rectangular tiles ?*

We consider the limit set of shape parameters (aspect ratios) of rectangular tiles as y tends to 0, when x is a fixed irrational number. If x is a fixed quadratic irrational, then it is shown in Theorem 2.9 that the limit set of shape parameters of rectangular tiles is a finite set written by quadratic irrationals. Moreover, if x is a fixed irrational number which is a linearity equivalent of the golden section τ, it is shown in Corollary 2.10 that the limit shape of the rectangular tiles is the square. It gives the extended result of the shape invariance under compression written in [49].

1.2.2 Voronoi spiral tilings

Part II gives mathematical description about the Voronoi spiral tilings. The Voronoi spiral tiling is a Voronoi tiling $\mathcal{T}(\zeta) = \{T_j\}_{j\in\mathbb{Z}}$ of $\mathbb{C}^*$ with the spiral site set $S = \{\zeta^j\}_{j\in\mathbb{Z}}$ generated by a single element $\zeta = re^{i\theta} \in \mathbb{D}\backslash\mathbb{R}$, $0 < r < 1$. First, we address the following essential question:

- *What is a Voronoi spiral multiple tiling geometrically possible ?*

In Section 3.1, we consider a Voronoi tiling $\mathcal{T}(\zeta)$ with the spiral site set S on an open Riemann surface M_v such that the exponential function is an isomorphism of the additive group $C_v := \mathbb{C}/2\pi v i\mathbb{Z}$ onto the multiplicative group M_v, where $v \neq 0$ is an integer. It is shown that a Voronoi tiling of the open Riemann surface M_v is a polygonal tiling. We call these polygonal tilings *the Voronoi spiral multiple tilings*. Moreover, it is shown in Lemma 3.3 that tiles T_j of Voronoi spiral multiple tilings are hexagons or quadrilaterals. In particular, the case of quadrilateral tilings is a special case which is called *the degenerate case* in the subject of the Voronoi diagram [6, 56]. In the phyllotaxis theory, the pair $\{m, n\}$ of a Voronoi spiral multiple tiling is called an *opposed parastichy pair* if T_0 is adjacent to T_m, T_n and $\arg(\zeta^m)\arg(\zeta^n) < 0$, and a *non-opposed parastichy pair* if T_0 is adjacent to T_m, T_n and $\arg(\zeta^m)\arg(\zeta^n) > 0$, where $\arg(\zeta) \in (-|\pi v|, |\pi v|]$ be an argument of $\zeta \in M_v$. It is the remarkable feature that the Voronoi spiral multiple tilings by quadrilaterals have opposed parastichy pairs, whereas there exists a triangular spiral multiple tiling with a non-opposed parastichy pair.

In Section 3.2, we show that transitions of opposed parastichy pairs of the Voronoi spiral multiple tilings are described by the continued fraction approximations of $\theta/2\pi v$ when $\theta/2\pi v$ is fixed and $1/r$ is decreased monotonically from a sufficiently large value to a sufficiently small value.

By Section 3.1 and 3.2, there are not generators $\zeta \in \mathbb{D}\backslash\mathbb{R}$ which produce Voronoi spiral multiple tilings by quadrilaterals with non-opposed parastichy pairs, and an opposed parastichy pair of a quadrilateral tiling is a pair of denominators of principal or intermediate convegents of $\theta/2\pi v$, at least one of which is principal.

If a Voronoi spiral multiple tiling of multiplicity v becomes a degenerate quadrilateral tiling with an opposed parastichy pair $\{m, n\}$, then the four points 1, ζ^m, ζ^{m+n} and ζ^n lie on a same circle in $U \subset M_v$. In this section, we address the following question about the quadrilateral Voronoi spiral multiple tilings:

- *Which generators $\zeta \in M_v$ produce quadrilateral Voronoi spiral multiple tilings ?*

In Section 3.3, we consider the set $B_{m,n,v}$ of generators $\zeta \in M_v$ which produce quadrilateral Voronoi spiral multiple tilings of multiplicity v, with an opposed parastichy pair $\{m, n\}$. It is shown in Theorem 3.12 and Lemma 3.13 that $B_{m,n,v}$ is a branch of a real algebraic curve

which is parameterized by the divergence angle $\theta = \arg(\zeta)$, in $\mathbb{D}$. Next, we consider the union $B_v := \bigcup_{(m,n)\in R} B_{m,n,v}$ for each v, where $R = \{(m,n) \in \mathbb{Z}^2 : m > n > 0 \text{ are relatively prime}\}$. Figure 3.5 shows the set $B_1 \cup B_{-1}$. This set is not a dense subset of $\mathbb{D}$. Moreover, it is shown in Theorem 3.15 that the union of $B := \bigcup_{v\neq 0} \bigcup_{(m,n)\in R} B_{m,n,v}$ gives a dense subset of $\mathbb{D}$.

In Section 3.4, we consider the shape convergence property of the quadrilateral Voronoi spiral multiple tilings. We address the following question:

- *What are limit shapes of quadrilateral tiles ?*

We consider the limit set of shape parameters of quadrilateral tiles for quadrilateral Voronoi spiral multiple tilings as $1/r \to 1$, when $\theta/2\pi v$ is a fixed irrational number. If $\theta/2\pi v$ is a fixed quadratic irrational, then it is shown in Theorem 3.18 that the limit set of shape parameters of quadrilateral tiles is a finite set written by quadratic irrationals. Moreover, if $\theta/2\pi v$ is a fixed irrational number which is a linearity equivalent of the golden section τ, it is shown in Corollary 3.19 that the limit shape of the quadrilateral tiles is the square.

1.2.3 Triangular spiral tilings

Part III gives a mathematical description of the triangular spiral tilings. First, we address the following essential question:

- *What is a quadrilateral spiral multiple tiling geometrically possible ?*

In Section 4.1, first, we define a spiral multiple tiling as a tiling of a covering space of the punctured plane $\mathbb{C}^*$. Second, we consider the spiral sequence $S = \{\zeta^j\}_{j\in\mathbb{Z}}$ of $\mathbb{C}^*$ generated by a single element $\zeta = re^{i\theta} \in \mathbb{D}\backslash\mathbb{R}$ with $0 < r < 1$, and we show that a quadrilateral spiral multiple tiling is determined by a triplet (ζ, m, n), where $m, n > 0$ are relatively prime integers. If $T_0 := \square(1, \zeta^m, \zeta^{m+n}, \zeta^n)$ is a quadrilateral of $\mathbb{C}^*$ in this order of vertices, it is shown in Theorem 4.2 that the family of quadrilaterals $\mathcal{T} = \{T_j := \square(\zeta^j, \zeta^{j+m}, \zeta^{j+m+n}, \zeta^{j+n})\}_{j\in\mathbb{Z}}$ gives a spiral multiple tiling of $\mathbb{C}^*$, with multiplicity $v := |n\mathrm{Arg}(\zeta^m) - m\mathrm{Arg}(\zeta^n)|/2\pi$, where $-\pi < \mathrm{Arg}(z) \leq \pi$ denotes the principal argument of $z \neq 0$.

In the phyllotaxis theory, the pair $\{m, n\}$ of a quadrilateral spiral multiple tiling $\mathcal{T}$ is called an *opposed parastichy pair* if $\mathrm{Arg}(\zeta^m)\mathrm{Arg}(\zeta^n) < 0$, and a *non-opposed parastichy pair* if $\mathrm{Arg}(\zeta^m)\mathrm{Arg}(\zeta^n) > 0$. In Section 4.2, we show that it has a natural extension to spiral multiple tilings. If $\{m, n\}$ is an opposed parastichy pair of a quadrilateral spiral multiple tiling of multiplicity v, it is shown in Theorem 4.3 that m, n are denominators of principal or intermediate convergents of $\theta/2\pi v$, at least one of which is principal.

If three vertices of the quadrilateral T_0 lie on a same line, then T_0 becomes a triangle, that is, a triangular spiral multiple tiling is a special case of quadrilateral spiral multiple tilings. In Section 4.3, we consider triangular spiral multiple tilings with opposed parastichy pairs or non-opposed parastichy pairs. In this section, we address the following questions about the triangular spiral multiple tilings:

- *What triangles admit spiral multiple tilings ?*

- *Which generators $\zeta \in \mathbb{D}\backslash\mathbb{R}$ produce triangular spiral multiple tilings ?*

About the first question, it is shown in Theorem 4.7 and Theorem 4.21 that, for each multiplicity $v > 0$, the set of shapes of triangles which admit spiral multiple tiling with opposed parastichy pairs or non-opposed parastichy pairs, is a nowhere dense subset of the parameter space Δ_+. Moreover, it is shown in Theorem 4.7 and Theorem 4.22 that the union of these sets for all multiplicity v gives a dense subset of the parameter space Δ_+. By Theorem 4.5 and Theorem 4.13, we can consider whether a fixed triangle admits a spiral multiple tiling. For example, we could obtain spiral tilings by equilateral triangles, right triangles with the angles 30°, 60°, 90°

or right triangles with the angles 45°, 45°, 90° (See Figure 4.7, 4.17 and 4.18). About multiple tilings, we could obtain a spiral multiple tiling of multiplicity $v = 2$ by right triangles with the angles 30°, 60°, 90° (See Figure 4.9). Moreover, we present origami sheets of Figure 4.7 and 4.9.

About the second question, we show the followings. It is shown that the set $P_{m,n,v}$ of generators $\zeta \in \mathbb{D}\backslash\mathbb{R}$ which produce triangular spiral multiple tilings of multiplicity v with an opposed parastichy pair $\{m, n\}$ is a branch of a real algebraic curve which are parameterized by the divergence angle $\theta = \mathrm{Arg}(\zeta)$. Next, we consider the union $P_v := \bigcup_{(m,n)\in R} P_{m,n,v}$ for each v. Figure 4.13 shows the set $P_1 \cup P_{-1}$. This set is not a dense subset of $\mathbb{D}$. However, it has an interesting resemblance to a diagram in the topology of knot complements [23, Fig.4] which has $PSL(2;\mathbb{Z})$ symmetry. It is shown in Theorem 4.12 that the union $P := \bigcup_{v\neq 0} P_v$ is a dense subset of $\mathbb{D}$.

On the other hand, it is shown in Theorem 4.15 that the set $Q_{m,n,v}$ of generators $\zeta \in \mathbb{D}\backslash\mathbb{R}$ which produce triangular spiral multiple tilings of multiplicity v with non-opposed parastichy pair $\{m, n\}$ is a branch of a real algebraic curve which are parameterized by the plastochrone ratio $r = |\zeta|$. For each v, it is shown in Theorem 4.20 that the union $Q_v := \bigcup_{(m,n)\in R} Q_{m,n,v}$ is a dense subset of $\mathbb{D}$.

In Section 4.4, we consider the shape convergence property of the triangular spiral multiple tilings with opposed parastichy pairs. We address the following question:

- *What are limit shapes of triangle tiles ?*

It is shown in Theorem 4.26 that if the divergence angle θ is written by a fixed quadratic irrational, then the limit set of shape parameters (ratios of line segments) of triangle tiles is a finite set. In particular, when the divergence angle is written as an irrational number of the golden section τ, it is shown in Corollary 4.27 that the limit set of the shape parameters of the triangle tiles is written by the golden section τ.

Finally, we give conclusion remarks in Chapter 5.

Part I

Helical Voronoi tilings on the cylinder

Chapter 2

Helical Voronoi tilings on the cylinder

2.1 Voronoi tilings for cylindrical lattices

In the thesis, we deal with a tiling of a two dimensional manifold defined as follows, where the following definition is based on the tiling theory [21].

Definition 2.1. *A tiling of a two dimensional manifold X is a family $\mathcal{T} = \{T_j\}_j$ of topological disks $T_j \subset X$ which covers X without gaps or overlaps, that is, $X = \bigcup_j T_j$ and $\mathrm{int}(T_j) \cap \mathrm{int}(T_k) = \emptyset$, $j \neq k$. Each T_j is called a tile.*

Let $z = x + \mathrm{i}y \in \mathbb{H}$, where $\mathbb{H} = \{z \in \mathbb{C} : \mathrm{Im}(z) > 0\}$. In the phyllotaxis theory, $x = \mathrm{Re}(z)$ is called the *divergence* and $\mathrm{e}^y = \mathrm{e}^{\mathrm{Im}(z)} = |\mathrm{e}^{-\mathrm{i}z}|$ is called the *plastochrone ratio*. Next, we consider a Voronoi tiling of the complex plane $\mathbb{C}$ with the site set $\Lambda(z) := z\mathbb{Z} + \mathbb{Z}$, which is defined as follows. The following definition is based on the subject of Voronoi diagram [6, 56].

Definition 2.2. *The Voronoi region of the site $\lambda \in \Lambda(z)$ is defined by*

$$V(\lambda) = V(\lambda; z) := \{\zeta \in \mathbb{C} : |\zeta - \lambda| \leq |\zeta - \lambda'|,\ \forall \lambda' \in \Lambda(z)\}. \tag{2.1.1}$$

The family $\mathcal{V}(z) := \{V(\lambda)\}_{\lambda \in \Lambda(z)}$ is called the Voronoi tiling or the Voronoi diagram, with the site set $\Lambda(z)$.

It is easy to see that the Voronoi region $V(\lambda)$, $\lambda \in \Lambda(z)$ is a bounded polygon of $\mathbb{C}$. The Voronoi tiling $\mathcal{V}(z)$ is a *periodic tiling* with respect to the additive group of translations $\Lambda(z)$, since $V(\lambda) = V(0) + \lambda$ for each $\lambda \in \Lambda(z)$. Moreover, we have $\mathcal{V}(z) = \mathcal{V}(-z) = \mathcal{V}(z+1) = z \cdot \mathcal{V}(z^{-1})$ because $z\mathbb{Z} + \mathbb{Z} = (-z)\mathbb{Z} + \mathbb{Z} = (z+1)\mathbb{Z} = z(z^{-1}\mathbb{Z} + \mathbb{Z})$.

By the canonical projection $\pi : \mathbb{C} \to \mathbb{C}/\mathbb{Z}$, $\mathbb{C}$ is a covering space of the cylinder $\mathbb{C}/\mathbb{Z}$. The Euclidean metric of $\mathbb{C}$ induces a canonical distance in $\mathbb{C}/\mathbb{Z}$. The Voronoi regions in $\mathbb{C}/\mathbb{Z}$ with respect to the site set $\pi(\Lambda(z))$ are given by

$$T(\lambda) := \{\zeta \in \mathbb{C}/\mathbb{Z} : \mathrm{dist}(\zeta, \pi(\lambda)) \leq \mathrm{dist}(\zeta, \pi(\lambda')),\ \forall \lambda' \in \Lambda(z)\},\ \lambda \in \Lambda(z).$$

Note that $T(\lambda) = \pi(V(\lambda))$. The family $\mathcal{T}(z) := \{T(\lambda)\}_{\lambda \in \Lambda(z)}$ admits a transitive action of an additive group of translations $\pi(z\mathbb{Z} + \mathbb{Z}) = \pi(z)\ \mathbb{Z}$, generated by a single element $\pi(z)$.

Two distinct tiles T_1, T_2 are *adjacent* if $T_1 \cap T_2$ contains at least two points. Let $E = \{z \in \mathbb{C} : |z - \frac{1}{2}| \leq \frac{1}{2}\}$. If $z \notin \mathbb{Z} + E$, then the two tiles $V(0)$, $V(1) \in \mathcal{V}(z)$ are adjacent to each other, and hence the Voronoi region $T(0) = T(1)$ in the cylinder is not simply connected. If $z \in \mathbb{Z} + E \setminus \mathbb{R}$, then $T(\lambda)$, $\lambda \in \Lambda(z)$, are simply connected, and $\mathcal{T}(z)$ is a tiling of the cylinder by convex polygons. It is called the *helical Voronoi tiling* generated by z.

Suppose that $z \in \mathbb{Z} + E \cap \mathbb{H}$, and fix a lattice $\Lambda(z)$. A dual of a Voronoi diagram is called a *Delaunay diagram*. The line segment $\ell(\lambda, \lambda')$ joining $\lambda, \lambda' \in \Lambda(z)$ is called a *Delaunay edge* if $V(\lambda)$ is adjacent to $V(\lambda')$. Two distinct Delaunay edges may have a point in common only at their endpoint. A connected component of the complement $\mathbb{C} \setminus \bigcup \ell(\lambda, \lambda')$, where $\ell(\lambda, \lambda')$ runs through all the Delaunay edges, is called a *Delaunay polygon*. Each Delaunay polygon is inscribed in a circle. That is, a finite subset $\Lambda'(z) \subset \Lambda(z)$ is the set of the corners of a Delaunay polygon if and only if there exists a disk D such that $\partial D \cap \Lambda(z) = \Lambda'(z)$ and $\mathrm{int}(D) \cap \Lambda(z) = \emptyset$.

For distinct $z_1, z_2, z_3 \in \mathbb{C}$, let $\triangle(z_1, z_2, z_3)$ be a triangle in this order of vertices and

$$\angle(z_1, z_2, z_3) = \mathrm{Arg}\left(\frac{z_1 - z_2}{z_3 - z_2}\right),$$

where $-\pi < \mathrm{Arg}(z) \leq \pi$ denotes the principal argument of $z \neq 0$. If $\triangle(z_1, z_2, z_3)$ is a triangle in this order of vertices with counterclockwise, then interior angles of $\triangle(z_1, z_2, z_3)$ are given by $\angle(z_3, z_1, z_2)$, $\angle(z_1, z_2, z_3)$ and $\angle(z_2, z_3, z_1)$, and they are all positive.

Lemma 2.3. *Let $z \in \mathbb{Z} + E \cap \mathbb{H}$. Let $m, n > 0$ be integers, and suppose that $\square(0, \lambda, \lambda + \lambda', \lambda')$ is a quadrilateral in $\mathbb{C}$ in this order of vertices, where $\lambda = mz - a, \lambda' = nz - b \in \Lambda(z)$ for some $a, b \in \mathbb{Z}$. Suppose that $\mathrm{Re}(\lambda) \cdot \mathrm{Re}(\lambda') > 0$ and*

$$\angle(\lambda', 0, \lambda),\ \angle(\lambda', \lambda + \lambda', \lambda) > 0.$$

Then we have $\angle(\lambda', 0, \lambda) + \angle(\lambda', \lambda + \lambda', \lambda) < \pi$.

Proof. By the assumption, $\angle(\lambda', 0, \lambda) < \pi/2$. Moreover, we have $\angle(\lambda', 0, \lambda) = \angle(\lambda', \lambda + \lambda', \lambda)$. Hence, the proof is clear. □

Lemma 2.4. *Let $z \in \mathbb{Z} + E \cap \mathbb{H}$. For the tiling $\mathcal{V}(z)$ of the plane $\mathbb{C}$, there are $\lambda = mz - a, \lambda' = nz - b \in \Lambda(z)$ with integers $m, n > 0$, such that the followings hold.*

(i) The tile $V(0)$ is adjacent to $V(\lambda)$ and $V(\lambda')$,

(ii) $\lambda, \lambda', \lambda'/\lambda \in \mathbb{H}$, $mb - na = 1$, $\mathrm{Re}(\lambda') < 0 < \mathrm{Re}(\lambda)$, and

(iii) Either

(a) $\mathcal{V}(z)$ is a rectangular tiling, or

(b) $\mathcal{V}(z)$ is a hexagonal tiling such that $V(0)$ is adjacent to $V(\lambda + \lambda')$.

Proof. Since the site set $\Lambda(z)$ is a lattice of $\mathbb{C}$, its Delaunay diagram is also a periodic tiling with respect to the translation group $\Lambda(z)$. Since $V(\lambda)$, $\lambda \in \Lambda(z)$ is a bounded polygon, there exists $\lambda \neq \lambda'$ such that the tile $V(0)$ is adjacent to $V(\lambda)$ and $V(\lambda')$.

Suppose that $V(0)$ is adjacent to $V(\lambda), V(\lambda')$, $\lambda \neq \lambda'$. Then we have either:

1. the quadrilateral $\square(0, \lambda, \lambda + \lambda', \lambda')$ is a Delaunay polygon, or
2. $\ell(0, \lambda + \lambda')$ or $\ell(\lambda, \lambda')$ is a Delaunay edge.

In the case 1, the quadrilateral $\square(0, \lambda, \lambda + \lambda', \lambda')$ is a parallelogram which is inscribed in a circle. Hence it is a rectangle. By Lemma 2.3, $\mathrm{Re}(\lambda') \cdot \mathrm{Re}(\lambda) < 0$. Denote by $\lambda = mz - a$, $\lambda' = nz - b$. We may assume that $m, n > 0$ without loss of generality, which implies that $\lambda, \lambda' \in \mathbb{H}$. Since $\Lambda(z) = \lambda\mathbb{Z} + \lambda'\mathbb{Z}$, we have $|mb - na| = 1$. We may further assume that $\lambda'/\lambda \in \mathbb{H}$, $\mathrm{Re}(\lambda') < 0 < \mathrm{Re}(\lambda)$ and $mb - na = 1$.

In the case 2, we may assume without generality that $\lambda, \lambda', \lambda'/\lambda \in \mathbb{H}$, and that $V(0)$ is adjacent to $V(\lambda), V(\lambda'), V(\lambda + \lambda')$. Denote by $\lambda = mz - a$, $\lambda' = nz - b$. Then we have $m, n > 0$, and $mb - na = 1$ since $\Lambda(z) = \lambda\mathbb{Z} + \lambda'\mathbb{Z}$. Since $\triangle(0, \lambda, \lambda + \lambda')$ is a Delaunay polygon, λ' lies outside the circumscribing circle of $\triangle(0, \lambda, \lambda + \lambda')$, whereas $\square(0, \lambda, \lambda + \lambda', \lambda')$ is a parallelogram. This implies that $\angle(\lambda', 0, \lambda) > \pi/2$, and hence $\mathrm{Re}(\lambda') < 0 < \mathrm{Re}(\lambda)$. □

In the phyllotaxis theory, the pair $m, n > 0$ is called an *opposed parastichy pair* if $V(0)$ is adjacent to $V(mz - a), V(nz - b)$, and $\mathrm{Re}(nz - b) \cdot \mathrm{Re}(mz - a) < 0$, for some $a, b \in \mathbb{Z}$.

2.2 Parastichy transitions of helical Voronoi tilings

In this section, we rewrite that the bifurcation structure [12, Chapter 3] of the helical Voronoi tilings. First, we describe the set of generators $z \in \mathbb{Z} + E \cap \mathbb{H}$ which produce rectangular helical Voronoi tilings.

Let $z \in \mathbb{Z} + E \cap \mathbb{H}$, and suppose that $\mathcal{V}(z)$ is a rectangular tiling of $\mathbb{C}$ such that the tile $V(0)$ is adjacent to $V(\lambda), V(\lambda')$, where $\lambda = mz - a$, $\lambda' = nz - b$, $m, n > 0$, $mb - na = 1$. Then the angle $\angle(\lambda', 0, \lambda)$ is a right angle, and z lies on the circle

$$C\left(\frac{a}{m}, \frac{b}{n}\right) = \left\{ z \in \mathbb{C} : \frac{nz - b}{mz - a} \in \mathrm{i}\mathbb{R} \right\}. \tag{2.2.1}$$

The circle $C(\frac{a}{m}, \frac{b}{n})$ is symmetric with respect to the real axis, and passes through the points $a/m, b/n \in \mathbb{R}$. This, together with the assumption that $mb - na > 0$, implies that $a/m < \mathrm{Re}(z) < b/n$.

Lemma 2.5. *Let $z \in \mathbb{Z} + E \cap \mathbb{H}$. Suppose that $\mathcal{V}(z)$ is a hexagonal tiling such that the tile $V(0)$ is adjacent to $V(\lambda), V(\lambda'), V(\lambda + \lambda')$, where $\lambda = mz - a$, $\lambda' = nz - b$, $m, n > 0$, $mb - na = 1$. Then z lies inside the circle (2.2.1). In particular, we have $a/m < \mathrm{Re}(z) < b/n$.*

Proof. Let $z = x + \mathrm{i}y$, $y > 0$. Fix x, and consider $\lambda = \lambda(z) = mz - a$, $\lambda' = \lambda(z) = nz - b$ as functions of y. Since $\lambda(z), \lambda'(z) \in \mathbb{H}$ and $\mathrm{Re}(\lambda'(z)) < 0 < \mathrm{Re}(\lambda(z))$, the angle $\angle(\lambda', 0, \lambda)$ is a decreasing function of $y > 0$. Since $\ell(0, \lambda + \lambda')$ is a Delaunay edge, we have $\angle(\lambda', 0, \lambda) > \pi/2$. This implies that z lies inside the circle (2.2.1). □

Now suppose that $|\mathrm{Re}(z)| < \frac{1}{2}$ for simplicity. For each pair of relatively prime integers $m, n > 0$ with $(m, n) \neq (1, 1)$, there exist $a, b \in \mathbb{Z}$ such that $mb - na = 1$ and $-\frac{1}{2} < \frac{a}{m} < \frac{b}{n} < \frac{1}{2}$. Denote by $\lambda = \lambda(z) := mz - a$, $\lambda' = \lambda'(z) := nz - b$. Lemma 2.5 implies that for $z \in E$ with $|\mathrm{Re}(z)| < \frac{1}{2}$, $\mathcal{V}(z)$ is a hexagonal tiling such that $V(0)$ is adjacent to $V(\lambda)$, $V(\lambda')$, $V(\lambda + \lambda')$ and $\lambda, \lambda', \lambda + \lambda' \in \mathbb{H}$, if and only if z lies inside the circle $C(\frac{a}{m}, \frac{b}{n})$ and outside $C(\frac{a}{m}, \frac{a+b}{m+n})$ and $C(\frac{a+b}{m+n}, \frac{b}{n})$, that is, $z \in H_{m,n}$ where

$$H_{m,n} := \left\{ z \in \mathbb{H} : |\mathrm{Re}(z)| < \frac{1}{2}, \frac{\lambda'}{\lambda} \in \mathrm{i}\mathbb{H},\ \frac{\lambda + \lambda'}{\lambda}, \frac{\lambda'}{\lambda + \lambda'} \in -\mathrm{i}\mathbb{H} \right\}.$$

Figure 2.1 is the set of $z \in \mathbb{H} \cap \{|\mathrm{Re}(z)| < \frac{1}{2}\}$ that generate rectangular tilings of $\mathbb{C}$ (and $\mathbb{C}/\mathbb{Z}$). In the figure, (m, n) denotes the half-circle $C(\frac{a}{m}, \frac{b}{n}) \cap \mathbb{H}$, where a, b are integers such that $mb - na = 1$ and $-\frac{1}{2} < \frac{a}{m} < \frac{b}{n} < \frac{1}{2}$.

Figure 2.2 shows the *parastichy transition* of helical Voronoi tilings with the fixed divergence angle $\theta = 2\pi\tau$, $\tau = \frac{1+\sqrt{5}}{2}$, from a hexagonal tiling with opposed parastichy pairs $\{3, 5\}$, $\{5, 8\}$, through a rectangular tiling with an opposed parastichy pair $\{5, 8\}$, to a hexagonal tiling with opposed parastichy pairs $\{5, 8\}$, $\{8, 13\}$.

2.3 Parastichies and continued fraction expansions

In this section, we recall the continued fractions [22] and we show that opposed parastichy pairs of helical Voronoi tilings are drived by the continued fraction approximations of the divergence $x = \mathrm{Re}(z)$.

For $x \in \mathbb{R}$, let

$$x = a_0 + \cfrac{1}{a_1 + \cfrac{1}{a_2 + \cdots}} = [a_0, a_1, a_2, \cdots],\ a_0 \in \mathbb{Z},\ a_i \in \mathbb{Z}_+,\ i \geq 1$$

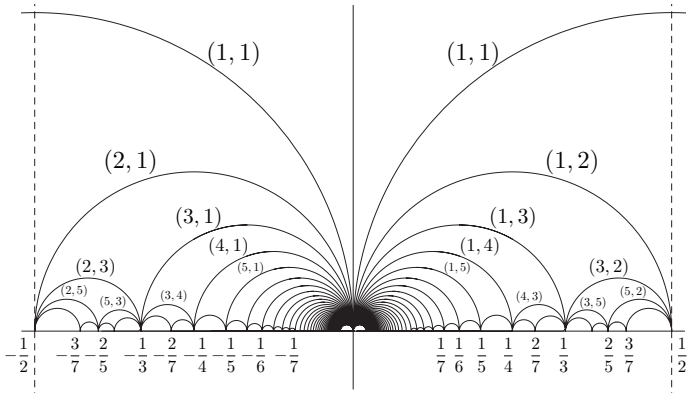

Figure 2.1: The set of generators $z \in \mathbb{H}$ of rectangular tilings, consisting of half circles. For each pair of relatively prime integers $m, n > 0$, there exist $a, b \in \mathbb{Z}$ such that $0 < a/m < b/n < 1$ and $mb - na = 1$. The half circle with the endpoints $a/m, b/n$, denoted by (m, n), is the set of generators $z \in \mathbb{H}$, $|\mathrm{Re}(z)| < \frac{1}{2}$, of rectangular tilings with an opposed parastichy pair $\{m, n\}$.

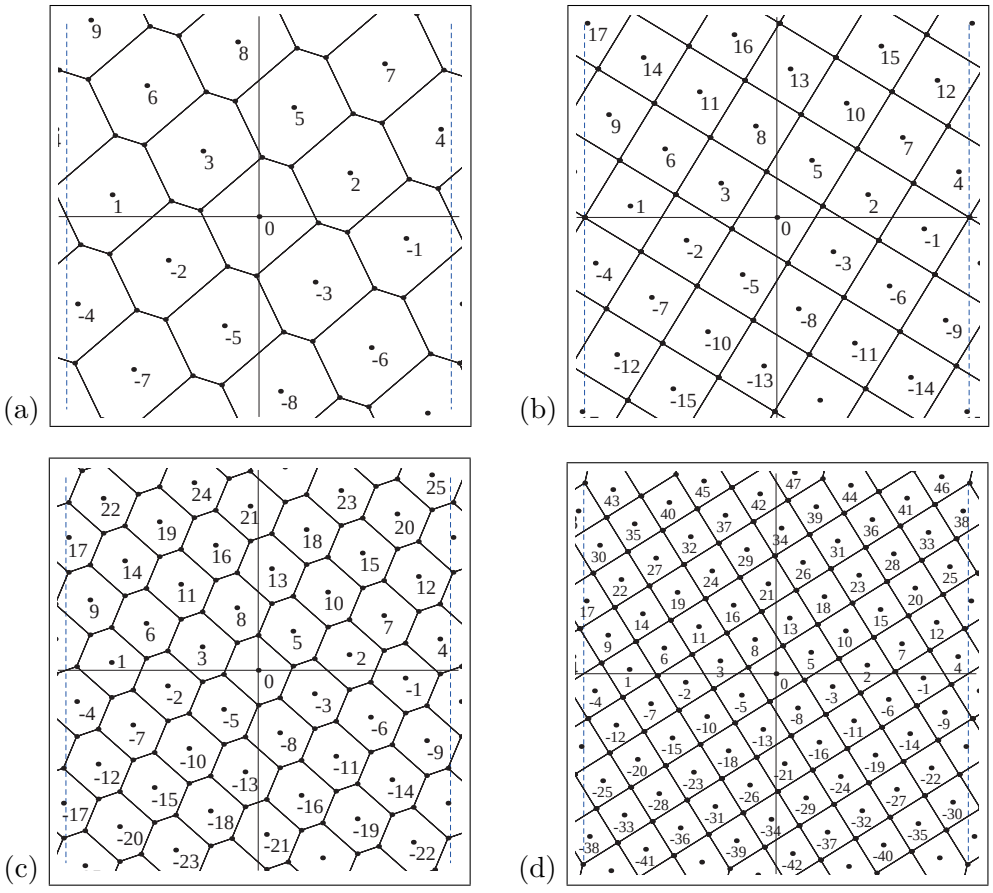

Figure 2.2: Helical Voronoi tilings generated by $z = (\tau - 2) + \mathrm{i}y$, where $\tau = \frac{1+\sqrt{5}}{2}$ is the golden section. The Fibonacci parastichy numbers are decreasing functions of $y > 0$. (a) $y = 0.056$, hexagonal tiling with opposed parastichy pairs $\{2, 3\}$, $\{5, 3\}$. (b) $y = 0.0296149\cdots$, rectangular tiling with an opposed parastichy pair $\{5, 3\}$. (c) $y = 0.02$, hexagonal tiling with opposed parastichy pairs $\{5, 3\}$, $\{5, 8\}$. (d) $y = 0.0112083\cdots$, rectangular tiling with an opposed parastichy pair $\{5, 8\}$.

be a continued fraction expansion of x, where $\mathbb{Z}_+$ denotes the set of positive integers. Define the following sequences. $\{p_j\}_{j\geq -1}$, $p_{-1}=1$, $p_0=a_0$, $p_1=a_0a_1+1$, $p_j=p_{j-2}+a_jp_{j-1}$, $j\geq 2$; $\{q_j\}_{j\geq -1}$, $q_{-1}=0$, $q_0=1$, $q_1=a_1$, $q_j=q_{j-2}+a_jq_{j-1}$, $j\geq 2$. Then

$$\frac{p_j}{q_j}=a_0+\cfrac{1}{a_1+\cfrac{1}{a_2+\cfrac{1}{\ddots+\frac{1}{a_j}}}}=[a_0,a_1,a_2,\cdots,a_j],\ j\geq 0$$

is called a *principal convergent* of x. Let $p_{j,k}=p_{j-1}+kp_j$ and $q_{j,k}=q_{j-1}+kq_j$, $j\geq 0$, $0\leq k\leq a_{j+1}$. Then

$$\frac{p_{j,k}}{q_{j,k}}=a_0+\cfrac{1}{a_1+\cfrac{1}{a_2+\cfrac{1}{\ddots+\frac{1}{a_j+\frac{1}{k}}}}}=[a_0,a_1,a_2,\cdots,a_j,k],\ j\geq 0,\ 0<k<a_{j+1}$$

is called an *intermediate converegent* of x. If $x\in\mathbb{Q}$, there are only finitely many convergents of x. Note that $p_{j,0}=p_{j-1}$, $q_{j,0}=q_{j-1}$, $p_{j,a_{j+1}}=p_{j+1}$, $q_{j,a_{j+1}}=q_{j+1}$.

Lemma 2.6. *Let $x\in\mathbb{R}\backslash\mathbb{Q}$. Suppose that a/m, b/n be irreducible fractions such that $a/m<x<b/n$, $mb-na=1$. Then a/m, b/n are principal or intermediate convergents of x, at least one of which is principal.*

Proof. This is a well-known result of the theory of numbers. For example, see Theorem 2.5, Theorem 2.6, the first part of Theorem 2.8 and Problem 2 (pp.153) in [68]. □

In the elementary numbers theory, a pair of rational numbers $a/m, b/n$ is called a *pair of convergents* of $x\in\mathbb{R}$ if $|bm-an|=1$ and either $a/m<x<b/n$ or $b/n<x<a/m$. It is known that if $a/m, b/n$ is a pair of convergents of x, then either $a=p_j$, $m=q_j$, $b=p_{j,k}$, $m=q_{j,k}$ with j even, or $a=p_{j,k}$, $m=q_{j,k}$, $b=p_j$, $n=q_j$ with j odd, and $0<k\leq a_{j+1}$.

Lemma 2.7. *Let $z=x+\mathrm{i}y\in\mathbb{Z}+E\cap\mathbb{H}$, and suppose that $\mathcal{V}(z)$ is a hexagonal tiling such that $V(0)$ is adjacent to $V(\lambda), V(\lambda'), V(\lambda+\lambda')$, where $\lambda=mz-a$, $\lambda'=nz-b$, $m,n>0$ and $mb-na=1$. Then $a/m, b/n$ are principal or intermediate convergents of x, at least one of which is principal.*

Proof. We have $mb-na=1$, and $a/m<x<b/n$ by Lemma 2.5. Hence, $a/m, b/n$ are a pair of convergents of x. □

2.4 Shape limit of rectangular helical Voronoi tilings

Fix an irrational number x such that $|x|<\frac{1}{2}$, and define the sequences a_j, q_j and $q_{j,k}$, $j\geq 0$, $0<k\leq a_{j+1}$, in Section 2.3. For each $j\geq 0$ and $0<k\leq a_{j+1}$, let $a_{j,k}/m_{j,k}<b_{j,k}/n_{j,k}$ be a pair of convergents of x such that $\{m_{j,k},n_{j,k}\}=\{q_j,q_{j,k}\}$. Denote by $C_{j,k}(x)=C(\frac{a_{j,k}}{m_{j,k}},\frac{b_{j,k}}{n_{j,k}})$. There exists a unique $y_{j,k}>0$ such that $z_{j,k}:=x+\mathrm{i}y_{j,k}\in C_{j,k}(x)$. Let $\lambda_{j,k}=m_{j,k}z_{j,k}-a_{j,k}$, $\lambda'_{j,k}=n_{j,k}z_{j,k}-b_{j,k}$. The ratio

$$R_{j,k}(x)=\frac{\lambda'_{j,k}}{\lambda_{j,k}}\in\mathrm{i}\mathbb{R}$$

is called a *shape parameter* of the tiling $\mathcal{V}(z_{j,k})$. It is defined as the aspect ratio, or the modulus, of the Delaunay polygon $\square(0,\lambda_{j,k},\lambda_{j,k}+\lambda'_{j,k},\lambda'_{j,k})$, which is the same as that of the rectangular tile $T(0)$ in $\mathcal{T}(z_{j,k})$.

Denote by $\langle\xi\rangle\in(-1/2,1/2]$ a fractional part of $\xi\in\mathbb{R}$, such that $[\![\xi]\!]:=\xi-\langle\xi\rangle$ is an integer which is the nearest to ξ. We have $\langle xm_{j,k}\rangle=xm_{j,k}-a_{j,k}=\mathrm{Re}(\lambda_{j,k})$, $\langle xn_{j,k}\rangle=xn_{j,k}-b_{j,k}=\mathrm{Re}(\lambda'_{j,k})$.

Lemma 2.8. $R_{j,k}(x) = \mathrm{i}\left(-\dfrac{q_{j,k}\langle xq_{j,k}\rangle}{q_j\langle xq_j\rangle}\right)^{(-1)^j/2}$

Proof. Since $\lambda'/\lambda \in \mathrm{i}\mathbb{R}$, we have

$$|\lambda_{j,k}|^2 \cdot \mathrm{Re}(\frac{\lambda'}{\lambda}) = (m_{j,k}x - a_{j,k})(n_{j,k}x - b_{j,k}) + m_{j,k}n_{j,k}y_{j,k}^2 = 0.$$

So we have

$$y_{j,k} = \left(-\frac{(m_{j,k}x - a_{j,k})(n_{j,k}x - b_{j,k})}{m_{j,k}n_{j,k}}\right)^{1/2},$$
$$|\lambda_{j,k}|^2 = (m_{j,k}x - a_{j,k})^2 + m_{j,k}^2 y_{j,k}^2 = \frac{m_{j,k}x - a_{j,k}}{n_{j,k}},$$

and hence

$$\mathrm{Im}(\frac{\lambda'_{j,k}}{\lambda_{j,k}}) = \frac{y_{j,k}^2}{|\lambda_{j,k}|^2} = \left(-\frac{n_{j,k}(n_{j,k}x - b_{j,k})}{m_{j,k}(m_{j,k}x - a_{j,k})}\right)^{1/2}.$$

□

Suppose that x is a quadratic irrational. Then it has a periodic continued fraction expansion

$$\begin{aligned} x &= [a_0, a_1, a_2, \dots] \\ &= [a_0, a_1, \dots, a_{j_0}, \overline{b_1, \cdots, b_d}] \\ &= [a_0, a_1, \dots, a_{j_0}, b_1, \dots, b_d, b_1, \cdots, b_d, \dots]. \end{aligned}$$

We may assume that j_0, d are even, by choosing bigger ones if necessary. For each $1 \le s \le d$, let $\omega_s = [\overline{b_s, \dots, b_d, b_1, \dots, b_{s-1}}]$ be a purely periodic continued fraction, and $h_s(x) = x^2 - \alpha_s x - \beta_s \in \mathbb{Q}[x]$ a quadratic polynomial such that $h_s(\omega_s) = 0$. Recall that the conjugate of ω_s is written as $\omega'_s := -1/[\overline{b_{s-1}, \dots, b_1, b_d, \dots, b_s}]$, that is, we have $h_s(\omega'_s) = 0$, see [19].

Let $\Omega(x) := \Omega(\{R_{j,k}(x)\}_{j,k})$ be the limit set, i.e., the set of the accumulation points, of $\{R_{j,k}(x)\}_{j,k}$.

Theorem 2.9. *If x is a quadratic irrational, the limit set $\Omega(x)$ is written as*

$$\Omega(x) = \left\{-\mathrm{i}h_{s+1}(k)^{(-1)^s/2} : 1 \le s \le d, 1 \le k \le b_s\right\}.$$

In particular, it is a finite set.

Proof. By using the continued fractions, we have

$$\frac{q_{j,k}}{q_j} = [k, a_j, a_{j-1}, \dots, a_1],\ -\frac{\langle xq_{j,k}\rangle}{\langle xq_j\rangle} = [a_{j+1} - k, a_{j+2}, a_{j+3}, \dots] \tag{2.4.1}$$

for $j \ge 0$, $0 < k \le a_{j+1}$. As $j \to +\infty$, they tend to the periodic sequence of continued fractions

$$[k, \overline{b_s, \dots, b_1, b_d, \dots, b_{s+1}}] \text{ and } [b_{s+1} - k, \overline{b_{s+2}, \dots, b_d, b_1, \dots, b_{s+1}}].$$

However, we have

$$\begin{aligned} &[k, \overline{b_s, \dots, b_1, b_d, \dots, b_{s+1}}] \cdot [b_{s+1} - k, \overline{b_{s+2}, \dots, b_d, b_1, \dots, b_{s+1}}] \\ &= (k - \omega'_{s+1})(-k + \omega_{s+1}) \\ &= -h_{s+1}(k) \end{aligned}$$

for $0 \le s < d$, $0 < k \le b_{s+1}$. This completes the proof. □

In the number theory of phyllotaxis [10], it is known that the most common divergences x are the quadratic irrationals such that $a_j = 1$ for sufficiently large j.

Corollary 2.10. *Let x be a quadratic irrational such that $a_j = 1$ for sufficiently large j. Then $\Omega(x) = \{\mathrm{i}\}$.*

Proof. The golden section has the purely periodic continued fraction expansion $\tau = [1, 1, \dots] = [1, \overline{1, 1}]$, and it is a root of a quadratic polynomial $h(x) = x^2 - x - 1$. Thus we have $-h(1) = 1$, and hence $\Omega(x) = \{\mathrm{i}\}$. □

In Figure 2.2 (b) and (d), the shape of the rectangle tiles is not the square because $R_{3,1}(2-\tau) = (0.9853\cdots)\mathrm{i}$ and $R_{4,1}(2-\tau) = (0.9944\cdots)\mathrm{i}$. The ratio $R_{j,1}(2-\tau)$ is close to i for sufficiently large j. That is, this implies that the shape of the rectangle tiles with a fixed divergence $x = \tau - 2$, as $y \to 0$, tend to the square.

Figure 2.3 shows helical Voronoi tilings generated by $z = (\frac{5+\sqrt{5}}{10}) + \mathrm{i}y$. The parastichy numbers are the Lucas numbers $1, 3, 4, 7, 11, 18, \cdots$, and these are decreasing functions of $y > 0$. Since $\frac{5+\sqrt{5}}{10}$ is a quadratic irrational which is a linearity equivalent of the golden section, the limit set is $\Omega(\frac{5+\sqrt{5}}{10}) = \{\mathrm{i}\}$, that is, the limit shape of rectangle tiles is the square.

Figure 2.4 shows helical Voronoi tilings generated by $z = (\sqrt{2}+1) + \mathrm{i}y$. $\sqrt{2}+1$ is called the *silver mean*, and its continued faction expansion is given by $\sqrt{2}+1 = [2, 2, 2, \cdots]$. The silver parastichy numbers $1, 2, 5, 7, 12, 19, \cdots$ are decreasing function of $y > 0$. The limit set is given by $\Omega(\sqrt{2}+1) = \{\mathrm{i}, \mathrm{i}\sqrt{2}, \mathrm{i}/\sqrt{2}\}$. That is, the limit shapes of the rectangle tiles are the square and the rectangle with the aspect ratio $1 : \sqrt{2}$.

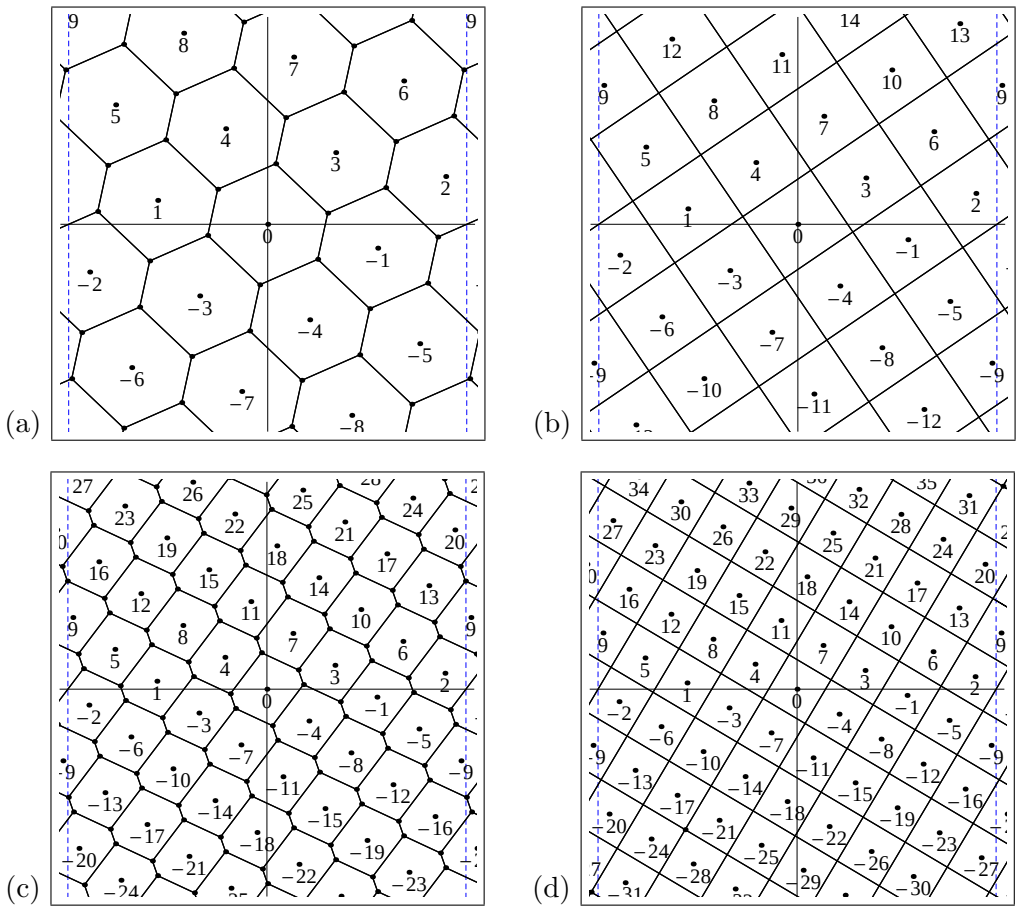

Figure 2.3: Helical Voronoi tilings generated by $z = (\frac{5+\sqrt{5}}{10}) + \mathrm{i}y$, (a) $y = 0.056$, hexagonal tiling with opposed parastichy pairs $\{1, 3\}$, $\{4, 3\}$. (b) $y = 0.0387664\cdots$, rectangular tiling with an opposed parastichy pair $\{4, 3\}$. (c) $y = 0.02$, hexagonal tiling with opposed parastichy pairs $\{4, 7\}$, $\{4, 3\}$. (d) $y = 0.0156848\cdots$, rectangular tiling with an opposed parastichy pair $\{4, 7\}$.

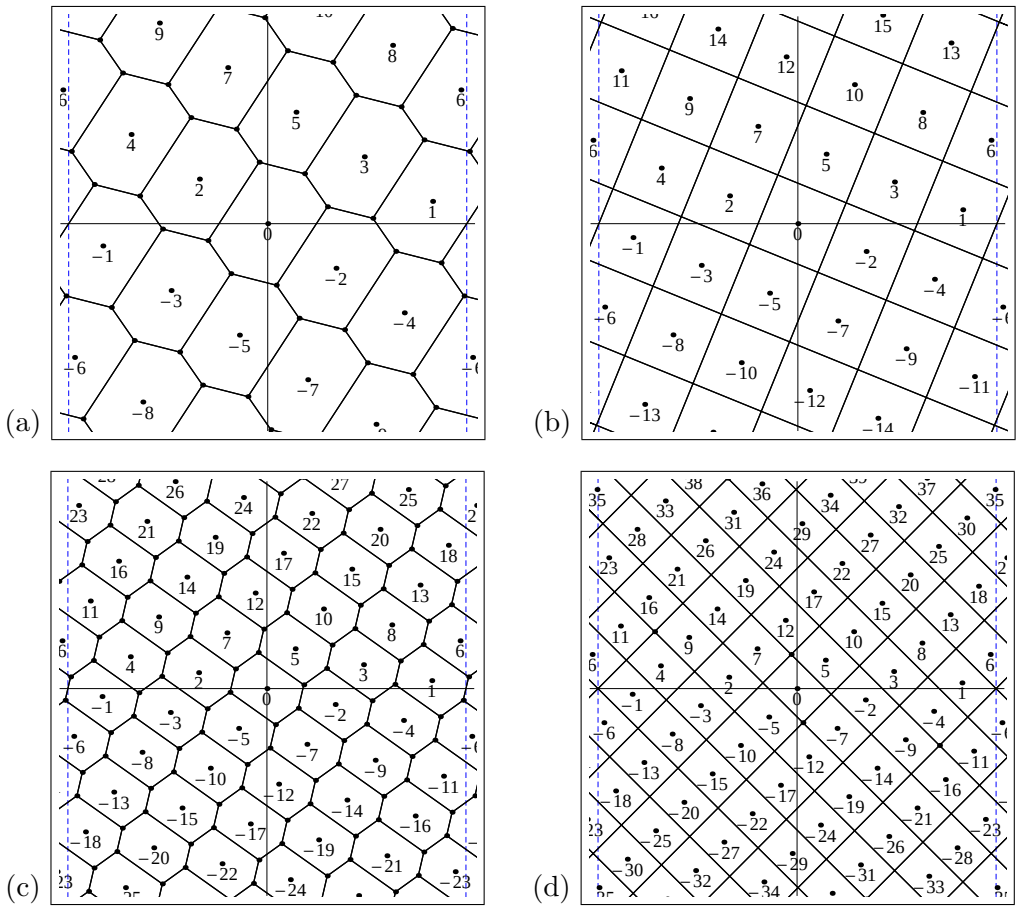

Figure 2.4: Helical Voronoi tilings generated by $z = (\sqrt{2}+1) + \mathrm{i}y$, (a) $y = 0.056$, hexagonal tiling with opposed parastichy pairs $\{2,3\}$, $\{2,5\}$. (b) $y = 0.0349189\cdots$, rectangular tiling with an opposed parastichy pair $\{2,5\}$. (c) $y = 0.02$, hexagonal tiling with opposed parastichy pairs $\{2,5\}$, $\{7,5\}$. (d) $y = 0.0142855\cdots$, rectangular tiling with an opposed parastichy pair $\{7,5\}$.

Part II

Voronoi spiral tilings

Chapter 3

Voronoi spiral tilings

3.1 Voronoi multiple tilings for spiral lattices

In this section, we consider a Voronoi multiple tiling as a tiling of a covering space of the punctured plane $\mathbb{C}^* = \mathbb{C}\backslash\{0\}$.

Let $C_v := \mathbb{C}/2\pi v\mathrm{i}\mathbb{Z}$ be a cylinder, where $v \neq 0$ is an integer. By the exponential function $\exp : C_v \to \mathbb{C}^*$ which maps $w+2\pi v\mathrm{i}\mathbb{Z}$ to $z = e^w$, C_v is a covering space of degree $|v|$ of $\mathbb{C}^*$. Let M_v be a covering space of $\mathbb{C}^*$ of degree $|v|$ such that the exponential function is an isomorphism of the additive group C_v onto the multiplicative group M_v. By the canonical projection $p : M_v \to \mathbb{C}^*$, the Euclidean metric on $\mathbb{C}^*$ is induced into M_v, so that p is a local isometry. Thus M_v is a metric space with the distance function

$$\mathrm{dist}(\zeta_0, \zeta_1) = \inf\{\int_0^1 |\phi'(t)|\, dt : \phi : [0,1] \to M_v, \phi(0) = \zeta_0, \phi(1) = \zeta_1\},$$

$\zeta_0, \zeta_1 \in M_v$. For $\zeta \in M_v$, denote by $\|\zeta\| := |p(\zeta)|$. Let $\arg(\zeta) \in (-|\pi v|, |\pi v|]$ be an argument of $\zeta \in M_v$. A tiling of M_v is called a *multiple tiling* of multiplicity $|v|$.

Let $U := \{\zeta \in M_v : -\pi < \arg(\zeta) < \pi\} \subset M_v$. Let $s : \mathbb{C}\backslash\mathbb{R}_- \to U$ be a continuous map such that $p \circ s = \mathrm{id}$ and $s(1) = 1$, where $\mathbb{R}_- = \{x \in \mathbb{R} : x \leq 0\}$. If $\zeta \in U$, $p(\zeta)$ is often identified with ζ. For $\zeta \in M_v$, $U\zeta$ is a neighborhood of ζ which is isometric to $\mathbb{C}\backslash\mathbb{R}_-$. For two points $\zeta_0, \zeta_1 \in M_v$ with $\zeta_1 \in U\zeta_0$, we can define a straight line segment $\ell(\zeta_0, \zeta_1) \subset M_v$ joining ζ_0, ζ_1.

Let $\zeta = r\mathrm{e}^{\mathrm{i}\theta} \in M_v$ with $0 < r < 1$ and $0 < |\theta| < |\pi v|$. Let $S = \{\zeta^j\}_{j\in\mathbb{Z}}$ be a spiral sequence of M_v generated by a single element $\zeta \in M_v$. Note that, in the complete metric space $\overline{M_v} = M_v \cup \{0\}$, the origin is an accumulation point of S. Suppose that

$$S \cap H_+ \neq \emptyset, \tag{3.1.1}$$

where $H_+ := s(\{z \in \mathbb{C} : \mathrm{Im}(z) > 0\})$ is an upper half-plane embedded in M_v. Note that the condition (3.1.1) is independent of r, see Lemma 3.5. Let

$$T_j = T(\zeta^j, S) := \{\xi \in M_v : \mathrm{dist}(\xi, \zeta^j) \leq \mathrm{dist}(\xi, \zeta^k), \forall k \neq j\} \tag{3.1.2}$$

be *the Voronoi region* for *the site* ζ^j, $j \in \mathbb{Z}$. By the assumption (3.1.1), it is not difficult to see that the following conditions hold for $j, k \in \mathbb{Z}$.

(i) $T_j \subset H\zeta^j$, where $H = s(\{z \in \mathbb{C} : \mathrm{Re}(z) > \frac{1}{2}\})$.

(ii) If $\zeta^k \notin U\zeta^j$, then $T_j \cap T_k = \emptyset$.

(iii) T_j is a bounded polygon.

Thus we obtain a polygonal tiling $\mathcal{T} := \{T_j\}_{j\in\mathbb{Z}}$ of M_v, which is called a *Voronoi spiral multiple tiling* with multiplicity $|v|$.

Two distinct Voronoi regions T_j, T_k are called *adjacent* if the intersection $T_j \cap T_k \subset M_v$ contains at least two points. In fact, if two distinct polygonal regions T_j, T_k are adjacent, $T_j \cap T_k$ is a line segment of positive length. If T_0 is adjacent to T_m, the multiplicative symmetry of S implies that T_j is adjacent to T_{j+m} for all $j \in \mathbb{Z}$. In the phyllotaxis theory, the pair $\{m, n\}$ of positive integers is called the *opposed parastichy pair* if T_0 is adjacent to T_m, T_n and $\arg(\zeta^m)\arg(\zeta^n) < 0$; the pair $\{m, n\}$ is called the *non-opposed parastichy pair* if T_0 is adjacent to T_m, T_n and $\arg(\zeta^m)\arg(\zeta^n) > 0$.

A dual of a Voronoi diagram is called a Delaunay diagram. If T_j is adjacent to T_k, the line segment $\ell(\zeta^j, \zeta^k) \subset U\zeta^j$ joining the sites ζ^j and ζ^k is called a *Delaunay edge*. Denote the set of Delaunay edges for the site set S by $\mathcal{E}$. A *Delaunay polygon* is a connected component of the complement in M_v of the union of the Delaunay edges. An important property is that two Delaunay edges have a point in common only at their endpoint. Thus a line segment is a side of a Delaunay polygon if and only if it is a Delaunay edge. A finite set $S' \subset S$ is equal to the set of the corners of a Delaunay polygon if and only if there exists a disk $D \subset M_v$ such that $\partial D \cap S = S'$ and $\mathrm{int}(D) \cap S = \emptyset$. Hence each Delaunay polygon is inscribed in a circle.

For distinct $a_1, a_2, a_3 \in \mathbb{C}$, let

$$\angle(a_1, a_2, a_3) := \mathrm{Arg}\left(\frac{a_1 - a_2}{a_3 - a_2}\right),$$

where $-\pi < \mathrm{Arg}(z) \le \pi$ denotes the principal argument of $z \in \mathbb{C}^*$. For distinct $\alpha_1, \alpha_2, \alpha_3 \in M_v$ with $\alpha_1, \alpha_2, \alpha_3 \in U\alpha_1 \cap U\alpha_2 \cap U\alpha_3$, let

$$\angle(\alpha_1, \alpha_2, \alpha_3) := \angle(p(\alpha_1), p(\alpha_2), p(\alpha_3)).$$

Lemma 3.1. *Let $\zeta = re^{i\theta} \in M_v$ with $0 < r < 1$, and suppose the condition (3.1.1). Let $\mathcal{T} := \{T_j\}_{j\in\mathbb{Z}}$ be a Voronoi tiling of M_v with the site set $S = \{\zeta^j\}_{j\in\mathbb{Z}}$. Let $j \ne k \in \mathbb{Z}$, and suppose that $\zeta^k \in U\zeta^j$. Then the following conditions are mutually equivalent.*

(i) The Voronoi regions T_j, T_k are adjacent.

(ii) The line segment $\ell(\zeta^j, \zeta^k)$ is a Delaunay edge.

(iii) There exists a disk $D \subset U\zeta^j$ such that $\partial D \cap S = \{\zeta^j, \zeta^k\}$ and $\mathrm{int}(D) \cap S = \emptyset$.

(iv) For any $\zeta^{i_1}, \zeta^{i_2} \in U\zeta^j \cap U\zeta^k$, we have

$$\angle(\zeta^j, \zeta^{i_1}, \zeta^k) + \angle(\zeta^k, \zeta^{i_2}, \zeta^j) < \pi \tag{3.1.3}$$

whenever $\angle(\zeta^j, \zeta^{i_1}, \zeta^k) > 0$ and $\angle(\zeta^k, \zeta^{i_2}, \zeta^j) > 0$.

Proof. (i) $\Leftrightarrow$ (ii): Obvious.

(iii) $\Leftrightarrow$ (iv): Obvious.

(ii) $\Rightarrow$ (iv): A Delaunay edge $\ell(\zeta^j, \zeta^k)$ is a side of two Delaunay polygons, say W_1, W_2. Let $\zeta^\alpha \notin \{\zeta^j, \zeta^k\}$ be a corner of W_1. We may suppose that $\angle(\zeta^j, \zeta^\alpha, \zeta^k) > 0$ without loss of generality. Any $\zeta^{i_2} \in U\zeta^j \cap U\zeta^k$ with $\angle(\zeta^j, \zeta^{i_2}, \zeta^k) < 0$ is out of the circumscribed circle of W_1, so we have $\angle(\zeta^j, \zeta^\alpha, \zeta^k) + \angle(\zeta^k, \zeta^{i_2}, \zeta^j) < \pi$. For any $\zeta^{i_1} \in U\zeta^j \cap U\zeta^k$ with $\angle(\zeta^j, \zeta^{i_1}, \zeta^k) > 0$, we have $\angle(\zeta^j, \zeta^{i_1}, \zeta^k) \le \angle(\zeta^j, \zeta^\alpha, \zeta^k)$. Thus we obtain 3.1.3.

(iv) $\Rightarrow$ (ii): Suppose that $\ell(\zeta^j, \zeta^k)$ is not a Delaunay edge. If ζ^j, ζ^k are corners of a Delaunay polygon W, then there exist $\zeta^{i_1}, \zeta^{i_2} \notin \{\zeta^j, \zeta^k\}$ which are corners of W, such that $\angle(\zeta^j, \zeta^{i_1}, \zeta^k) > 0$ and $\angle(\zeta^k, \zeta^{i_2}, \zeta^j) > 0$. In this case we have

$$\angle(\zeta^j, \zeta^{i_1}, \zeta^k) + \angle(\zeta^k, \zeta^{i_2}, \zeta^j) = \pi$$

since W is inscribed in a circle.

If ζ^j, ζ^k are not corners of a same Delaunay polygon, then the line segment $\ell(\zeta^j, \zeta^k)$ intersects some Delaunay edge $\ell(\zeta^{i_1}, \zeta^{i_2})$. We may suppose that $\angle(\zeta^{i_1}, \zeta^k, \zeta^{i_2})$, $\angle(\zeta^{i_2}, \zeta^j, \zeta^{i_1}) > 0$ without loss of generality. This implies that

$$\angle(\zeta^j, \zeta^{i_1}, \zeta^k),\ \angle(\zeta^k, \zeta^{i_2}, \zeta^j) > 0.$$

Since we have already shown that (ii) $\Rightarrow$ (iv), we obtain

$$\angle(\zeta^{i_1}, \zeta^k, \zeta^{i_2}) + \angle(\zeta^{i_2}, \zeta^j, \zeta^{i_1}) < \pi,$$

and hence $\angle(\zeta^j, \zeta^{i_1}, \zeta^k) + \angle(\zeta^k, \zeta^{i_2}, \zeta^j) \geq \pi$. This completes the proof. □

Lemma 3.2. *Let $\zeta = r\mathrm{e}^{\mathrm{i}\theta} \in M_v$ with $0 < r < 1$. Let $m, n > 0$ be positive integers. Suppose that $\zeta^m, \zeta^n \in U$, and $\square(\zeta^m, \zeta^{m+n}, \zeta^n, 1)$ is a quadrilateral in this order of vertices. If $\arg(\zeta^m)\arg(\zeta^n) \geq 0$, then we have*

$$|\angle(\zeta^m, \zeta^{m+n}, \zeta^n)| + |\angle(\zeta^n, 1, \zeta^m)| < \pi. \tag{3.1.4}$$

Proof. We may assume that $0 \leq \arg(\zeta^m), \arg(\zeta^n) < \pi$ without loss of generality, and we assume that $\angle(\zeta^m, \zeta^{m+n}, \zeta^n)$, $\angle(\zeta^n, 1, \zeta^m) > 0$. We have

$$\begin{aligned}\angle(\zeta^m, \zeta^{m+n}, \zeta^n) + \angle(\zeta^n, 1, \zeta^m) &= \angle(\zeta^{-n}, 1, \zeta^{-m}) + \angle(\zeta^n, 1, \zeta^m)\\ &\leq \angle(2, 1, \zeta^{-m}) + \angle(0, 1, \zeta^m)\\ &< \angle(2, 1, \mathrm{e}^{-m\theta}) + \angle(0, 1, \mathrm{e}^{m\theta}) = \pi.\end{aligned}$$

□

Lemma 3.3. *Let $\zeta = r\mathrm{e}^{\mathrm{i}\theta} \in M_v$, and suppose that $0 < r < 1$, $0 < |\theta| < |\pi v|$ and (3.1.1) for $S = \{\zeta^j\}_{j\in\mathbb{Z}}$. Let $\mathcal{T} := \{T_j\}_{j\in\mathbb{Z}}$ be a Voronoi tiling of M_v with the site set S. Then there exist $m, n > 0$ such that $\{m, n\}$ is an opposed parastichy pair of $\mathcal{T}$, and $T_0 \cap T_{m+n} \neq \emptyset$. If T_0 is adjacent to T_{m+n}, then it is a hexagon; if T_0 is not adjacent to T_{m+n}, then it is a quadrilateral.*

Proof. If T_0 is adjacent to T_m for some m, then by the multiplicative symmetry of S, T_0 is also adjacent to T_{-m}. A bounded polygon T_0 has at least three sides, so there exists $n > 0$, $n \neq m$, such that T_0 is also adjacent to $T_{\pm n}$. The Delaunay diagram contains the Delaunay edges $\ell(\zeta^j, \zeta^{j+m}), \ell(\zeta^j, \zeta^{j+n})$, $j \in \mathbb{Z}$, which form a lattice. In the quadrilateral $\square(1, \zeta^m, \zeta^{m+n}, \zeta^n)$ surrounded by Delaunay edges, there are three possibilities.

(i) $\square(1, \zeta^m, \zeta^{m+n}, \zeta^n)$ is a Delaunay polygon,

(ii) $\ell(1, \zeta^{m+n})$ is a Delaunay edge and the triangles

$$\triangle(\zeta^m, \zeta^{m+n}, 1),\ \triangle(1, \zeta^{m+n}, \zeta^n)$$

are Delaunay polygons, or

(iii) $\ell(\zeta^m, \zeta^n)$ is a Delaunay edge and the triangles

$$\triangle(\zeta^m, \zeta^n, 1),\ \triangle(\zeta^m, \zeta^{m+n}, \zeta^n)$$

are Delaunay polygons.

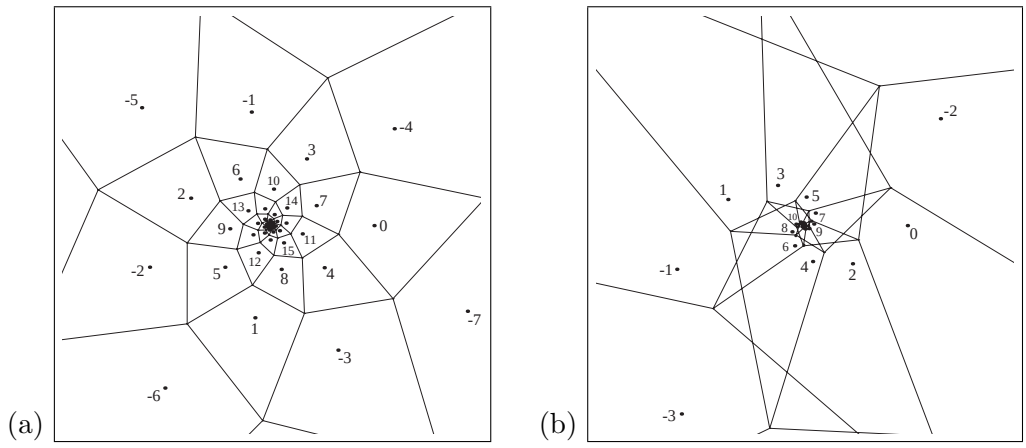

Figure 3.1: (a) A Voronoi spiral tiling with an opposed parastichy pair $\{7, 4\}$. The generator $\zeta = (0.9011\cdots)\exp(2\pi\mathrm{i}\cdot(5+\sqrt{5})/10)$ is marked $\star_1$ in Figure 3.4. (b) A Voronoi spiral multiple tiling of multiplicity $v = 2$, with an opposed parastichy pair $\{7, 4\}$. The generator $\zeta = (0.7730\cdots)\exp(2\pi\mathrm{i}/\sqrt{5})$ is marked $\star_2$ in Figure 3.4.

If $\arg(\zeta^m)\arg(\zeta^n) \geq 0$, we have (3.1.4) by Lemma 3.2, and so $\ell(\zeta^m, \zeta^n)$ is a Delaunay edge. This implies that if $\ell(1, \zeta^{m+n})$ is a Delaunay edge, we have $\arg(\zeta^m)\arg(\zeta^n) < 0$, and so $\{m, n\}$ is an opposed parastichy pair of $\mathcal{T}$, where T_0 is a hexagon which is adjacent to $T_{\pm m}, T_{\pm n}$ and $T_{\pm(m+n)}$.

If $\square(1, \zeta^m, \zeta^{m+n}, \zeta^n)$ is a Delaunay polygon, then we have $\arg(\zeta^m)\arg(\zeta^n) < 0$ again, and so $\{m, n\}$ is an opposed parastichy pair of $\mathcal{T}$. If this is the case, the intersection $T_0 \cap T_{m+n}$ consists of a point which is the center of the circumscribed circle of $\square(1, \zeta^m, \zeta^{m+n}, \zeta^n)$.

If $\ell(\zeta^m, \zeta^n)$ is a Delaunay edge, then T_0 is adjacent to $T_{\pm(m-n)}$. If we denote by $m' = \min(m, n)$, $n' = |m - n|$, the tile T_0 is a hexagon which is adjacent to $T_{\pm m'}$, $T_{\pm n'}$ and $T_{\pm(m'+n')}$. This completes the proof. □

Figure 3.1 shows two examples of Voronoi spiral (multiple) tilings with an opposed parastichy pair $\{4, 7\}$. Their generators are marked in Figure 3.4.

3.2 Parastichy transitions of Voronoi spiral tilings

Lemma 3.4. *Let $\zeta = re^{\mathrm{i}\theta} \in M_v$, and suppose that $0 < r < 1$, $0 < |\theta| < |\pi v|$ and (3.1.1). Let $\{m, n\}$ be an opposed parastichy pair of a Voronoi tiling $\mathcal{T} := \{T_j\}_{j\in\mathbb{Z}}$ of M_v generated by $S = \{\zeta^j\}_{j\in\mathbb{Z}}$. Let $a = [\![\frac{m\theta}{2\pi v}]\!]$, $b = [\![\frac{n\theta}{2\pi v}]\!]$. Then $\frac{a}{m}, \frac{b}{n}$ are a pair of convergents of $\frac{\theta}{2\pi v}$.*

Proof. Since $\{m, n\}$ is an opposed parastichy pair, we may suppose that $-\pi < \arg(\zeta^n) < 0 < \arg(\zeta^m) < \pi$, without loss of generality. Since $\arg(\zeta^n) = n\theta - 2\pi bv$, $\arg(\zeta^m) = m\theta - 2\pi av$, we obtain $\frac{a}{m} < \frac{\theta}{2\pi v} < \frac{b}{n}$.

The sides of the quadrilateral $W_0 = \square(1, \zeta^m, \zeta^{m+n}, \zeta^n)$ are Delaunay edges. By the multiplicative symmetry of S, the family of quadrilaterals

$$\{\zeta^j W_0\}_{j\in\mathbb{Z}} = \{\square(\zeta^j, \zeta^{j+m}, \zeta^{j+m+n}, \zeta^{j+n})\}_{j\in\mathbb{Z}}$$

is a tiling of M_v. Let

$$\begin{aligned}
\xi &:= \log r + \mathrm{i}\theta \in \log(\zeta),\\
\xi_m &:= m\log r + \mathrm{i}(m\theta - 2\pi av) \in \log(\zeta^m),\\
\xi_n &:= n\log r + \mathrm{i}(n\theta - 2\pi bv) \in \log(\zeta^n).
\end{aligned}$$

Let W_0' be a connected component of $\log(W_0) \subset \mathbb{C}$ which has corners $0, \xi_m, \xi_m + \xi_n, \xi_n$. Since M_v is connected, ξ is contained in the lattice $\xi_m\mathbb{Z} + \xi_n\mathbb{Z}$ in $\mathbb{C}$ and we have $\xi = k_1\xi_m + k_2\xi_n$ for some

$k_1, k_2 \in \mathbb{Z}$. Hence m, n are relatively prime, and we have

$$(\xi_m\mathbb{Z} + \xi_n\mathbb{Z}) \cap \mathrm{i}\mathbb{R} = \{k(n\xi_m - m\xi_n)\}_{k\in\mathbb{Z}} = 2\pi v(mb - na)\mathrm{i}\mathbb{Z}.$$

However, $\{(k_1\xi_m + k_2\xi_n)W_0' \mod 2v\pi\mathrm{i}\}_{k_1,k_2\in\mathbb{Z}}$ is a tiling of the cylinder $C_v = \mathbb{C}/2v\pi\mathrm{i}\mathbb{Z}$ by the assumption. Thus we obtain $mb - na = 1$. □

A (principal or intermediate) convergent $\frac{a}{m}$ of $x = \frac{\theta}{2\pi v}$ is called *admissible* if

$$0 < \left|\frac{\theta}{2\pi v} - \frac{a}{m}\right| < \left|\frac{1}{2mv}\right|, \tag{3.2.1}$$

i.e., $0 < |m\theta - 2\pi av| < \pi$. Let $H_+ := s(\{z \in \mathbb{C} : \mathrm{Im}(z) > 0\})$, $H_- := s(\{z \in \mathbb{C} : \mathrm{Im}(z) < 0\})$ be half-planes in M_v.

Lemma 3.5. *Let $v \neq 0$ be an integer. For $0 < |\theta| < |\pi v|$, the following conditions are mutually equivalent.*

(i) $\theta/2\pi v$ has a pair of convergents that are both admissible.

(ii) For any $r > 0$, we have $S \cap H_+ \neq \emptyset$, where $S = \{\zeta^j\}_{j\in\mathbb{Z}}$, $\zeta = r\mathrm{e}^{\mathrm{i}\theta} \in M_v$.

(iii) $k\theta \notin 2\pi v\mathbb{Z}$ for $k = 1, \ldots, |2v|$.

Proof. If $\frac{\theta}{2\pi v}$ is an irrational number, then it is easy to see that all of the conditions (i), (ii) and (iii) hold.

If $\frac{\theta}{2\pi v}$ is a rational number, there exists a pair of convergents $\frac{a}{m} < \frac{b}{n}$ of $\theta/2\pi v$ such that $\frac{\theta}{2\pi v} = \frac{a+b}{m+n}$. If $v > 0$, we see the equivalence: (3.2.1) $\Leftrightarrow m\theta - 2\pi av < \pi$, $-\pi < n\theta - 2\pi bv \Leftrightarrow m + n > 2v \Leftrightarrow \frac{k\theta}{2\pi v} \notin \mathbb{Z}$ for $0 < k \leq 2v$. The case $v < 0$ is similarly shown. □

Let $m_0 = \min\{m > 0 : \zeta^m \in H_+\}$, $n_0 = \min\{n > 0 : \zeta^n \in H_-\}$, $a_0 = [\![\frac{m_0\theta}{2\pi v}]\!]$, $b_0 = [\![\frac{n_0\theta}{2\pi v}]\!]$. Then $\frac{a_0}{m_0} < \frac{b_0}{n_0}$ is a pair of convergents of $x = \frac{\theta}{2\pi v}$ that are both admissible.

Lemma 3.6. *Let $v \neq 0$ be an integer. Let $\zeta = r\mathrm{e}^{\mathrm{i}\theta} \in M_v$ with $0 < r < 1$ and $0 < |\theta| < |\pi v|$, and assume the condition (3.1.1). Let $\mathcal{T} := \{T_j\}_{j\in\mathbb{Z}}$ be a Voronoi tiling of M_v generated by $S = \{\zeta^j\}_{j\in\mathbb{Z}}$. If r is small, T_0 is adjacent to $T_{\pm m_0}$, $T_{\pm n_0}$ and $T_{\pm(m_0+n_0)}$.*

Proof. If $j > 0$ and $\zeta^j \in U\zeta^{m_0} \cup U$, then the minimality of m_0 and the multiplicative symmetry of S imply that $j \geq m_0$. Since r is small, we have

$$\angle(\zeta^{m_0}, \zeta^j, 1) < \angle(p(\zeta^{m_0}), 0, 1) + \varepsilon,$$

where $\varepsilon > 0$ is a sufficiently small. If $k < 0$ and $\zeta^k \in U \cap U\zeta^{m_0}$, then we have

$$|\angle(1, \zeta^k, \zeta^{m_0})| = |\angle(\zeta^{-k}, 1, \zeta^{m_0-k})| < \varepsilon$$

because $\|\zeta^{-k}\|, \|\zeta^{m_0-k}\|$ are small. Therefore, we have

$$\angle(\zeta^{m_0}, \zeta^j, 1) + \angle(1, \zeta^k, \zeta^{m_0}) < \angle(p(\zeta^{m_0}), 0, 1) + 2\epsilon < \pi$$

for any $\zeta^j, \zeta^k \in U \cap U\zeta^{m_0}$ with $\angle(\zeta^{m_0}, \zeta^j, 1), \angle(1, \zeta^k, \zeta^{m_0}) > 0$. By Lemma 3.1, $\ell(1, \zeta^{m_0})$ is a Delaunay edge, and hence T_0 is adjacent to T_{m_0}. The argument for the Delaunay edge $\ell(1, \zeta^{n_0})$ is similar.

There are three possibilities:

(i) $\ell(1, \zeta^{m_0+n_0})$ is an Delaunay edge,

(ii) $\ell(\zeta^{m_0}, \zeta^{n_0})$ is an Delaunay edge, or

(iii) $\square(1, \zeta^{m_0}, \zeta^{m_0+n_0}, \zeta^{n_0})$ is a Delaunay polygon.

By the minimality condition of m_0, n_0 and the multiplicative symmetry of S, we have $\zeta^{m_0} \notin H_+\zeta^{n_0}$ or $\zeta^{n_0} \notin H_-\zeta^{m_0}$, which are mutually equivalent. Thus $\square(\zeta^{m_0}, 0, \zeta^{n_0}, 1)$ and $\square(1, \zeta^{m_0}, \zeta^{m_0+n_0}, \zeta^{n_0})$ are concave quadrilaterals, and we have

$$\angle(1, \zeta^{m_0}, \zeta^{m_0+n_0}) + \angle(\zeta^{m_0+n_0}, \zeta^{n_0}, 1) < \pi.$$

Hence $\ell(1, \zeta^{m_0+n_0})$ is a Delaunay edge. □

We fix θ, $0 < |\theta| < |\pi v|$, and denote by $\zeta(r) := re^{i\theta} \in M_v$, $0 < r < 1$. Let $S(r) := \{\zeta(r)^j\}_{j\in\mathbb{Z}}$. Let $\mathcal{T}(r) := \{T_j(r)\}_{j\in\mathbb{Z}}$ be the corresponding Voronoi tiling. Let

$$\Lambda = \{0 < r < 1 : T_0(r) \text{ is a quadrilateral}\}.$$

Lemma 3.7. *Fix v and θ, and suppose that $0 < |\theta| < |\pi v|$. Let $\zeta = \rho e^{i\theta}$, $0 < \rho < 1$. Suppose that the tiling $\mathcal{T}(\rho)$ has an opposed parastichy pair $\{m, n\}$ and a Delaunay polygon $\square(\zeta(\rho)^m, \zeta(\rho)^{m+n}, \zeta(\rho)^n, 1)$. Then there exists a small $\varepsilon > 0$ such that the followings hold.*

(i) For $r \in (\rho, \rho + \varepsilon)$, the tile $T_0(r)$ in $\mathcal{T}(r)$ is adjacent to $T_{\pm m}(r)$, $T_{\pm n}(r)$ and $T_{\pm(m+n)}(r)$.

(ii) For $r \in (\rho - \varepsilon, \rho)$, the tile $T_0(r)$ in $\mathcal{T}(r)$ is adjacent to $T_{\pm m}(r)$, $T_{\pm n}(r)$ and $T_{\pm(m-n)}(r)$.

Proof. We may suppose that $-\pi < \arg(\zeta(\rho)^n) < 0 < \arg(\zeta(\rho)^m) < \pi$ without loss of generality. Since Lemma 3.1 (iv) is an open condition, $\ell(1, \zeta(r)^m)$ and $\ell(1, \zeta(r)^n)$ are Delaunay edges if r is close to ρ. The sum of the angles

$$\begin{aligned} \phi(r) &:= \angle(1, \zeta(r)^m, \zeta(r)^{m+n}) + \angle(\zeta(r)^{m+n}, \zeta(r)^n, 1) \\ &= \angle(\zeta(r)^{-m}, 1, \zeta(r)^n) + \angle(\zeta(r)^m, 1, \zeta(r)^{-n}) \end{aligned} \tag{3.2.2}$$

is a decreasing function of r. Therefore, for $\rho < r < \rho + \varepsilon$ with $\varepsilon > 0$ small, we have $\phi(r) < \phi(\rho) = \pi$, and hence $\ell(1, \zeta(r)^{m+n})$ is a Delaunay edge. For $\rho - \epsilon < r < \rho$, we have $\phi(r) > \pi$, and so $\ell(\zeta(r)^m, \zeta(r)^n)$ is a Delaunay edge. □

In Lemma 3.7, the opposed parastichy pair $\{m, n\}$ is called an *extension* of the opposed parastichy pair $\{|m - n|, \min(m, n)\}$, and the pair $\{|m - n|, \min(m, n)\}$ is called a *contraction* of $\{m, n\}$. Lemma 3.7 implies that Λ is a discrete subset of the open interval $(0, 1)$.

Lemma 3.8. *Let $0 < \rho < 1$, and suppose that the tiling $\mathcal{T}(\rho)$ has opposed parastichy pairs $\{m, n\}$ and $\{m + n, n\}$. Then there exists $\rho' \in (\rho, 1)$ such that the followings hold.*

(i) For each $r \in [\rho, \rho')$, the tiling $\mathcal{T}(r)$ has opposed parastichy pairs $\{m, n\}$ and $\{m + n, n\}$.

(ii) The tiling $\mathcal{T}(\rho')$ has an opposed parastichy pair $\{m + n, n\}$, and $T_0(\rho')$ is a quadrilateral.

Proof. Without loss of generality we may assume that

$$-\pi < \arg(\zeta(\rho)^n) < 0 < \arg(\zeta(\rho)^{m+n}) < \arg(\zeta(\rho)^m) < \pi$$

and $\angle(\zeta(\rho)^m, \zeta(\rho)^{m+n}, \zeta(\rho)^n), \angle(\zeta(\rho)^n, 1, \zeta(\rho)^m) > 0$. Let

$$\rho' := \sup\{r \geq \rho : \ell(1, \zeta(r)^j) \in \mathcal{E}(r),\ j = m, n, m + n\},$$

where $\mathcal{E}(r)$ denotes the set of the Delaunay edges for the site set $S(r)$. Since

$$\angle(\zeta(1)^m, \zeta(1)^{m+n}, \zeta(1)^n) < 0,$$

there exist $r' \in (\rho, 1)$ such that

$$\angle(\zeta(r')^m, \zeta(r')^{m+n}, \zeta(r')^n) < 0,$$

where $\zeta(r')^{m+n}$ lands on the line segment $\ell(1, \zeta(r')^m)$. Then, $\ell(1, \zeta(r')^m)$ is not a Delaunay edge, and we obtain $\rho' < 1$.

There are three possibilities:

(i) $\ell(1, \zeta(\rho')^m) \notin \mathcal{E}(\rho')$,

(ii) $\ell(1, \zeta(\rho')^{m+n}) \notin \mathcal{E}(\rho')$, or

(iii) $\ell(1, \zeta(\rho')^n) \notin \mathcal{E}(\rho')$.

Since $\mathcal{T}(\rho')$ has an opposed parastichy pair by Lemma 3.3, we have $\ell(1, \zeta(\rho')^n) \in \mathcal{E}(\rho')$. Since the sum of the angles $\phi(r)$ given in (3.2.2) is a decreasing function of $0 < r < 1$, we have $\phi(\rho') < \phi(\rho) < \pi$, and hence $\ell(1, \zeta(\rho')^{m+n}) \in \mathcal{E}(\rho')$. Therefore, we have $\ell(1, \zeta(\rho')^m) \notin \mathcal{E}(\rho')$. Hence $\square(1, \zeta(\rho')^{m+n}, \zeta(\rho')^{m+2n}, \zeta(\rho')^n)$ is a Delaunay polygon. □

The following is a converse of Lemma 3.4.

Proposition 3.9. *Fix v, θ such that $0 < |\theta| < |\pi v|$. Let $a/m < b/n$ be a pair of convergents of $\theta/2\pi v$ that are both admissible. Then there exists $\rho \in (0,1)$ such that $T_0(\rho)$ is adjacent to $T_{\pm m}(\rho)$, $T_{\pm n}(\rho)$ and $T_{\pm(m+n)}(\rho)$.*

If, in addition, $(a-b)/(m-n)$ is an admissible convergent of $\theta/2\pi v$, then there exists $\rho' \in (0, \rho)$ such that $\mathcal{T}(\rho')$ is a quadrilateral tiling with an opposed parastichy pair $\{m, n\}$.

Proof. It is known in elementary number theory that a pair of convergents of x is written as a pair p_j/q_j, $p_{j,k}/q_{j,k}$ where $j \geq 0$ and $0 < k \leq a_{j+1}$. Hence, an opposed parastichy pair is written as $\{m, n\} = \{q_j, q_{j,k}\}$ for some $j \leq 0$, $0 < k \leq a_{j+1}$. The extension of $\{q_j, q_{j,k}\}$ is equal to $\{q_j, q_{j,k+1}\}$ if $k + 1 < a_{j+1}$; $\{q_j, q_{j+1}\}$ if $k = a_{j+1}$.

Lemmas 3.6, 3.7 and 3.8 imply that the sequence of extensions of the opposed parastichy pairs for $\mathcal{T}(r)$, as $r \to 1$, is written as the sequence of the pairs $\{q_j, q_{j,k}\}$. Thus, for any admissible pair p_j/q_j, $p_{j,k}/q_{j,k}$ of convergents of $\theta/2\pi v$, there exists $r \in (0,1)$ such that the tiling $\mathcal{T}(r)$ has an opposed parastichy pair $\{q_j, q_{j,k}\}$. □

Figure 3.2 shows the *parastichy transition* of Voronoi spiral tilings with the fixed divergence angle $\theta = 2\pi\tau$, $\tau = \frac{1+\sqrt{5}}{2}$, from a hexagonal tiling with opposed parastichy pairs $\{3, 5\}$, $\{5, 8\}$, through a quadrilateral tiling with an opposed parastichy pair $\{5, 8\}$, to a hexagonal tiling with opposed parastichy pairs $\{5, 8\}$, $\{8, 13\}$.

3.3 Quadrilateral Voronoi spiral tilings

Let $\zeta = re^{i\theta} \in M_v$ with $0 < r < 1$. Let $m, n > 0$ be relatively prime integers. If a Voronoi region of a Voronoi tiling for the spiral sequence $S = \{\zeta^j\}_{j\in\mathbb{Z}}$ becomes a quadrilateral, then the four points 1, ζ^m, ζ^{m+n} and ζ^n lie on a same circle in this order of vertices.

Let

$$\Psi_{m,n}(z) := \frac{(z^m - z^{m+n})(z^n - 1)}{(z^n - z^{m+n})(z^m - 1)} = \frac{z^m(z^n-1)^2}{z^n(z^m-1)^2}$$

be a rational function of one complex variable, and

$$\begin{aligned}\psi_{m,n,\theta}(r) &:= (1-r^m)(1-r^n)\cos\frac{m\theta}{2}\cos\frac{n\theta}{2} + (1+r^m)(1+r^n)\sin\frac{m\theta}{2}\sin\frac{n\theta}{2} \\ &= (1+r^{m+n})\cos\frac{m-n}{2}\theta - (r^m + r^n)\cos\frac{m+n}{2}\theta.\end{aligned}$$

We have

$$\Psi_{m,n}(z) = \Psi_{m,n}(1/z) = 1/\Psi_{n,m}(z),\ \psi_{m,n,\theta}(r) = \psi_{n,m,\theta}(r) = r^{m+n}\psi_{m,n,\theta}(1/r).$$

Lemma 3.10. *Let m, n be distinct positive integers. Let $z = re^{i\theta} \in \mathbb{C}\backslash\mathbb{R}$, and suppose that $z^m \neq 1$. The following conditions are mutually equivalent.*

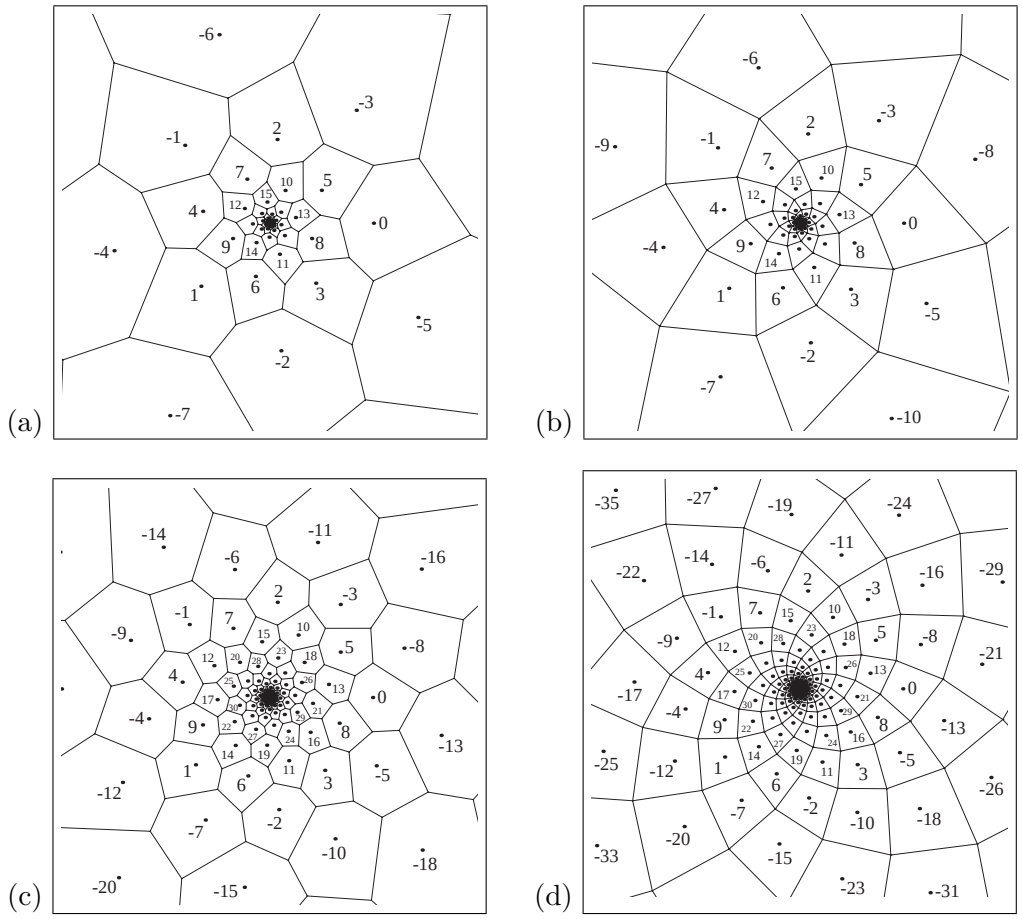

Figure 3.2: Voronoi spiral tilings generated by $\zeta = re^{i\theta}$ with the fixed divergence angle $\theta = 2\pi\tau$, $\tau = \frac{1+\sqrt{5}}{2}$. As r increases, the Fibonacci parastichy numbers also increase. (a) $r = 0.9$, hexagonal tiling with opposed parastichy pairs $\{3, 5\}$, $\{5, 8\}$. (b) $r = 0.92943\cdots$, quadrilateral tiling with an opposed parastichy pair $\{5, 8\}$. (c) $r = 0.96$, hexagonal tiling with opposed parastichy pairs $\{5, 8\}$, $\{8, 13\}$. (d) $r = 0.97328\cdots$, quadrilateral tiling with an opposed parastichy pair $\{13, 8\}$.

(i) The four points 1, z^m, z^{m+n}, z^n *form a quadrilateral* $\square(1, z^m, z^{m+n}, z^n)$ *which is inscribed in a circle, in this order of vertices.*

(ii) $\Psi_{m,n}(z) < 0$.

(iii) $\psi_{m,n,\theta}(r) = 0$.

Proof. (i) $\Leftrightarrow$ (ii): The cross ratio of 1, z^m, z^{m+n}, z^n is given as $\Psi_{m,n}(z)$.
(ii) $\Leftrightarrow$ (iii): We have $\mathrm{Re}\sqrt{\Psi_{m,n}(z)} = \mathrm{Re}(z^{\frac{m-n}{2}}\frac{z^n-1}{z^m-1}) = \frac{|z|^{\frac{m-n}{2}}}{|z^m-1|^2}\psi_{m,n,\theta}(r)$. □

3.3.1 Generators of quadrilateral Voronoi spiral tilings

In this section, we consider a set of generators ζ which produce quadrilateral Voronoi spiral tilings for each opposed parastichy pair.

Let $I = (-\pi, \pi]$ be a half-open interval, and consider an injective map

$$\iota_{m,n} : \mathbb{R} \to I^2, \qquad \iota_{m,n}(\theta) = \left(2\pi\langle\frac{m\theta}{2\pi}\rangle, 2\pi\langle\frac{n\theta}{2\pi}\rangle\right),$$

where $\langle x\rangle \in (-\frac{1}{2}, \frac{1}{2}]$ denotes a fractional part of $x \in \mathbb{R}$, such that $[\![x]\!] := x - \langle x\rangle \in \mathbb{Z}$ is an integer which is the nearest to x. The image of $\iota_{m,n}$ is a *stripe* in the square I^2 written as

$$\iota_{m,n}(\mathbb{R}) = \bigcup_{|v|<(m+n)/2} \{(\theta_1, \theta_2) \in I^2 : n\theta_1 - m\theta_2 = 2\pi v\}.$$

Let $\Delta = \Delta_+ \cup \Delta_-$,

$$\Delta_+ = \{(\theta_1, \theta_2) \in I^2 :\ 0 < \theta_1 < \theta_2 + \pi < \pi\},$$
$$\Delta_- = \{(\theta_1, \theta_2) \in I^2 :\ 0 < \theta_2 < \theta_1 + \pi < \pi\}.$$

Then $\iota_{m,n}(\mathbb{R}) \cap \Delta$ is a union of line segments written as

$$\iota_{m,n}(\mathbb{R}) \cap \Delta = \bigcup_{0<|v|<\max(m,n)/2} \ell_{m,n,v},\ \ell_{m,n,v} := \{(\theta_1, \theta_2) \in \Delta : n\theta_1 - m\theta_2 = 2\pi v\}.$$

Lemma 3.11. *Let* $m, n > 0$ *be relatively prime integers, and* $\theta \in \mathbb{R}$. *Then the followings conditions are mutually equivalent.*

(i) $\iota_{m,n}(\theta) \in \Delta$.

(ii) $(\cos\frac{m}{2}\theta\cos\frac{n}{2}\theta)(\sin\frac{m}{2}\theta\sin\frac{n}{2}\theta) < 0$ *and* $|\cos\frac{m}{2}\theta\cos\frac{n}{2}\theta| > |\sin\frac{m}{2}\theta\sin\frac{n}{2}\theta|$.

(iii) The equation $\psi_{m,n,\theta}(r) = 0$ *has a (unique) solution* r *in* $(0, 1)$.

Proof. (i) $\Leftrightarrow$ (ii): Obvious.
(ii) $\Leftrightarrow$ (iii): Since $(1 - r^m)(1 - r^n)$ is a decreasing function and $(1 + r^m)(1 + r^n)$ is an increasing function of r, the Intermediate Value Theorem can be applied to $\psi_{m,n,\theta}$ in the interval $[0, 1]$, to show the existence and the uniqueness of the solution $r \in (0, 1)$. The converse is also obvious. □

Figure 3.3 shows the set $\iota_{7,4}(\mathbb{R}) \cap (\Delta_+ \cup \Delta_-)$, consisting of six solid lines. It is a parameter space for quadrilateral Voronoi spiral (multiple) tilings with an opposed parastichy pair $\{4, 7\}$.

Let $B_{m,n} = \{z \in \mathbb{D}\setminus\mathbb{R} : \Psi_{m,n}(z) < 0\}$. Let $B_{m,n,v}$ be the set of $\zeta = re^{\mathrm{i}\theta} \in M_v$, $0 < r < 1$, such that the Voronoi tiling $\mathcal{T} = \{T_j\}_{j\in\mathbb{Z}}$ of M_v generated by $S = \{\zeta^j\}_{j\in\mathbb{Z}}$ is a quadrilateral tiling with an opposed parastichy pair $\{m, n\}$ and $n\arg(\zeta^m) - m\arg(\zeta^n) = 2\pi v$. Note that $B_{m,n,v} = B_{n,m,-v}$.

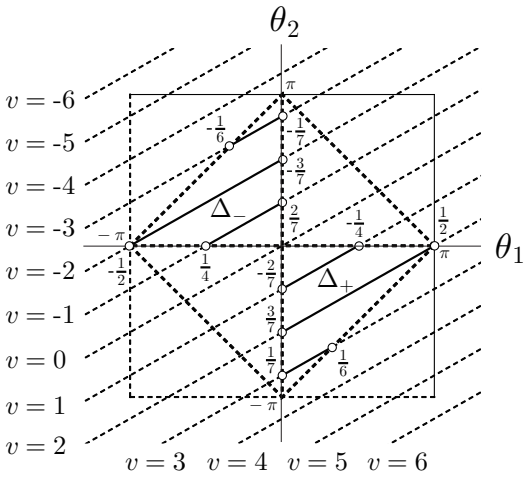

Figure 3.3: The set $\iota_{7,4}(\mathbb{R}) \cap (\Delta_+ \cup \Delta_-)$, consisting of six solid lines, denotes the set of the points $(\arg(\zeta^7), \arg(\zeta^4))$, where ζ generates a quadrilateral (multiple) spiral tiling with an opposed parastichy pair $\{4, 7\}$. The dotted lines are the lines $4\theta_1 - 7\theta_2 = 2\pi v$, $-6 \le v \le 6$. On each endpoint $\iota_{7,4}(\theta)$ of solid lines the rational number $\theta/2\pi$ is shown in the figure.

Theorem 3.12. *Let $m > n > 0$ be relatively prime integers. Then we have*

$$B_{m,n} = \bigcup_{0<|v|<m/2} p(B_{m,n,v}).$$

Proof. If $\zeta \in B_{m,n,v}$, then the Delaunay polygon $T_0 = \square(1, \zeta^m, \zeta^{m+n}, \zeta^n)$ is inscribed in a circle. By Lemma 3.10, we see that $f_{m,n}(p(\zeta)) < 0$, and hence $p(\zeta) \in B_{m,n}$. Thus we obtain $B_{m,n} \supset \bigcup_{0<|v|<m/2} p(B_{m,n,v})$.

Suppose that $z_0 = r_0 \mathrm{e}^{\mathrm{i}\theta} \in B_{m,n}$, $0 < r_0 < 1$, $0 < \theta < 2\pi$. Let a, b be positive integers such that $0 \le a/m < b/n \le 1$ and $mb - na = 1$. Let $v := n\langle \frac{m\theta}{2\pi} \rangle - m\langle \frac{n\theta}{2\pi} \rangle$, $a' := [\![\frac{m\theta}{2\pi}]\!]$, $b' := [\![\frac{n\theta}{2\pi}]\!]$, $d := ab' - a'b$, $\theta' := \theta + 2\pi d$, and $\zeta_0 := r_0 \mathrm{e}^{\mathrm{i}\theta'} \in M_v$. Then we have $v = mb' - na' \in \mathbb{Z}$, $0 < \theta'/2\pi v < 1$, and $\frac{a}{m} < \frac{\theta'}{2\pi v} < \frac{b}{n}$. The rational numbers a/m, b/n are a pair of convergents of $\theta'/2\pi v$ that are both admissible. For v, θ' fixed, Proposition 3.9 implies the existence of r such that $\zeta = r\mathrm{e}^{\mathrm{i}\theta'} \in M_v$ gives rise to a quadrilateral Voronoi tiling $\mathcal{T}$ with an opposed parastichy pair $\{m, n\}$, and Lemma 3.11 implies the uniqueness of r such that $\psi_{m,n,\theta'}(r) = 0$. Since $\square(1, \zeta_0^m, \zeta_0^{m+n}, \zeta_0^n) \subset M_v$ is indeed inscribed in a circle, it is a Delaunay polygon, and ζ_0 generates a quadrilateral Voronoi spiral multiple tiling. $\square$

Here we describe the details of the branches $B_{m,n,v}$. Let $I_v = (-|\pi v|, |\pi v|]$, and consider the mappings

$$\iota_{m,n,v} : \mathbb{R} \to I_v \times I_v, \qquad \iota_{m,n,v}(\theta) = \left(|2\pi v| \langle \frac{m\theta}{|2\pi v|} \rangle, |2\pi v| \langle \frac{n\theta}{|2\pi v|} \rangle \right).$$

Let $\Delta_v := \Delta_v^+ \cup \Delta_v^-$, $\Delta_v^+ := \{(\theta_1, \theta_2) \in I_v \times I_v : 0 < \theta_1 < \theta_2 + \pi < \pi\}$, $\Delta_v^- := \{(\theta_1, \theta_2) \in I_v \times I_v : 0 < \theta_2 < \theta_1 + \pi < \pi\}$, and $\ell'_{m,n,v} := \{(\theta_1, \theta_2) \in \Delta_v : n\theta_1 - m\theta_2 = 2\pi v\}$.

Lemma 3.13. *Let $m > n > 0$ be relatively prime integers and $0 < |v| < \frac{m}{2}$. Let $a, b > 0$ be integers such that $0 \le \frac{a}{m} < \frac{b}{n} \le 1$ and $bm - an = 1$. Define the intervals $I_{m,n,v} \subset \mathbb{R}$ as follows. First, an endpoint of $I_{m,n,v}$ is $\frac{2\pi a v}{m}$. The other endpoint of $I_{m,n,v}$ is given as follows: $\frac{2\pi b v}{n}$ if $|v| < \frac{n}{2}$; $b\pi$ if $v = \frac{n}{2}$; $-b\pi$ if $v = -\frac{n}{2}$; $\frac{\pi(2(a-b)v+1)}{m-n}$ if $\frac{n}{2} < v < \frac{m}{2}$; and $\frac{\pi(2(a-b)v-1)}{m-n}$ if $-\frac{m}{2} < v < -\frac{n}{2}$. Then*

$$\iota_{m,n,v} | I_{m,n,v} : I_{m,n,v} \to \ell'_{m,n,v}$$

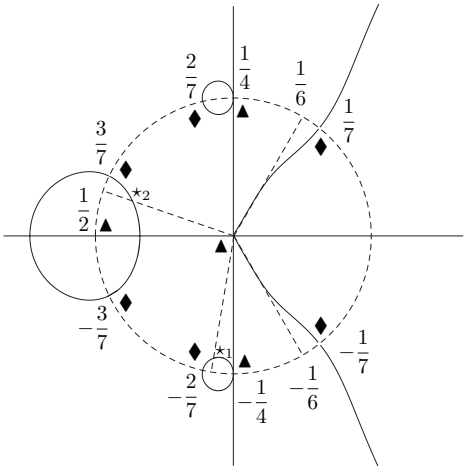

Figure 3.4: The set $B_{7,4}$ of the generators consists of the arcs $p(B_{7,4,v})$, $v = \pm1, \pm2, \pm3$, which are branches of the real algebraic curve $\mathrm{Re}\sqrt{\Psi_{7,4}(z)} = 0$. A rational number x on the unit circle denotes the point $\mathrm{e}^{2\mathrm{i}\pi x}$. The marks ▲ and ♦ indicate the points z where $\Psi_{7,4}(z) = 0$ and $-\infty$ respectively. The arc $p(B_{7,4,1})$ connects the point $\mathrm{e}^{(-2/7)\cdot 2\mathrm{i}\pi}$ with $\mathrm{e}^{(-1/4)\cdot 2\mathrm{i}\pi}$. The arc $p(B_{7,4,2})$ connects the point $\mathrm{e}^{(3/7)\cdot 2\mathrm{i}\pi}$ with $-0.6776\cdots$, where $r = 0.6776\cdots$ is a root of the equation $7(1-r^7)(1-r^4) - 4(1+r^7)(1+r^4) = 0$. The arc $p(B_{7,4,3})$ connects the point $\mathrm{e}^{(1/7)\cdot 2\mathrm{i}\pi}$ with the origin. The arc $p(B_{7,4,-v})$ is a complex conjugate of $p(B_{7,4,v})$, for each $v = 1, 2, 3$.

is a homeomorphism. Moreover, there exists a real analytic function $\rho_{m,n,v} : I_{m,n,v} \to \mathbb{R}$ *such that the mapping*

$$\varphi_{m,n,v} : I_{m,n,v} \to B_{m,n,v}, \qquad \varphi_{m,n,v}(\theta) = \rho_{m,n,v}(\theta)\mathrm{e}^{\mathrm{i}\theta}$$

is a homeomorphism.

Proof. First, we have $\iota_{m,n,v}(\frac{2\pi av}{m}) = (0, -\frac{2\pi v}{m})$. If $|v| < \frac{n}{2}$, we have $\iota_{m,n,v}(\frac{2\pi bv}{n}) = (\frac{2\pi v}{n}, 0)$. If $v = \frac{n}{2}$, we have $\iota_{m,n,v}(b\pi) = (\pi, 0)$. If $v = -\frac{n}{2}$, we have $\iota_{m,n,v}(-b\pi) = (-\pi, 0)$. If $\frac{n}{2} < v < \frac{m}{2}$, then $\iota_{m,n,v}(2\pi\frac{(a-b)v+\frac{1}{2}}{m-n}) = (\frac{m-2v}{m-n}\pi, \frac{n-2v}{m-n}\pi)$ lies on the boundary line $\theta_1 - \theta_2 = \pi$ of Δ_v^+. If $-\frac{m}{2} < v < -\frac{n}{2}$, then $\iota_{m,n,v}(2\pi\frac{(a-b)v-\frac{1}{2}}{m-n}) = (\frac{-m-2v}{m-n}\pi, \frac{-n-2v}{m-n}\pi)$ lies on the boundary line $\theta_1 - \theta_2 = -\pi$ of Δ_v^-. Finally confirm that the length of $I_{m,n,v}$ is less than or equal to $1/2m$.

The function $0 < r = \rho_{m,n,v}(\theta) < 1$ is given as a unique solution of $\psi_{m,n,v}(r) = 0$. □

Lemma 3.14. *Let $m > n > 0$ be relatively prime integers and $0 < |v| < m/2$. Let a, b be positive integers such that $0 \le a/m < b/n \le 1$ and $mb - na = 1$. The endpoints of the arc $B_{m,n,v}$ are given as follows. First, $\lim_{\theta\to 2\pi av/m} \rho_{m,n,v}(\theta) = 1$. For $0 < |v| < \frac{n}{2}$, we have $\lim_{\theta\to 2\pi bv/n} \rho_{m,n,v}(\theta) = 1$. For $|v| = \frac{n}{2}$, we have $\lim_{\theta\to\pm b\pi} \rho_{m,n,v}(\theta) = -\tilde{r}$, where $\tilde{r} \in (0,1)$ is a unique root of the equation*

$$m(1-r^m)(1-r^n) - n(1+r^m)(1+r^n) = 0. \tag{3.3.1}$$

For $\frac{n}{2} < |v| < \frac{m}{2}$, we have $\lim_{\theta\to\pi\frac{2(a-b)v\pm1}{m-n}} \rho_{m,n,v}(\theta) = 0$.

Proof. As $\theta \to 2\pi\frac{av}{m}$ or $\theta \to 2\pi\frac{bv}{n}$, we have $\sin m\theta \to 0$ or $\sin n\theta \to 0$, respectively, and so the positive root r of $\psi_{m,n,\theta}(r) = 0$ tends to a root of the equation $(1-r^m)(1-r^n)\cos\frac{\pi v}{m} = 0$ or $(1-r^m)(1-r^n)\cos\frac{\pi v}{n} = 0$, either of which is equal to 1. As $\theta \to \pm b\pi$, where n is even, the positive root of $\psi_{m,n,\theta}(r) = 0$ tends to a root of the equation

$$(\frac{m}{2}(1-r^m)(1-r^n) - \frac{n}{2}(1+r^m)(1+r^n))\sin\frac{m\pi}{2}\cos\frac{n\pi}{2} = 0,$$

which has a unique root $0 < \tilde{r} < 1$.

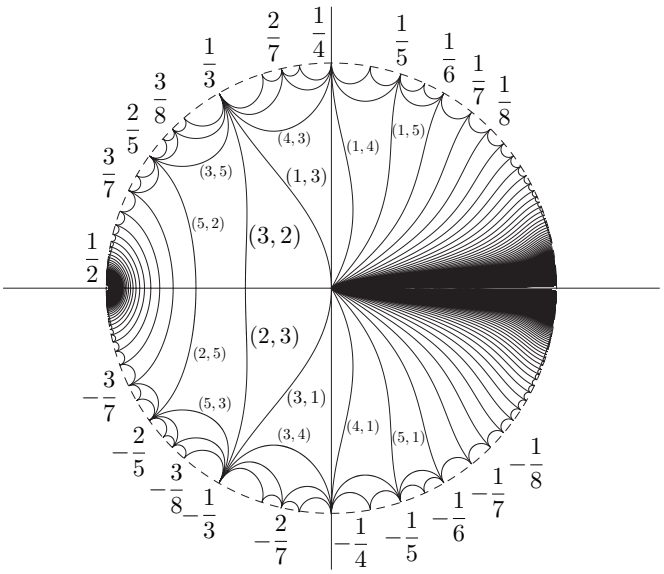

Figure 3.5: The set $B_1 \cup B_{-1}$ of generators of quadrilateral Voronoi spiral tilings. The arc $B_{m,n,1}$ is denoted by (m, n), and $B_{m,n,-1} = B_{n,m,1}$ by (n, m). The arcs $B_{m,1,\pm 1}$ accumulate to the interval $[0, 1]$ on the real axis, as $m \to \infty$.

As $\theta \to \pi \frac{2(a-b)v \pm 1}{m-n}$, we have $\cos \frac{m-n}{2}\theta \to 0$, and so the positive root of $\psi_{m,n,\theta}(r) = 0$ tends to a root of the equation $(r^m + r^n) \cos \frac{-4v \pm (m+n)}{2(m-n)}\pi = 0$, which is equal to 0. □

Figure 3.4 shows thet set $B_{7,4} = \cup_{=\pm 1,\pm 2,\pm 3} p(B_{7,4,v})$, which is a subset of a real algebraic curve defined by an inequality $\Psi_{7,4}(z) < 0$, i.e., by an equation $\mathrm{Re}\sqrt{\Psi_{7,4}(z)} = 0$. Each arc $B_{7,4,v}$ consists of the generators of Voronoi quadrilateral (multiple) spiral tilings with an opposed parastichy pair $\{4, 7\}$. The polynomial (3.3.1) for $m = 7$, $n = 4$, has a root $\tilde{r} = 0.6776\cdots$. So the arc $p(B_{7,4,2})$ has an endpoint $-\tilde{r} = -0.6776\cdots$. It is a critical point of the function $\Psi_{7,4}$.

Let $R := \{(m, n) \in \mathbb{Z}^2 : m > n > 0 \text{ are relatively prime}\}$. Let $\delta(\theta) = \{re^{\sqrt{-1}\theta} : 0 < r < 1\}$ be a radial line segment in $\mathbb{D}$.

Theorem 3.15. *Let $B_v := \bigcup_{(m,n)\in R} p(B_{m,n,v})$. The union $B := \bigcup_{v>0} B_v$ is a dense subset of $\mathbb{D}$.*

Proof. For each $v > 0$, we shall show that a radial line segment $\delta(2\pi bv/n)$ is contained in the closure of $B_v := \bigcup_{(m,n)\in R} p(B_{m,n,v})$, whenever n, b are relatively prime and $1 \le b < n < 2v$.

Let $0 < a < m$ be integers, such that $m > 2v$ and $mb - na = 1$. Let $m_j = nj + m$ and $a_j = bj + a$ for $j \ge 0$. Then, we have $m_j b - n a_j = 1$, and $a_j/m_j \to b/n$ as $j \to +\infty$. Since $n/2 < v < m_j/2$, the arc $p(B_{m_j,n,v})$ connects the m_j th root of unity $\mathrm{e}^{2\pi\sqrt{-1}a_j v/m_j}$ with the origin. As $j \to +\infty$, the length of the interval $I_{m_j,n,v} = (2\pi a_j v/m_j, 2\pi((a_j - b)v + \frac{1}{2})/(m_j - n))$ tends to 0. Thus, the curves $p(B_{m_j,n,v})$ accumulate to the radial line segment $\delta(2\pi bv/n)$ as $j \to +\infty$. □

Figure 3.5 shows the set $B_1 \cup B_{-1}$ of generators of quadrilateral Voronoi spiral tilings. This indicates that the arcs $B_{m,1,\pm 1}$ accumulate to the unit interval $[0, 1] = \delta(0)$ as $m \to +\infty$.

3.3.2 Shape limit of quadrilateral Voronoi spiral tilings

Let $v > 0$, $\theta \in (-\pi v, \pi v]$. In this section we suppose that $\theta/2\pi v$ is a fixed irrational number. In the continued fraction expansion of $x = \theta/2\pi v$, we defined the sequences q_j and $q_{j,k}$, $j > 0$, $0 \le k \le a_{j+1}$, in Section 2.3. For each $j > 0$ and $0 \le k \le a_{j+1}$, let $a_{j,k}/m_{j,k} < b_{j,k}/n_{j,k}$ be a pair of convergents of $x = \theta/2\pi v$ such that $\{m_{j,k}, n_{j,k}\} = \{q_j, q_{j,k}\}$. If the convergents

$a_{j,k}/m_{j,k}, b_{j,k}/n_{j,k}$ are admissible, let $0 < r = r_{j,k} < 1$ be the root of the equation $\psi_{m_{j,k},n_{j,k},\theta}(r) = 0$, and $\zeta_{j,k} = r_{j,k}\mathrm{e}^{\mathrm{i}\theta} \in M_v$. The Voronoi tiling $\mathcal{T} = \mathcal{T}(\zeta_{j,k})$ for the spiral site set S generated by $\zeta_{j,k}$ is a quadrilateral Voronoi spiral multiple tiling.

Lemma 3.16. *Let $v > 0$, $\theta \in (-\pi v, \pi v]$, and suppose that $\frac{\theta}{2\pi v}$ is an irrational number. Then, all the angles of the quadrilateral $\square(1, \zeta_{j,k}^{m_{j,k}}, \zeta_{j,k}^{m_{j,k}+n_{j,k}}, \zeta_{j,k}^{n_{j,k}})$ tend to $\pi/2$ as $j \to \infty$.*

Proof. Denote by $m = m_{j,k}$, $n = n_{j,k}$, $\zeta = \zeta_{j,k}$ for the sake of simplicity. First note that we have $-\pi < \arg(\zeta^n) < 0 < \arg(\zeta^m) < \pi$, where $-\pi v < \arg(z) < \pi v$ denotes an argument of $z \in M_v$. Since the quadrilateral $\square(1, \zeta^m, \zeta^{m+n}, \zeta^n)$ is inscribed in a circle, we obtain

$$\begin{aligned}\angle(\zeta^n, 1, \zeta^m) &= \pi - \angle(\zeta^m, \zeta^{m+n}, \zeta^n),\\ \angle(1, \zeta^m, \zeta^{m+n}) &= \pi - \angle(\zeta^{m+n}, \zeta^n, 1).\end{aligned}$$

Moreover we have

$$\begin{aligned}\pi &= \angle(\zeta^n, 1, \zeta^m) + \angle(1, \zeta^m, \zeta^{m+n}) + \arg(\zeta^m),\\ \pi &= \angle(\zeta^n, 1, \zeta^m) + \angle(\zeta^{m+n}, \zeta^n, 1) - \arg(\zeta^n).\end{aligned}$$

Solving these equations, we obtain

$$\begin{aligned}\angle(\zeta^n, 1, \zeta^m) &= \frac{\pi}{2} - \frac{1}{2}\arg(\zeta^{m-n}),\ \angle(1, \zeta^m, \zeta^{m+n}) = \frac{\pi}{2} - \frac{1}{2}\arg(\zeta^{m+n}),\\ \angle(\zeta^m, \zeta^{m+n}, \zeta^n) &= \frac{\pi}{2} + \frac{1}{2}\arg(\zeta^{m-n}),\ \angle(\zeta^{m+n}, \zeta^n, 1) = \frac{\pi}{2} + \frac{1}{2}\arg(\zeta^{m+n}),\end{aligned}$$

all of which tend to $\pi/2$ as $j \to \infty$, since

$$\lim_{j\to+\infty} \arg(\zeta^{m+n}) = \lim_{j\to+\infty} \arg(\zeta^{m-n}) = 0.$$

□

Lemma 3.17. *Suppose that the coefficients $\{a_j\}_{j\geq 0}$ in the continued fraction expansion*

$$\frac{\theta}{2\pi v} = [a_0, a_1, a_2, \dots]$$

are bounded. Then we have

$$0 < 1 - r_{j,k} \leq \frac{C}{m_{j,k}^2},$$

$$0 < 1 - r_{j,k} - \sqrt{\frac{-(2\pi v)^2}{m_{j,k}n_{j,k}}\langle\frac{m_{j,k}\theta}{2\pi v}\rangle\langle\frac{n_{j,k}\theta}{2\pi v}\rangle} \leq \frac{C}{m_{j,k}^3}, \tag{3.3.2}$$

where $C > 0$ is a constant independent of j, k.

Proof. For the (principal or intermediate) convergents $p_{j,k}/q_{j,k}$ of $\theta/2\pi v$, we have

$$\left|\frac{\theta}{2\pi v} - \frac{p_{j,k}}{q_{j,k}}\right| \leq \frac{C}{q_{j,k}^2}$$

where the constant $C > 0$ is independent of j, k. This implies that

$$\left|\pi v\langle\frac{q_{j,k}\theta}{2\pi v}\rangle\right| = \pi v\left|\frac{q_{j,k}\theta}{2\pi v} - p_{j,k}\right| \leq \frac{C\pi v}{q_{j,k}}$$

for sufficiently large j. This implies that

$$\left|\tan\frac{q_{j,k}\theta}{2}\right| \le \frac{C'}{q_{j,k}}$$

where C' is independent of j,k. Denote by $m = m_{j,k}$, $n = n_{j,k}$, $\zeta = \zeta_{j,k}$ for the sake of simplicity. Since a_j are bounded, the ratios $n_{j,k}/m_{j,k}$ are also bounded. By abuse of notation we shall sometimes denote the constants that are independent of j,k by the same letter C. The plastochrone ratio $0 < r = r_{j,k} < 1$ is a root of the equation

$$(1-r^m)(1-r^n) + (1+r^m)(1+r^n)\tan\frac{m\theta}{2}\tan\frac{n\theta}{2} = 0. \tag{3.3.3}$$

We have

$$\begin{aligned}(1-r)^2 &= \frac{(1+r^m)(1+r^n)}{(1+r+\cdots+r^{m-1})(1+r+\cdots+r^{n-1})}\left|\tan\frac{m\theta}{2}\tan\frac{n\theta}{2}\right| \\ &\le \frac{2\cdot 2}{1\cdot 1}\cdot(\frac{C}{m})^2 = \frac{C}{m^2},\end{aligned}$$

and hence

$$1-r \le \frac{C}{m}.$$

This implies that

$$\sum_{s=0}^{m-1} r^s \ge \sum_{s=0}^{m-1}(1-\frac{C}{m})^s = \frac{m}{C}(1-(1-\frac{C}{m})^m) \ge C'm \tag{3.3.4}$$

with $C' > 0$, since $\lim_{m\to\infty}(1-\frac{C}{m})^m = \mathrm{e}^{-C} < 1$. By applying (3.3.4) to (3.3.3) again, we obtain

$$\begin{aligned}(1-r)^2 &= \frac{(1+r^m)(1+r^n)}{(1+r+\cdots+r^{m-1})(1+r+\cdots+r^{n-1})}\left|\tan\frac{m\theta}{2}\tan\frac{n\theta}{2}\right| \\ &\le \frac{2\cdot 2}{Cm\cdot Cm}\cdot(\frac{C}{m})^2 = \frac{C}{m^4},\end{aligned}$$

and hence

$$1-r \le \frac{C}{m^2}.$$

Here we adopt a notation $\varphi = O(m^{-s})$ when there exists a constant C independent of j,k such that $|\varphi| \le C/m^s$. Then we have

$$\begin{aligned} t := 1-r &= O(m^{-2}), \\ r^m = (1-t)^m &= 1-mt+O(m^{-2}), \\ r^n = (1-t)^n &= 1-nt+O(m^{-2}), \\ \tan\tfrac{m\theta}{2} &= \pi v\langle\tfrac{m\theta}{2\pi v}\rangle + O(m^{-3}), \\ \tan\tfrac{n\theta}{2} &= \pi v\langle\tfrac{n\theta}{2\pi v}\rangle + O(m^{-3}).\end{aligned}$$

By (3.3.3) we obtain

$$mt\cdot nt + (2\pi v)^2\langle\frac{m\theta}{2\pi v}\rangle\langle\frac{n\theta}{2\pi v}\rangle + O(m^{-3}) = 0,$$

thus $t^2 = -\frac{(2\pi v)^2}{mn}\langle\frac{m\theta}{2\pi v}\rangle\langle\frac{n\theta}{2\pi v}\rangle + O(m^{-5})$, where we note that $\langle\frac{n\theta}{2\pi v}\rangle < 0 < \langle\frac{m\theta}{2\pi v}\rangle$, and hence we obtain (3.3.2). □

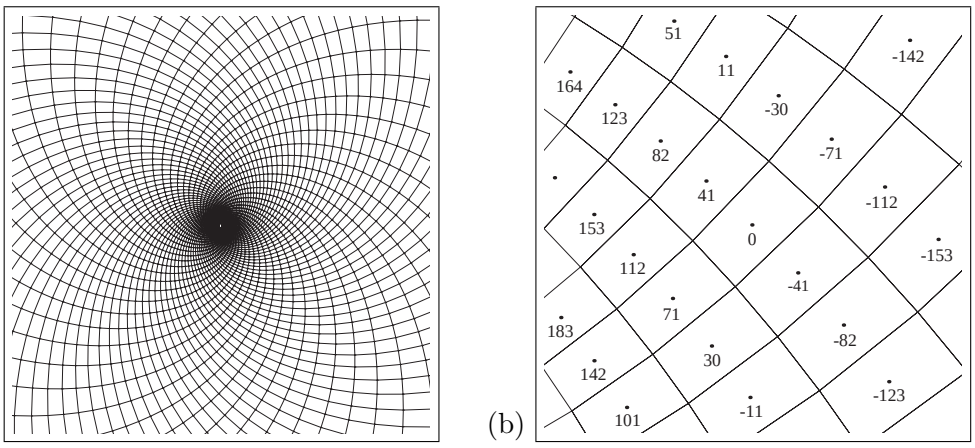

Figure 3.6: A quadrilateral Voronoi spiral tiling generated by $(0.9989\cdots)\mathrm{e}^{\mathrm{i}\theta}$, $\theta = 2\pi \cdot \frac{1+\sqrt{3}}{2}$, with an opposed parastichy pair $\{41, 71\}$. (a) Global view around the origin. (b) Local view around the tile T_0. The shapes of the quadrilaterals are close to the rectangle with the aspect ratio $\sqrt{3}$.

Similar to the rectangular helical Voronoi tilings, we suppose that $\theta/2\pi v$ is a quadratic irrational number.

Let $R(\theta, v) \subset \mathbb{C}$ be the set of ratios $(\zeta_{j,k}^{n_{j,k}} - 1)/(\zeta_{j,k}^{m_{j,k}} - 1)$, where $j > 0$, $0 < k \leq a_{j+1}$ and such that the convergents $a_{j,k}/m_{j,k}$, $b_{j,k}/n_{j,k}$ of $\theta/2\pi v$ are admissible. Let

$$\Omega(\theta, v) := \Omega(R(\theta, v))$$

be the limit set, i.e., the set of the accumulation points, of $R(\theta, v)$.

Theorem 3.18. *Suppose that $\theta/2\pi v$ is a quadratic irrational number. Then we have*

$$\Omega(\theta, v) = \{\mathrm{i}\,(-\psi_{s+1}(k))^{(-1)^s/2} : 0 \leq s < d, 0 < k \leq b_{s+1}\}. \tag{3.3.5}$$

In particular, it is a finite set.

Proof. Since $\theta/2\pi v$ is a quadratic irrational number, there exists a constant $C_1, C_2 > 0$, independent of $j > 0$, $0 < k \leq a_{j+1}$, such that

$$\frac{C_1}{q_{j,k}^2} < \left| \frac{p_{j,k}}{q_{j,k}} - \frac{\theta}{2\pi v} \right| < \frac{C_2}{q_{j,k}^2}.$$

See Theorem 188 in [22]. This implies that

$$\frac{C_1}{m_{j,k}} < |\langle \frac{m_{j,k}\theta}{2\pi v} \rangle| < \frac{C_2}{m_{j,k}}.$$

We have

$$\begin{aligned}
\frac{\zeta_{j,k}^{n_{j,k}}-1}{\zeta_{j,k}^{m_{j,k}}-1} &= \frac{-1+r^n\cos n\theta+\mathrm{i}r^n\sin n\theta}{-1+r^m\cos m\theta+\mathrm{i}r^m\sin\theta} \\
&= \frac{-nt+\mathrm{i}2\pi v\langle\frac{n\theta}{2\pi v}\rangle+O(m^{-2})}{-mt+\mathrm{i}2\pi v\langle\frac{m\theta}{2\pi v}\rangle+O(m^{-2})} \\
&= \frac{-\sqrt{\frac{-n}{m}\langle\frac{m\theta}{2\pi v}\rangle\langle\frac{n\theta}{2\pi v}\rangle}+\mathrm{i}\langle\frac{n\theta}{2\pi v}\rangle+O(m^{-2})}{-\sqrt{\frac{-m}{n}\langle\frac{m\theta}{2\pi v}\rangle\langle\frac{n\theta}{2\pi v}\rangle}+\mathrm{i}\langle\frac{m\theta}{2\pi v}\rangle+O(m^{-2})} \\
&= \frac{-\sqrt{\frac{-n}{m}\langle\frac{m\theta}{2\pi v}\rangle\langle\frac{n\theta}{2\pi v}\rangle}+\mathrm{i}\langle\frac{n\theta}{2\pi v}\rangle}{-\sqrt{\frac{-m}{n}\langle\frac{m\theta}{2\pi v}\rangle\langle\frac{n\theta}{2\pi v}\rangle}+\mathrm{i}\langle\frac{m\theta}{2\pi v}\rangle}(1+O(m^{-1})) \\
&= \mathrm{i}\sqrt{\frac{-n\langle\frac{n\theta}{2\pi v}\rangle}{m\langle\frac{m\theta}{2\pi v}\rangle}}(1+O(m^{-1}))
\end{aligned}$$

since $\langle\frac{n\theta}{2\pi v}\rangle < 0 < \langle\frac{m\theta}{2\pi v}\rangle$, where we denote by $m = m_{j,k}$, $n = n_{j,k}$. Thus it is written as

$$\frac{\zeta_{j,k}^{n_{j,k}}-1}{\zeta_{j,k}^{m_{j,k}}-1} = \mathrm{i}\left(\frac{q_{j,k}}{q_j}\frac{(-\langle\frac{q_{j,k}\theta}{2\pi v}\rangle)}{\langle\frac{q_j\theta}{2\pi v}\rangle}\right)^{(-1)^j/2}(1+O(q_j^{-1})).$$

By using the continued fractions, we have

$$\begin{aligned}
q_{j,k}/q_j &= [k, a_j, a_{j-1}, \dots, a_1], \\
-\langle\frac{q_{j,k}\theta}{2\pi v}\rangle/\langle\frac{q_j\theta}{2\pi v}\rangle &= [a_{j+1}-k, a_{j+2}, a_{j+3}, \dots]
\end{aligned}$$

for $j \geq 1$, $0 \leq k \leq a_{j+1}$. As $j \to +\infty$, they tend to the periodic sequence of continued fractions

$$[k, \overline{b_s, \dots, b_1, b_d, \dots, b_{s+1}}] \text{ and } [b_{s+1}-k, \overline{b_{s+2}, \dots, b_d, b_1, \dots, b_{s+1}}].$$

However, we have

$$\begin{aligned}
&[k, \overline{b_s, \dots, b_1, b_d, \dots, b_{s+1}}] \cdot [b_{s+1}-k, \overline{b_{s+2}, \dots, b_d, b_1, \dots, b_{s+1}}] \\
&= (k-\omega'_{s+1})(-k+\omega_{s+1}) \\
&= -\psi_{s+1}(k)
\end{aligned}$$

for $0 \leq s < d$, $0 < k \leq b_{s+1}$. This completes the proof. □

Figure 3.6 shows a quadrilateral Voronoi tiling generated by $\zeta = (0.9989\cdots)\mathrm{e}^{\mathrm{i}\theta}$, $\theta = 2\pi \cdot (1+\sqrt{3})/2$, with an opposed parastichy pair $\{41, 71\}$. Note that $(1+\sqrt{3})/2 = [\overline{1,2}]$ is a purely periodic continued fraction expansion. The defining polynomial of $\omega_1 = [\overline{2,1}] = 1+\sqrt{3}$ is $\psi_1(x) = x^2-2x-2$, and the defining polynomial of $\omega_2 = [\overline{1,2}] = (1+\sqrt{3})/2$ is $\psi_1(x) = x^2-x-1/2$. We have $(-\psi_1(1))^{1/2} = \sqrt{3}$, $(-\psi_1(2))^{1/2} = \sqrt{2}$ and $(-\psi_2(1))^{-1/2} = \sqrt{2}$, and so $\Omega(\theta = (1+\sqrt{3})/2, v = 1) = \{\mathrm{i}\sqrt{2}, \mathrm{i}\sqrt{3}\}$. This implies that the limit set of the shapes of quadrilateral tiles, as $r \to 1$, is the rectangles whose aspect ratios are $\sqrt{3}$ and $\sqrt{2}$. The opposed parastichy pair $\{41, 71\}$ in Figure 3.6 corresponds to the pair of convergents $p_6/q_6 = 56/41 < \theta/2\pi < p_{6,1}/q_{6,1} = 97/71$, and $r = 0.998921$ is a root of the polynomial $\psi_{m,n,\theta}(r)$ for $\{m, n\} = \{41, 71\}$. The ratio $(\zeta_{6,1}^{71}-1)/(\zeta_{6,1}^{41}-1) = 0.102397 + 1.70098\mathrm{i}$ is close to $\mathrm{i}\sqrt{3}$.

Corollary 3.19. *If the coefficients $a_j = 1$ of the continued fraction expansion of $\theta/2\pi v$ for sufficiently large j, then $\Omega(\theta, v) = \{\mathrm{i}\}$.*

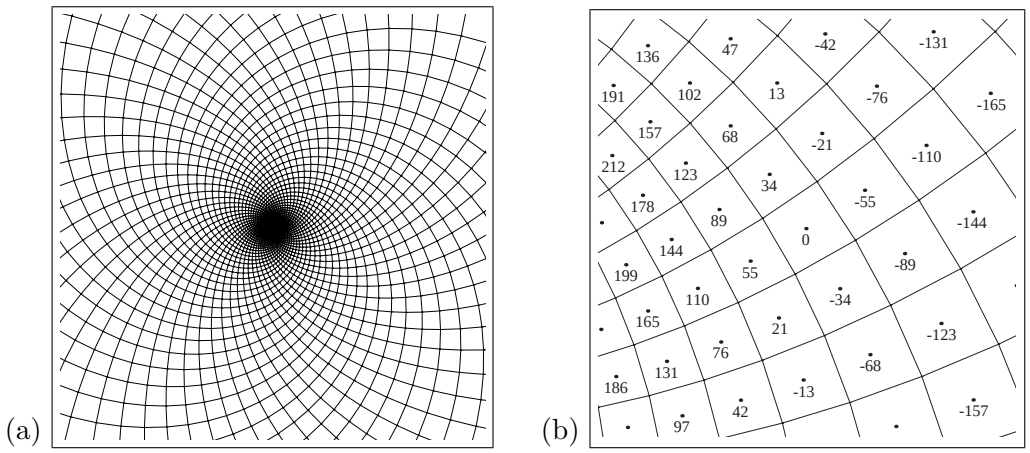

Figure 3.7: A quadrilateral Voronoi spiral tiling generated by $(0.9994\cdots)\exp(2\pi\mathrm{i}\cdot\tau)$, $\tau=\frac{1+\sqrt{5}}{2}$, with an opposed parastichy pair $\{34,55\}$. (a) Global view around the origin. (b) Local view around the tile T_0. The quadrilateral tiles are close to the squares.

Proof. The golden section $\tau=[1,1,\dots]=[1,\overline{1,1}]$ is a root of a quadratic polynomial $\psi(x)=x^2-x-1$, and we have $-\psi(1)=1$. □

Figure 3.7 shows a quadrilateral Voronoi tiling generated by $\zeta=(0.9994\cdots)\mathrm{e}^{2\pi\mathrm{i}\tau}$, $\tau=\frac{1+\sqrt{5}}{2}$, with an opposed parastichy pair $\{34,55\}$. The tiles are close to the squares.

Figure 3.8 shows the parastichy transition of Voronoi spiral tilings with the fixed divergence angle $\theta=2\pi(\sqrt{2}+1)$, from a hexagonal tiling with opposed parastichy pairs $\{5,2\}$, $\{5,7\}$, through a quadrilateral tiling with an opposed parastichy pair $\{5,7\}$, to a hexagonal tiling with opposed parastichy pairs $\{5,7\}$, $\{5,12\}$. The limit set is given by $\Omega(\theta=2\pi(\sqrt{2}+1),v=1)=\{\mathrm{i},\mathrm{i}\sqrt{2},\mathrm{i}/\sqrt{2}\}$.

Figure 3.9 shows the parastichy transition of Voronoi spiral multiple tilings of multiplicity $v=2$, with the fixed divergence angle $\theta=2\pi(\tau-1)$, from a hexagonal tiling with opposed parastichy pairs $\{10,13\}$, $\{13,3\}$, through a quadrilateral tiling with an opposed parastichy pair $\{13,3\}$, to a hexagonal tiling with opposed parastichy pairs $\{13,3\}$, $\{13,16\}$. The limit set is given by $\Omega(\theta=2\pi(\tau-1),v=2)=\{\mathrm{i},\mathrm{i}\sqrt{2},\mathrm{i}/\sqrt{2},\mathrm{i}\sqrt{3},\mathrm{i}/\sqrt{3}\}$.

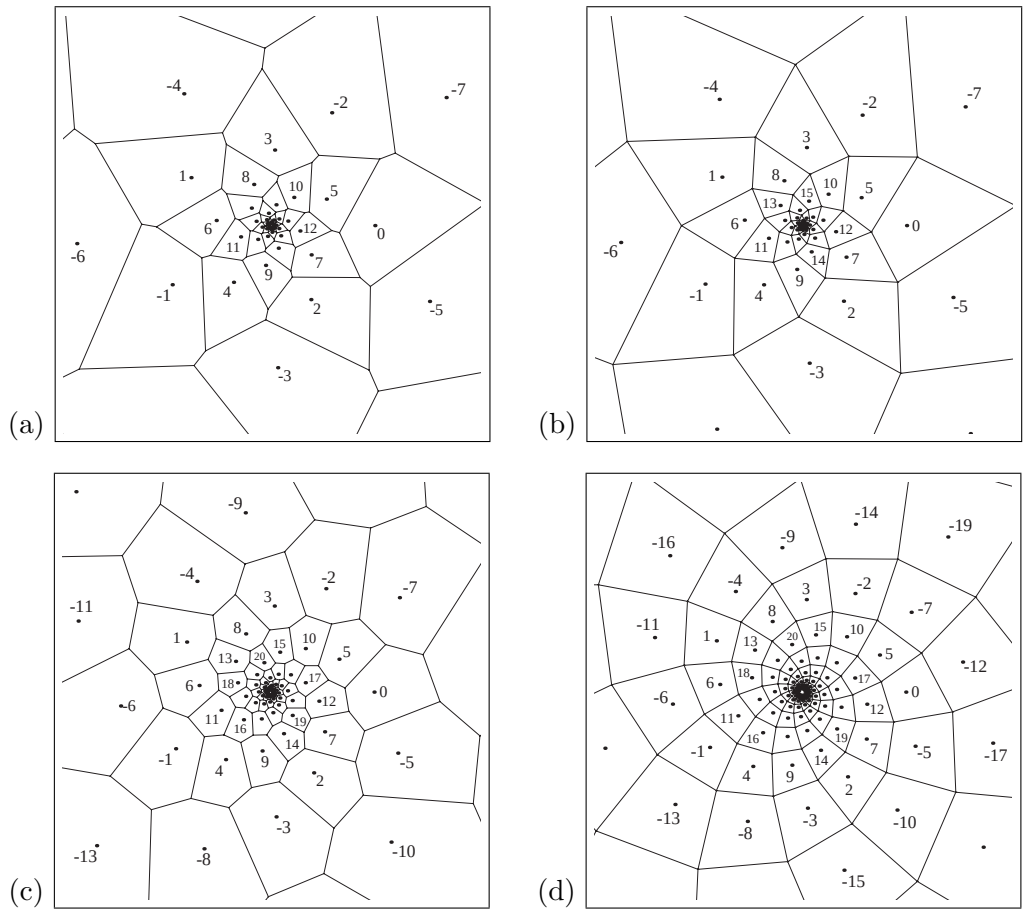

Figure 3.8: Voronoi spiral tilings generated by $\zeta = re^{i\theta}$ with the fixed divergence angle $\theta = 2\pi(\sqrt{2}+1)$, $\sqrt{2}+1$ is the silver mean. (a) $r = 0.9$, hexagonal tiling with opposed parastichy pairs $\{5, 2\}$, $\{5, 7\}$. (b) $r = 0.90974$, quadrilateral tiling with an opposed parastichy pair $\{5, 7\}$. (c) $r = 0.94$, hexagonal tiling with opposed parastichy pairs $\{5, 7\}$, $\{5, 12\}$. (d) $r = 0.96286$, quadrilateral tiling with an opposed parastichy pair $\{5, 12\}$.

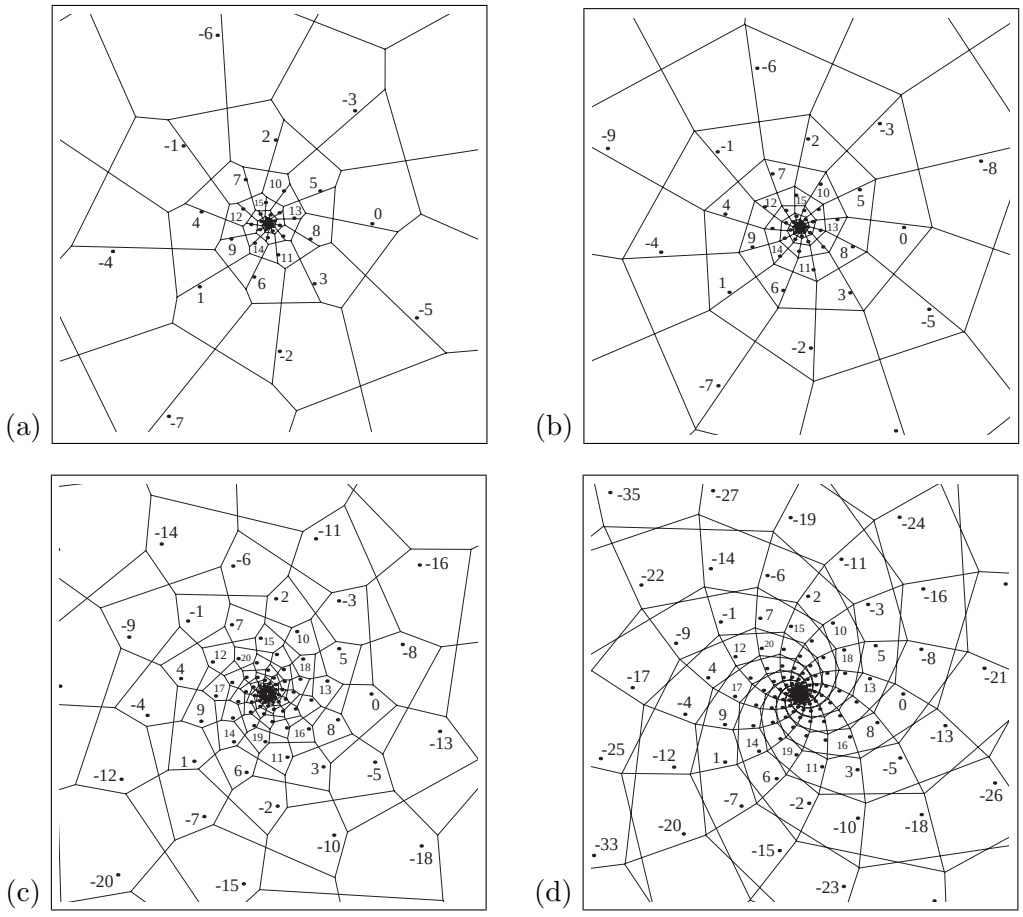

Figure 3.9: Voronoi spiral multiple tilings of multiplicity $v = 2$, which is generated by $\zeta = re^{i\theta} \in M_2$ with the fixed divergence angle $\theta = 2\pi(\tau - 1)$, $\tau = \frac{1+\sqrt{5}}{2}$. (a) $r = 0.9$, hexagonal tiling with opposed parastichy pairs $\{10, 13\}$, $\{13, 3\}$. (b) $r = 0.92559$, quadrilateral tiling with an opposed parastichy pair $\{13, 3\}$. (c) $r = 0.96$, hexagonal tiling with opposed parastichy pairs $\{13, 3\}$, $\{13, 16\}$. (d) $r = 0.97238$, quadrilateral tiling with an opposed parastichy pair $\{13, 16\}$.

Part III

Triangular spiral tilings

Chapter 4

Triangular spiral tilings

4.1 Quadrilateral spiral multiple tilings

In this section, we define a spiral multiple tiling as a tiling of a covering space of the punctured plane $\mathbb{C}^* := \mathbb{C}\backslash\{0\}$.

Let $C_v := \mathbb{C}/2\pi v\mathrm{i}\mathbb{Z}$ be a cylinder, where $v \neq 0$ is an integer. By the exponential function $\exp : \mathbb{C}_v \to \mathbb{C}^*$ which maps $w + 2\pi v\mathrm{i}\mathbb{Z}$ to $z = \mathrm{e}^w$, C_v is a covering space of $\mathbb{C}^*$, with degree v. The metric on C_v is written by the Euclidean metric on $\mathbb{C}^*$, $ds^2 = dzd\overline{z} = \mathrm{e}^{2\mathrm{Re}(w)}dwd\overline{w}$.

Definition 4.1. *Let $\mathcal{T}'$ be a tiling of C_v. Then $\exp(\mathcal{T}') = \{\exp(T')\}_{T'\in\mathcal{T}'}$ is called a multiple tiling of $\mathbb{C}^*$ of multiplicity $|v|$. Let Λ be an additive subgroup of C_v. We say that $\mathcal{T}'$ admits a transitive action by Λ if*

(i) for each $T' \in \mathcal{T}'$ and $\eta \in \Lambda$, we have $T' + \eta \in \mathcal{T}'$, and

(ii) for any pair $T'_1, T'_2 \in \mathcal{T}'$, there exists $\eta \in \Lambda$ such that $T'_2 = T'_1 + \eta$.

If $\mathcal{T}'$ admits a transitive action by an additive group $\xi\mathbb{Z}$ which is generated by a single element $\xi \in C_v$, then $\mathcal{T} = \exp(\mathcal{T}')$ is called a spiral multiple tiling of multiplicity $|v|$.

Let $\zeta = r\mathrm{e}^{\mathrm{i}\theta} \in \mathbb{D}\backslash\mathbb{R}$ with $0 < r < 1$, and consider the spiral sequence $S = \{\zeta^j\}_{j\in\mathbb{Z}}$ of $\mathbb{C}^*$, which is generated by a single element ζ. In the phyllotaxis theory, $1/r$ is called *the plastochrone ratio* and $\theta = \mathrm{Arg}(\zeta)$ is called *the divergence angle*, where $-\pi < \mathrm{Arg}(z) \leq \pi$ denotes the principal argument of $z \in \mathbb{C}^*$. Let $m, n > 0$ be relatively prime integers. Suppose that $T_0 := \square(1, \zeta^m, \zeta^{m+n}, \zeta^n)$ is a quadrilateral of $\mathbb{C}^*$ in this order of vertices. Let

$$\xi_m := m\log(r) + \mathrm{i}\left(m\theta - 2\pi[\![\frac{m\theta}{2\pi}]\!]\right) \in \log(\zeta^m),$$
$$\xi_n := n\log(r) + \mathrm{i}\left(n\theta - 2\pi[\![\frac{n\theta}{2\pi}]\!]\right) \in \log(\zeta^n),$$

where $[\![x]\!]$ denotes an integer which is the nearest to $x \in \mathbb{R}$ such that $-\frac{1}{2} < \langle x\rangle := x - [\![x]\!] \leq \frac{1}{2}$. Let a, b be integers such that $mb - na = 1$. Let

$$\xi := b\xi_m - a\xi_n = \log(r) + \mathrm{i}(\theta + 2\pi\ell) \in \log(\zeta), \quad \ell = a[\![\frac{n\theta}{2\pi}]\!] - b[\![\frac{m\theta}{2\pi}]\!],$$

and

$$v := m[\![\frac{n\theta}{2\pi}]\!] - n[\![\frac{n\theta}{2\pi}]\!] = \frac{n\mathrm{Arg}(\zeta^m) - m\mathrm{Arg}(\zeta^n)}{2\pi}. \tag{4.1.1}$$

Theorem 4.2. *Let $\zeta = r\mathrm{e}^{\mathrm{i}\theta} \in \mathbb{D}\backslash\mathbb{R}$. Let $m, n > 0$ be relatively prime integers, and suppose that $\zeta^m, \zeta^n \notin \mathbb{R}_-$. If $T_0 := \square(1, \zeta^m, \zeta^{m+n}, \zeta^n)$ is a quadrilateral in $\mathbb{C}^*$ in this order of vertices, then*

$$\mathcal{T} = \{T_j := \square(\zeta^j, \zeta^{j+m}, \zeta^{j+m+n}, \zeta^{j+n})\}_{j\in\mathbb{Z}} \tag{4.1.2}$$

is a spiral multiple tiling of multiplicity $|v|$, where v is given by (4.1.1).

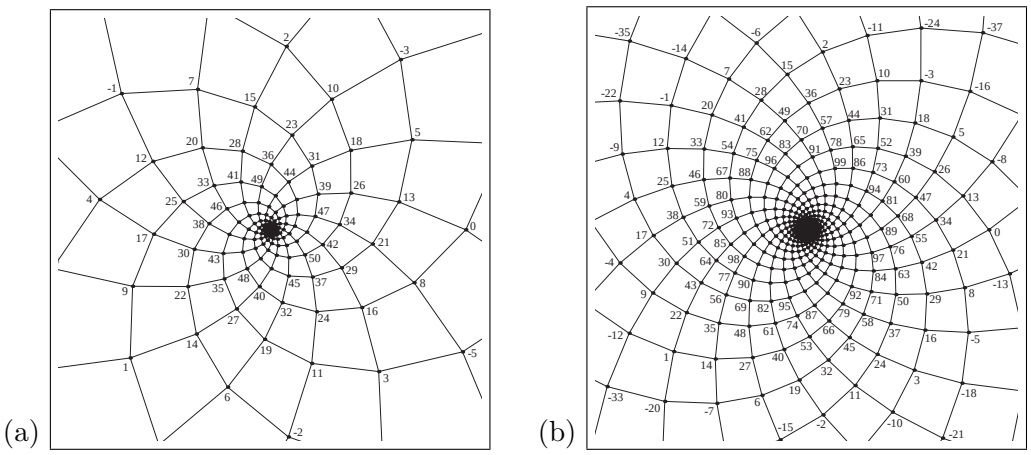

Figure 4.1: Quadrilateral spiral tilings with the divergence angle $\theta = 2\pi\tau$, where $\tau = \frac{1+\sqrt{5}}{2}$ is the golden section. Each $j \in \mathbb{Z}$ indicates the position of the complex coordinate $\zeta^j \in S$. (a) $r = 0.97$ and an opposed parastichy pair is $\{13, 8\}$. (b) $r = 0.99$ and an opposed parastichy pair is $\{13, 21\}$.

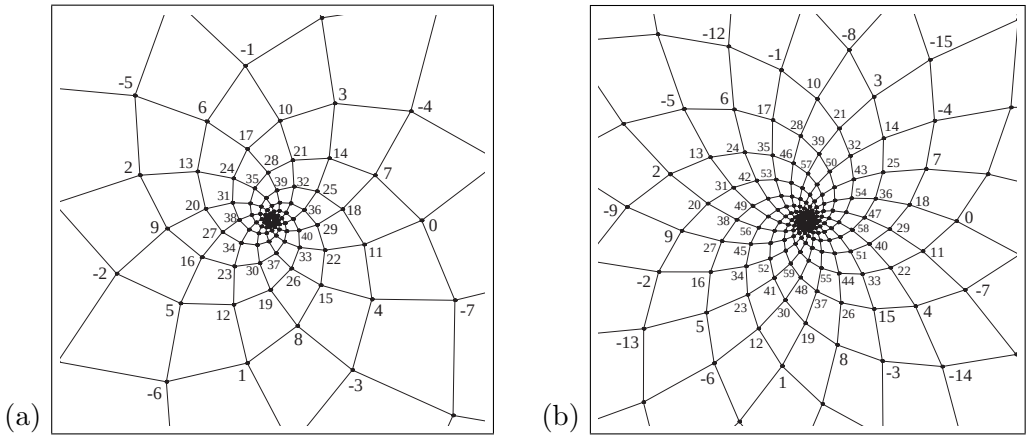

Figure 4.2: Quadrilateral spiral tilings with the divergence angle $\theta = 2\pi \cdot \frac{5+\sqrt{5}}{10}$. (a) $r = 0.96$ and an opposed parastichy pair is $\{7, 11\}$. (b) $r = 0.98$ and an opposed parastichy pair is $\{18, 11\}$.

Proof. Since the complex logarithmic function log is a multiple-valued function, $\log(T_0)$ has $|v|$ components in C_v. Let T_0' be a component of $\log(T_0)$ which has $0, \xi_m, \xi_m + \xi_n$ and ξ_n on its boundary. In C_v, we have $n\xi_m - m\xi_n \equiv 0$, $m\xi \equiv \xi_m$, $n\xi \equiv \xi_n$ and $\xi_m\mathbb{Z} + \xi_n\mathbb{Z} \equiv \xi\mathbb{Z} \bmod 2\pi v i\mathbb{Z}$. Let $\mathcal{T}' := \{T_0' + k_1\xi_m + k_2\xi_n\}_{k_1,k_2\in\mathbb{Z}} = \{T_0' + k\xi\}_{k\in\mathbb{Z}}$. Then $\mathcal{T}'$ is a tiling of C_v which admits a transitive action by $\xi\mathbb{Z}$. Hence we have $\mathcal{T} = \exp(\mathcal{T}')$. □

We call (4.1.2) *the quadrilateral spiral multiple tiling* of multiplicity $|v|$. In the quadrilateral spiral multiple tiling $\mathcal{T}$, we say that two quadrilateral tiles $T_1, T_2 \subset \mathcal{T}$ are *adjacent* if $\sharp(T_1 \cap T_2) > 1$, that is, $T_1 \cap T_2$ is a line segment with positive length, where $\sharp(T)$ denotes the potency of $T \subset \mathcal{T}$. That is, we do not say that T_1 and T_2 are not adjacent if $T_1 \cap T_2$ is a point or the empty set. For all $j \in \mathbb{Z}$, tiles T_j of a quadrilateral spiral multiple tiling $\mathcal{T}$ is adjacent to four tiles $T_{j\pm m}$ and $T_{j\pm n}$. In the phyllotaxis theory, the pair (m, n) of (4.1.2) is called the *parastichy pair* if T_0 is adjacent to T_m and T_n. Moreover, the parastichy pair $\{m, n\}$ is called an *opposed parastichy pair* if $\mathrm{Arg}(\zeta^m)\mathrm{Arg}(\zeta^n) < 0$ and a *non-opposed parastichy pair* if $\mathrm{Arg}(\zeta^m)\mathrm{Arg}(\zeta^n) > 0$.

Figure 4.1 shows two examples of quadrilateral spiral tilings with the divergence angle $\theta = 2\pi\tau$, where $\tau = \frac{1+\sqrt{5}}{2}$ is the golden section. The opposed parastichy pairs $\{13, 8\}$ and $\{13, 21\}$ are pairs of successive terms of the Fibonacci sequence. Figure 4.2 shows two examples of quadrilateral

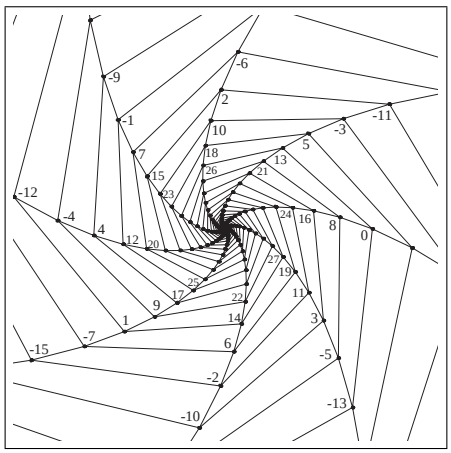

Figure 4.3: A quadrilateral spiral tiling with a non-opposed parastichy pair $\{13, 8\}$ generated by $\zeta = 0.97\mathrm{e}^{2\pi(1.627)\mathrm{i}}$.

spiral tilings with the divergence angle $\theta = 2\pi \cdot \frac{5+\sqrt{5}}{10}$. The opposed parastichy pairs $\{7, 11\}$ and $\{18, 11\}$ are pairs of successive terms of the Lucas sequence.

4.2 Continued fractions and quadrilateral spiral multiple tilings with opposed parastichy pairs

In the phyllotaxis theory, it is shown that the relationship between the opposed parastichy pair $\{m, n\}$ and the continued fraction approximation of $\theta/2\pi$. It has a natural extension to spiral multiple tilings as shown below.

Theorem 4.3. *Let $\zeta = r\mathrm{e}^{\mathrm{i}\theta} \in \mathbb{D}\backslash\mathbb{R}$. Let $m, n > 0$ be relatively prime integers. Suppose that $\zeta^m, \zeta^n \notin \mathbb{R}_-$. If (4.1.2) is a spiral multiple tiling and (m, n) is an opposed parastichy pair, then a/m, b/n are principal or intermediate convergents of $x = (\theta/2\pi + \ell)/v$, at least one of which is principal.*

Proof. We may suppose that $\mathrm{Arg}(\zeta^n) < 0 < \mathrm{Arg}(\zeta^m)$ without loss of generality. In the setting of the theorem 4.2, we have $\ell = a[\![n\theta/2\pi]\!] - b[\![m\theta/2\pi]\!]$ and $v = m[\![n\theta/2\pi]\!] - n[\![m\theta/2\pi]\!]$. Thus

$$n\left(\frac{\theta}{2\pi} + \ell\right) - bv = \frac{n\theta}{2\pi} - [\![\frac{n\theta}{2\pi}]\!] < 0 < \frac{m\theta}{2\pi} - [\![\frac{m\theta}{2\pi}]\!] = m\left(\frac{\theta}{2\pi} + \ell\right) - av,$$

and hence

$$\frac{a}{m} < \frac{1}{v}\left(\frac{\theta}{2\pi} + \ell\right) < \frac{b}{n}, \quad mb - na = 1. \tag{4.2.1}$$

Thus a/m, b/n are principal or intermediate convergents of $x = (\theta/2\pi + \ell)/v$, at least one of which is principal. □

Figure 4.3 shows an example of a quadrilateral spiral tiling with an non-opposed parastichy pair $\{13, 8\}$, where the divergence angle is $2\pi(1.627)$. This pair $\{13, 8\}$ is not a pair of denominators of two successive terms of convergents of 1.627 which satisfy the condition (4.2.1).

4.3 Triangular spiral multiple tilings

Let $m, n > 0$ be relatively prime integers. Let $\zeta = r\mathrm{e}^{\mathrm{i}\theta} \in \mathbb{D}\backslash\mathbb{R}$ with $0 < r < 1$, and suppose that $\zeta^m, \zeta^n \notin \mathbb{R}_-$. If three of the four points 1, ζ^m, ζ^{m+n} and ζ^n lie on a same line, then (4.1.2) becomes a triangular spiral multiple tiling. In this section, we consider triangular spiral multiple tilings given as a special case of quadrilateral spiral multiple tilings.

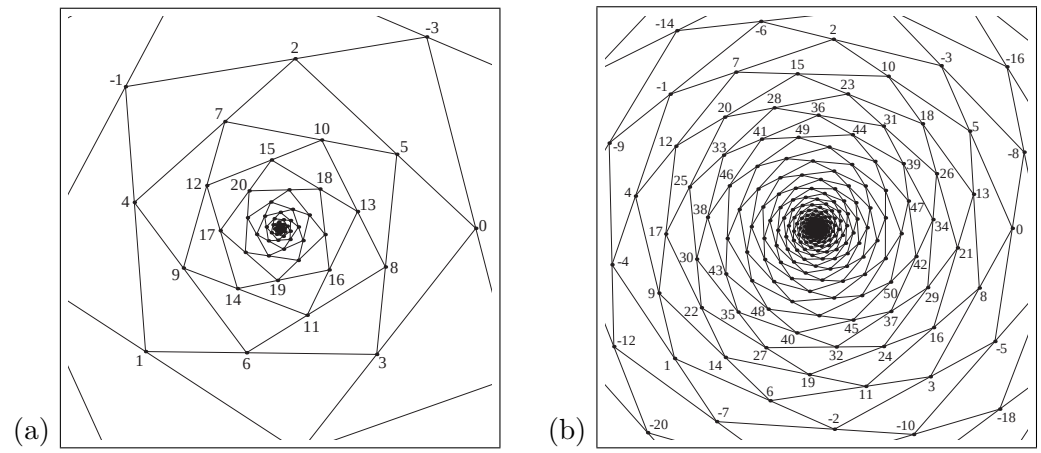

Figure 4.4: Phyllotactic triangular spiral tilings with the divergence angle $\theta = 2\pi\tau$. (a) $r = 0.9328\cdots$ and the opposed parastichy pair is $\{5, 3\}$. (b) $r = 0.9849\cdots$ and the opposed parastichy pair is $\{5, 8\}$.

Let

$$\phi_{m,k}(z) = \frac{z^k - 1}{z^m - 1} \tag{4.3.1}$$

be a rational function of one complex variable.

Lemma 4.4. *Let $m > n > 0$ be relatively prime integers. Let $\zeta = re^{i\theta} \in \mathbb{C}\backslash\mathbb{R}$, and suppose that $\zeta^m \neq 1$. Then the following conditions are mutually equivalent.*

(i) The three points ζ^m, ζ^{m+n} and ζ^n lie on a same line.

(ii) The four points 0, 1, ζ^m and ζ^n lie on a same circle.

(iii) $f_{m,n}(r, \theta) = 0$, where

$$f_{m,n}(r, \theta) := r^m \sin n\theta - r^n \sin m\theta + \sin(m - n)\theta. \tag{4.3.2}$$

(iv) $\phi_{m,m-n}(\zeta) \in \mathbb{R}$.

Proof. (i) $\Leftrightarrow$ (iv): We have $\zeta^m - \zeta^n = t(\zeta^{m+n} - \zeta^n)$ holds for some $t \in \mathbb{R}$.
(ii) $\Leftrightarrow$ (iv): The cross ratio of 1, ζ^m, ζ^{m+n} and ζ^n is given as $\phi_{m,m-n}(\zeta)$.
(iii) $\Leftrightarrow$ (iv): We have $\mathrm{Im}(\phi_{m,m-n}(\zeta)) = -\frac{|\zeta^{m-n}|}{|\zeta^m - 1|^2} f_{m,n}(r, \theta)$. □

Figure 4.4 shows two examples of triangular spiral tilings with the divergence angle $\theta = 2\pi\tau$, which are called Fibonacci Tornado. In Figure 4.4 (a), an opposed parastichy pair is $\{5, 3\}$. In Figure 4.4 (b), an opposed parastichy pair is $\{5, 8\}$. See [36, Fig.1] for a biological triangular spiral tiling by Suaeda vera. Figure 4.5 shows an origami development for the triangular spiral tiling of Figure 4.4 (a).

4.3.1 Triangles which admit spiral multiple tilings with opposed parastichy pairs

In this section, we consider shapes of triangles which admit spiral multiple tilings with opposed parastichy pairs.

Let $m, n > 0$ be relatively prime integers. Let $I = (-\pi, \pi]$ be a half-open interval, and consider an injective map

$$\iota_{m,n} : I \to I^2, \quad \iota_{m,n}(\theta) = \left(2\pi\langle\frac{m\theta}{2\pi}\rangle, 2\pi\langle\frac{n\theta}{2\pi}\rangle\right),$$

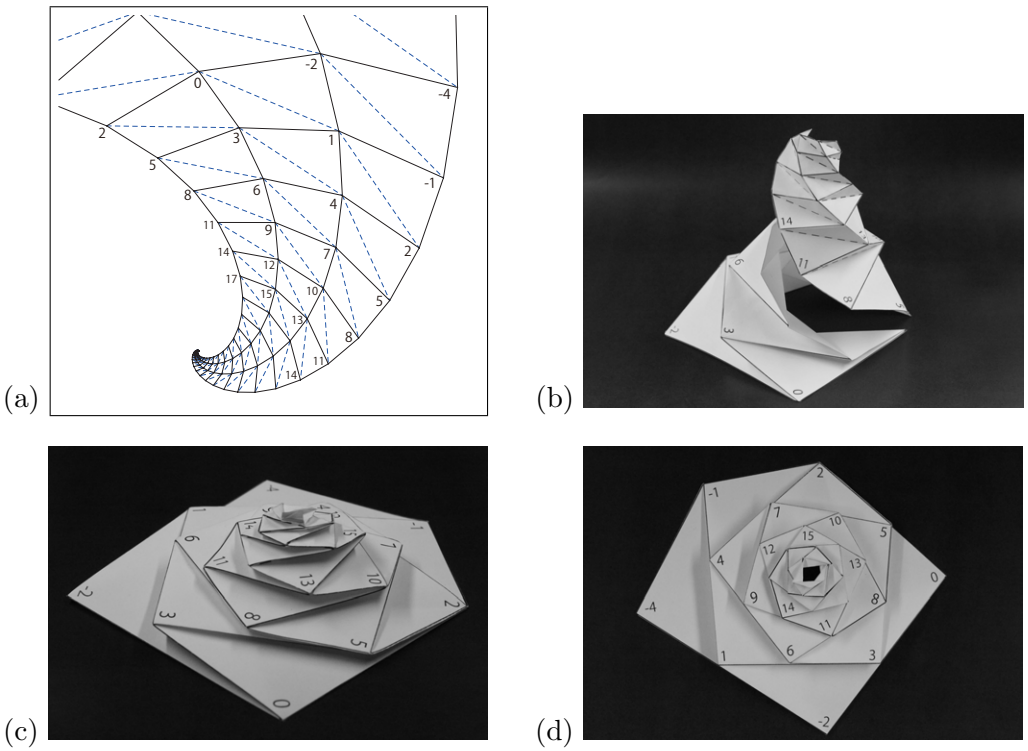

Figure 4.5: An origami for the phyllotactic triangular spiral tiling of Figure 4.4 (a). (a) An origami sheet. Solid lines are mountain fold and dashed lines are valley fold. (b) Side view from right, before squash. (c) Side view from right, after squashed. (d) Top-down view.

where $\langle x \rangle \in (-\frac{1}{2}, \frac{1}{2}]$ denotes a fractional part of $x \in \mathbb{R}$ such that $[\![x]\!] := x - \langle x \rangle \in \mathbb{Z}$. The image of $\iota_{m,n}$ is a *stripe* in the square I^2 written by

$$\iota_{m,n}(I) = \bigcup_{|v|<(m+n)/2} \{(\theta_1, \theta_2) \in I^2 : \ n\theta_1 - m\theta_2 = 2\pi v\}.$$

Let $\Delta = \Delta_+ \cup \Delta_-$,

$$\Delta_+ = \{(\theta_1, \theta_2) \in I^2 : \ 0 < \theta_1 < \theta_2 + \pi < \pi\},$$
$$\Delta_- = \{(\theta_1, \theta_2) \in I^2 : \ 0 < \theta_2 < \theta_1 + \pi < \pi\}.$$

Then $\iota_{m,n}(I) \cap \Delta$ is a union of line segments written by

$$\iota_{m,n}(I) \cap \Delta = \bigcup_{0<|v|<\frac{\max(m,n)}{2}} \ell_{m,n,v}, \quad \ell_{m,n,v} = \{(\theta_1, \theta_2) \in \Delta : n\theta_1 - m\theta_2 = 2\pi v\}.$$

Theorem 4.5. *Let $m > n > 0$ be relatively prime integers. Let $v > 0$ be an integer. The followings are mutually equivalent.*

(i) There exists $\zeta \in \mathbb{D}\backslash\mathbb{R}$ such that

$$\mathcal{T} = \{T_j = \square(\zeta^j, \zeta^{j+m}, \zeta^{j+m+n}, \zeta^{j+n}) = \triangle(\zeta^j, \zeta^{j+m}, \zeta^{j+n})\}_{j\in\mathbb{Z}} \tag{4.3.3}$$

is a triangular spiral multiple tiling of multiplicity v with an opposed parastichy pair $\{m, n\}$, where

$$|\angle(\zeta^{j+m}, \zeta^{j+n}, \zeta^j)| = \alpha \text{ and } |\angle(\zeta^j, \zeta^{j+m}, \zeta^{j+n})| = \beta \ (j \in \mathbb{Z}),$$

(ii) $n\alpha + m\beta = 2\pi v$.

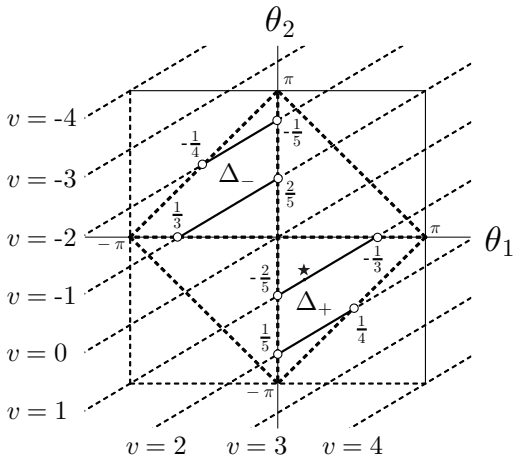

Figure 4.6: The set $\iota_{5,3}(I) \cap (\Delta_+ \cup \Delta_-)$ consisted of four solid lines, denotes the set of the pair of angles $\iota_{5,3}(\theta) = (2\pi\langle\frac{5\theta}{2\pi}\rangle, 2\pi\langle\frac{3\theta}{2\pi}\rangle)$ of triangles that admit spiral multiple tilings with an opposed parastichy pair $\{5, 3\}$. The dotted lines are the lines $3\theta_1 - 5\theta_2 = 2\pi v$, $-4 \le v \le 4$. For each endpoint $\iota_{5,3}(\theta)$ of a solid line, $\theta/2\pi$ is a rational number as shown in this figure. The mark $\bigstar$ denotes the point $\iota_{5,3}(2\pi\tau)$ which produce the triangular spiral tiling of Figure 4.4 (a).

(iii) $(\alpha, -\beta) \in \ell_{m,n,v}$,

Proof. (i) $\Rightarrow$ (ii): By taking complex conjugates if necessary, we may suppose that $\mathrm{Arg}(\zeta^n) < 0 < \mathrm{Arg}(\zeta^m)$. Since the quadrilateral $\square(1, \zeta^m, \zeta^{m+n}, \zeta^n)$ is a quadrilateral in this order of vertices, the three points ζ^m, ζ^{m+n} and ζ^n lie on a same line. By Lemma 4.4, the four points 0, 1, ζ^m and ζ^n lie on a same circle. Thus we have $\mathrm{Arg}(\zeta^m) = \alpha$, $\mathrm{Arg}(\zeta^n) = -\beta$, and hence $n\alpha + m\beta = 2\pi v$.
(ii) $\Leftrightarrow$ (iii): Obvious.
(iii) $\Rightarrow$ (i): We assume that $(\alpha, -\beta) \in \ell_{m,n,v}$. Let $\theta = \iota_{m,n}^{-1}(\alpha, -\beta) \in I_{m,n,v}$. Then we have $\sin m\theta > 0$, $\sin(-n\theta) > 0$ and $\sin(m-n)\theta > 0$, and so we have

$$\begin{aligned} f_{m,n,\theta}(0) &= \sin(m-n)\theta > 0, \\ f_{m,n,\theta}(1) &= (\cos n\theta - 1)\sin m\theta + (1 - \cos m\theta)\sin n\theta < 0, \\ df_{m,n,\theta}(r)/dr &= (mr^m \sin n\theta - nr^n \sin m\theta) < 0, \end{aligned}$$

where note that $f_{m,n}(r, \theta)$ is rewritten by $f_{m,n,\theta}(r)$ because θ is given. The Intermediate Value Theorem implies that the equation $f_{m,n,\theta}(r) = 0$ has a unique root $0 < r < 1$. Let $\zeta = re^{\mathrm{i}\theta}$. Then, since $f_{m,n,\theta}(r) = 0$, the three points ζ^m, ζ^{m+n} and ζ^n lie on a same line by Lemma 4.4. Since $\mathrm{Arg}(\zeta^n) < 0 < \mathrm{Arg}(\zeta^m)$, we have $\mathrm{Arg}(\zeta^n) < \mathrm{Arg}(\zeta^{m+n}) < \mathrm{Arg}(\zeta^m)$. So ζ^{m+n} lies on the line segment $\ell(\zeta^m, \zeta^n)$. Thus (4.3.3) is a spiral multiple tiling of multiplicity v with an opposed parastichy pair $\{m, n\}$. By Lemma 4.4 again, the four points 0, 1, ζ^m and ζ^n lie on a same circle, and so we have $\angle(\zeta^m, \zeta^n, 1) = \angle(\zeta^m, 0, 1) = \alpha$ and $\angle(1, \zeta^m, \zeta^n) = \angle(1, 0, \zeta^n) = \beta$. $\square$

The set $\iota_{5,3}(I) \cap \Delta_+$ in Figure 4.6 consisted of two solid lines, denotes the set of the pairs of angles $(\alpha, -\beta)$ in Theorem 4.5. The dotted lines are the lines $3\theta_1 - 5\theta_2 = 2\pi v$, $-4 \le v \le 4$. For each endpoint $\iota_{5,3}(\theta)$ of a solid line, $\theta/2\pi$ is a rational number as shown in this figure. The mark $\bigstar$ denotes the point $\iota_{5,3}(2\pi\tau)$ which produce the triangular spiral tiling of Figure 4.4 (a).

Let $R = \{(m, n) \in \mathbb{Z}^2 : \ m > n > 0 \text{ are relatively prime}\}$. Theorem 4.5 implies that for each $v > 0$, $L_v := \bigcup_{(m,n)\in R} \ell_{m,n,v} \subset \Delta_+$ is the set of shapes of triangles which admit spiral multiple tilings of multiplicity v with an opposed parastichy pair $\{m, n\}$.

Definition 4.6. *A set X is called a nowhere dense subset of a topological space if the interior of the closure of X is the empty set.*

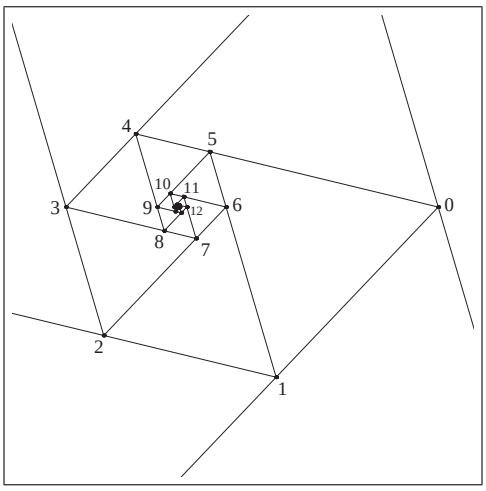

Figure 4.7: A spiral tiling by equilateral triangles. Opposed parastichy pair $\{m, n\} = \{5, 1\}$. $\theta = -\pi/3$, $r = 0.7548\cdots$. See Figures 4.8 for its origami development. The equilateral triangle does not admit a spiral tiling with a non-opposed parastichy pair.

Theorem 4.7. *For each $v > 0$, L_v is a nowhere dense subset of Δ_+. The union $L := \bigcup_{v>0} L_v$ is dense in Δ_+.*

Proof. Fix $v > 0$, and let $K \subset \Delta_+$ be a compact set. Since $\ell_{m,n,v} \subset [0, v/n] \times [-v/m, 0]$, K intersects $\ell_{m,n,v}$ for only finitely many $(m, n) \in R$. Hence L_v is nowhere dense. The union $L = \bigcup_{v>0} L_v = \bigcup_{(m,n)\in R} \iota_{m,n}(I) \cap \Delta_+$ is a union of stripes $\iota_{m,n}(I)$. Thus it is a dense subset of Δ_+. □

4.3.2 Examples of triangles which admit spiral multiple tilings with opposed parastichy pairs

By Theorem 4.5, we obtain the following examples of triangular spiral multiple tilings with opposed parastichy pairs.

(i) A spiral tiling by equilateral triangles: The equilateral triangle generates a spiral tiling with an opposed parastichy pair $\{5, 1\}$, of Figure 4.7, since $\frac{\pi}{3} + 5 \cdot \frac{\pi}{3} = 2\pi$. See figure 4.8 for its origami development. The generator $\zeta = re^{i\theta}$ is determined by the equation $\iota_{5,1}(\theta) = (\frac{\pi}{3}, -\frac{\pi}{3})$ and $r^5 + r - 1 = 0$, thus $\theta = -\frac{\pi}{3}$ and $r = 0.7548\cdots$.

(ii) A spiral multiple tiling by right triangles with angles 30°, 60° and 90°: The right triangle with angles 30° and 60° has a spiral multiple tiling of multiplicity $v = 2$ with an opposed parastichy pair $\{11, 2\}$, since $11 \cdot \frac{\pi}{3} + 2 \cdot \frac{\pi}{6} = 4\pi$. See Figure 4.9. The generator $\zeta = re^{i\theta}$ is given by the equation $\iota_{11,2}(\theta) = (\frac{\pi}{6}, -\frac{\pi}{3})$ and $\sqrt{3}r^{11} + r^2 - 2 = 0$, thus $\theta = -\pi/6$ and $r = 0.9581\cdots$. Figure 4.10(a) is its origami sheet, but the top-down view in Figure 4.10 (b) is apparently different from the multiple tiling in Figure 4.9. A problem is that the paper sheet is not penetrable. It is not possible to actualize a double-covering space of the punctured plane $\mathbb{C}^*$.

4.3.3 Generators of triangular spiral multiple tilings with opposed parastichy pairs

Let $m > n > 0$ be relatively prime integers. In this section, we consider a set of generators of triangular spiral multiple tilings for each opposed parastichy pair $\{m, n\}$.

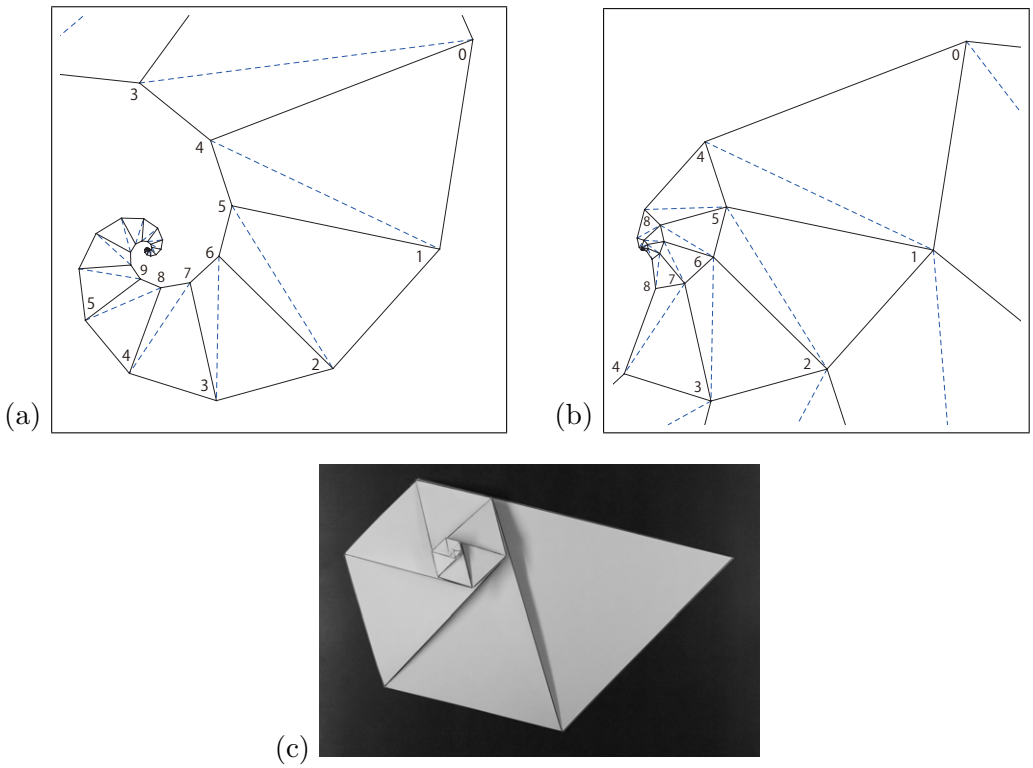

Figure 4.8: Two paper-folding sheets which build the same origami of Figure 4.7. (a) An origami sheet for beginners, very easy. (b) A sheet for experts, quite difficult. (c) Top-down view.

Lemma 4.8. *Let $m > n > 0$ be relatively prime integers. Let $\zeta \in \mathbb{C} \setminus \mathbb{R}$, and suppose that $\zeta^m, \zeta^n \notin \mathbb{R}$. The followings are mutually equivalent.*

(i) $|\zeta| < 1$, *and $\mathcal{T}$ in (4.3.3) is a triangular spiral multiple tiling with an opposed parastichy pair $\{m, n\}$.*

(ii) $\zeta \in P_{m,n}$ *where* $P_{m,n} := \{\zeta \in \mathbb{C}\setminus\mathbb{R} : \phi_{m,m-n}(\zeta) > 1\}$.

(iii) $\phi_{m,n}(1/\zeta) < 0$.

Proof. (i) $\Rightarrow$ (ii): We assume that ζ^{m+n} lies on the line segment $\ell(\zeta^m, \zeta^n)$. Then we have $(\zeta^m - \zeta^n) = t(\zeta^{m+n} - \zeta^n)$ for some $t > 1$. Thus $\phi_{m,m-n}(\zeta) > 1$ holds.
(ii) $\Rightarrow$ (i): We assume that $\phi_{m,m-n}(\zeta) > 1$. Then $(\zeta^m - \zeta^n) = t(\zeta^{m+n} - \zeta^n)$ holds for some $t > 1$. This implies that ζ^{m+n} lies on the line segment $\ell(\zeta^m, \zeta^n)$. Thus the quadrilateral $\square(1, \zeta^m, \zeta^{m+n}, \zeta^n)$ is a triangle with corners 1, ζ^m and ζ^n. Since ζ^{m+n} lies on the line segment $\ell(\zeta^m, \zeta^n)$, we have $|\zeta^{m+n}| < \max(|\zeta^m|, |\zeta^n|)$ on the line segment $\ell(\zeta^m, \zeta^n)$. Hence $|\zeta| < 1$. Since ζ^{m+n} lies in an angular region $\angle(\zeta^n, 1, \zeta^m)$, we obtain $\mathrm{Arg}(\zeta^m)\mathrm{Arg}(\zeta^n) < 0$.
(ii) $\Leftrightarrow$ (iii): This follows from the relation $\phi_{m,n}(1/\zeta) + \phi_{m,m-n}(\zeta) = 1$. □

Lemma 4.9. *Let $m > n > 0$ be relatively prime integers. Then we have $P_{m,n} = \bigcup_{0<|v|<m/2} P_{m,n,v}$, where*

$$P_{m,n,v} := \{\zeta \in P_{m,n} : n\mathrm{Arg}(\zeta^m) - m\mathrm{Arg}(\zeta^n) = 2\pi v\}.$$

For each $v \in \mathbb{Z}$ with $0 < |v| < m/2$, there exists a real analytic function $r : I_{m,n,v} \to \mathbb{R}$ such that the mapping

$$\varphi_{m,n,v} : I_{m,n,v} \to P_{m,n,v}, \qquad \varphi_{m,n,v}(\theta) = r(\theta)\mathrm{e}^{\mathrm{i}\theta},$$

is a homeomorphism.

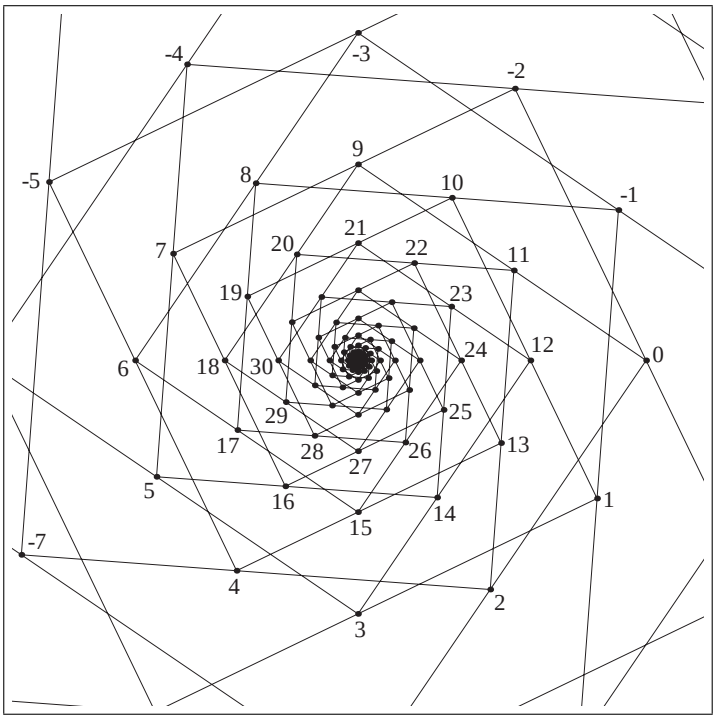

Figure 4.9: Spiral multiple tiling by right triangles with angles 30° and 60°, with multiplicity $v = 2$, opposed parastichy pair $\{m, n\} = \{11, 2\}$, $\theta = -\pi/6$, $r = 0.9581\cdots$.

(a)

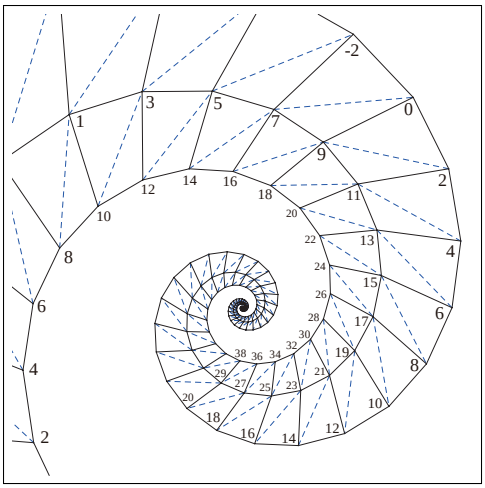

(b)

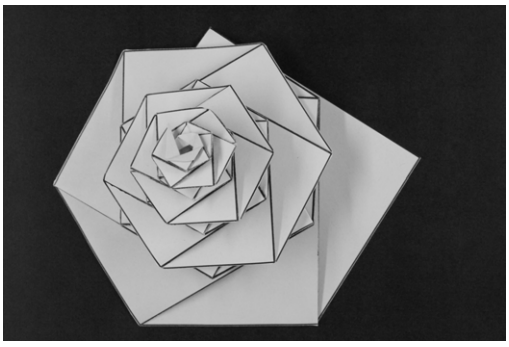

Figure 4.10: An origami development for the spiral multiple tiling of Figure 4.9. (a) An origami sheet. (b) Top-down view.

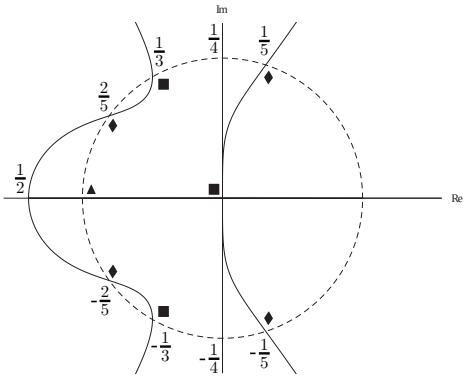

Figure 4.11: A real algebraic curve $\mathrm{Im}(\phi_{5,2}(\zeta)) = 0$. A rational number x on the unit circle denotes $\mathrm{e}^{2\mathrm{i}\pi x}$. The marks ▲, ■ and ♦ indicate the points ζ, where $\phi_{5,2}(\zeta) = 0$, 1 and ∞ respectively.

Proof. We have already shown that $r(\theta)$ is uniquely determined as a root of the equation $f_{m,n,\theta}(r) = 0$, in the proof of Theorem 4.5, where note that $f_{m,n}(r,\theta)$ is rewritten by $f_{m,n,\theta}(r) = 0$ because θ is given. □

Figure 4.11 shows the real algebraic curve $\mathrm{Im}(\phi_{5,2}(\zeta)) = 0$. Inside $\mathbb{D}\backslash\mathbb{R}$, it consists of four arcs $P_{5,3,v}$, $v = \pm 1, \pm 2$.

Lemma 4.10. *Let $m > n > 0$ be relatively prime integers and $0 < |v| < m/2$. Let a, b be integers such that $0 < b < a < m$ and $mb - na = 1$. The interval $I_{m,n,v}$ has an endpoint $2\pi\langle\frac{a}{m}\rangle$. The other endpoint of $I_{m,n,v}$ is given as follows: $2\pi\langle\frac{bv}{n}\rangle$ if $0 < |v| < \frac{n}{2}$; π if $v = \frac{n}{2}$; $-\pi$ if $v = -\frac{n}{2}$; $2\pi\langle\frac{(a-b)v+\frac{1}{2}}{m-n}\rangle$ if $\frac{n}{2} < v < \frac{m}{2}$; and $2\pi\langle\frac{(a-b)v-\frac{1}{2}}{m-n}\rangle$ if $-\frac{m}{2} < v < -\frac{n}{2}$.*

The arc $P_{m,n,v}$ has an endpoint $\lim_{\theta\to 2\pi\langle\frac{av}{m}\rangle}\varphi_{m,n,v}(\theta) = \mathrm{e}^{2\mathrm{i}\pi av/m}$. The other endpoint is given as follows: For $0 < |v| < n/2$, $\lim_{\theta\to 2\pi\langle\frac{bv}{n}\rangle}\varphi_{m,n,v}(\theta) = \mathrm{e}^{2\mathrm{i}\pi bv/n}$. For $|v| = n/2$, $\lim_{\theta\to\pi}\varphi_{m,n,v}(\theta) = -\tilde{r}$, where $\tilde{r}$ is a unique positive root of the equation

$$m - n = m\tilde{r}^n + n\tilde{r}^m. \tag{4.3.4}$$

For $n/2 < |v| < m/2$, $\lim_{\theta\to 2\pi\langle\frac{(a-b)v\pm\frac{1}{2}}{m-n}\rangle}\varphi_{m,n,v}(\theta) = 0$.

Proof. First, we see that $\iota_{m,n}(2\pi\langle\frac{av}{m}\rangle) = (0, -\frac{2\pi v}{m})$. Second, we see the other endpoint as follows. If $0 < |v| < \frac{n}{2}$, we have $\iota_{m,n}(2\pi\langle\frac{bv}{n}\rangle) = (\frac{2\pi v}{n}, 0)$. If $\frac{n}{2} < v < \frac{m}{2}$, $\iota_{m,n}(2\pi\langle\frac{(a-b)v+\frac{1}{2}}{m-n}\rangle) = (\frac{m-2v}{m-n}\pi, \frac{n-2v}{m-n}\pi)$ lies on the boundary line $\theta_1 - \theta_2 = \pi$ of Δ_+. If $\frac{-m}{2} < v < \frac{-n}{2}$, $\iota_{m,n}(2\pi\langle\frac{(a-b)v-\frac{1}{2}}{m-n}\rangle) = (\frac{-m-2v}{m-n}\pi, \frac{-n-2v}{m-n}\pi)$ lies on the boundary line $\theta_2 - \theta_1 = \pi$ of Δ_-. For each candidate θ of the endpoint of $I_{m,n,v}$, we confirm that $\iota_{m,n}(\theta)$ lies on the line $n\theta_1 - m\theta_2 = 2\pi v$.

Finally, we prove the latter half of Lemma 4.10. Note that $f_{m,n}(r,\theta)$ is rewritten by $f_{m,n,\theta}(r) = 0$ because θ is given. As $\theta \to 2\pi\langle\frac{av}{m}\rangle$ or $\theta \to 2\pi\langle\frac{bv}{n}\rangle$, we have $\sin m\theta \to 0$ or $\sin n\theta \to 0$ respectively, so the positive root r of the equation $f_{m,n,\theta}(r) = 0$ tends to 1. As $\theta \to 2\pi\langle\frac{(a-b)v\pm\frac{1}{2}}{m-n}\rangle$, we have $\sin(m-n)\theta \to 0$, so $r \to 0$. As $\theta \to \pi$, we have all $\sin m\theta, \sin n\theta, \sin(m-n)\theta \to 0$, so the limit $\tilde{r}$ of r is a root of (4.3.4). □

Figure 4.12 shows the stripe $\iota_{7,4}(I) \cap (\Delta_+ \cup \Delta_-)$ and the real algebraic curve $\mathrm{Im}(\phi_{7,3}(\zeta)) = 0$. At the endpoints of each arc $P_{7,4,v}$, $v = \pm 1, \pm 2, \pm 3$, we have $\phi_{7,3}(\zeta) = 1, \infty$. This example shows the three types of intervals in Lemma 4.10. The interval $I_{7,4,1} = 2\pi(-2/7, -1/4)$ corresponds to the line segment $\ell_{7,4,1}$ with endpoints on the θ_j-axis, $j = 1, 2$, and the arc $P_{7,4,1}$ with endpoints on the unit circle. For $I_{7,4,2} = 2\pi(3/7, 1/2)$, the line segment $\ell_{7,4,2}$ has an endpoint $(\pi, 0)$ on the corner of I^2, and the arc $P_{7,4,2}$ has an endpoint -0.7644 on the real axis which is a critical

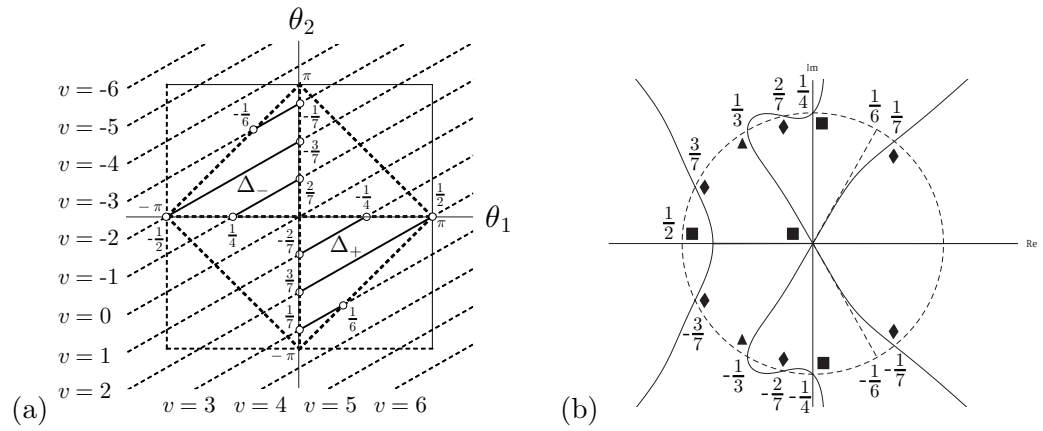

Figure 4.12: (a) The stripe $\iota_{7,4}(I) \cap (\Delta_+ \cup \Delta_-)$ consists of six solid lines. (b) The six arcs $P_{7,4,v}$, $v = \pm1, \pm2, \pm3$, connect ■ and ♦ on the real algebraic curve $\mathrm{Im}(\phi_{7,3}(\zeta)) = 0$.

point of the function $\phi_{7,3}(\zeta)$, where $\tilde{r} = 0.7644$ is a root of the equation $3 = 7\tilde{r}^4 + 4\tilde{r}^7$. For $I_{7,4,3} = 2\pi(1/7, 1/6)$, the line segment $\ell_{7,4,3}$ has an endpoint on the line $\theta_1 - \theta_2 = \pi$, and the arc $P_{7,4,3}$ has an endpoint at the origin. $1, 3, 4, 7, 11, 18, \ldots$ is the Lucas sequence.

In Theorem 4.3, a/m and b/n in (4.2.1) are successive convergents of $x = \frac{1}{v}(\frac{\theta}{2\pi} + \ell)$. The next (principal or intermediate) convergent is given as the Farey sum $(a+b)/(m+n)$. Thus we obtain

$$I_{m,n,v} \setminus \left\{ 2\pi\langle \frac{a+b}{m+n} \rangle \right\} \subset I_{m+n,n,v} \cup I_{m+n,m,v}.$$

The following Lemma shows that the plastochrone ratio $1/|\zeta|$ decreases in the *parastichy transition* $\{m, n\} \to \{m+n, n\}$ or $\{m+n, m\}$. In particular, the arcs $P_{m+n,n,v}$ and $P_{m+n,m,v}$ do not intersect $P_{m,n,v}$ in $\mathbb{D}$.

Lemma 4.11. *Let $\theta \in I_{m,n,v}$, $r_1 \mathrm{e}^{\mathrm{i}\theta} \in P_{m,n,v}$ and $r_2 \mathrm{e}^{\mathrm{i}\theta} \in P_{m+n,n,v} \cup P_{m+n,m,v}$. Then $r_1 < r_2$.*

Proof. Without loss of generality, we may suppose that $v > 0$ and $r_2 \mathrm{e}^{\mathrm{i}\theta} \in P_{m+n,n,v}$. By the equation $f_{m,n,\theta}(r) = 0$, we have

$$(r_1^m - \cos m\theta) \sin n\theta = (r_1^n - \cos n\theta) \sin m\theta. \tag{4.3.5}$$

Let $f_{m+n,n,\theta}(r) = r^{m+n} \sin n\theta - r^n \sin(m+n)\theta + \sin m\theta$. It is a decreasing function of r, because $\sin n\theta, -\sin(m+n)\theta < 0$. We have $f_{m+n,n,\theta}(r_2) = 0$ by $f_{m,n,\theta}(r) = 0$ and

$$\begin{aligned} f(r_1) &= r_1^n (r_1^m - \cos m\theta) \sin n\theta + (1 - r_1^n \cos n\theta) \sin m\theta \\ &= (r_1^{2n} - 2r_1^n \cos n\theta + 1) \sin m\theta > 0 \end{aligned}$$

by (4.3.5). Hence $r_1 < r_2$. □

Let $P_v := \bigcup_{(m,n)\in R} P_{m,n,v}$ for $v \neq 0$. Lemma 4.11 implies that for each $v \neq 0$, P_v is not a dense subset of $\mathbb{D}$. However, we have the following result.

Theorem 4.12. *The union $P := \bigcup_{v\neq 0} P_v$ is a dense subset of $\mathbb{D}$.*

Proof. Denote by $\delta(\theta) := \{r\mathrm{e}^{\mathrm{i}\theta} : 0 < r < 1\}$ a radial line segment of $\mathbb{D}^* = \mathbb{D} \setminus \{0\}$. We show that a radial line segment $\delta(2\pi\langle \frac{bv}{n} \rangle)$ is contained in the closure of P_v whenever $1 \le b < n < 2v$.

We may assume that n, b are relatively prime. Let $0 \le a_0 < m_0 < n$ be integers such that $m_0 b - n a_0 = 1$. Let $m_j = nj + m_0$ and $a_j = bj + a_0$ for $j > 0$. Then we have $m_j b - n a_j = 1$, and $a_j/m_j \to b/n$ as $j \to +\infty$. For a sufficiently large j, we have $\frac{n}{2} < v < \frac{m_j}{2}$, so the curve $P_{m_j,n,v}$ connects the m_j-th root of unity $\mathrm{e}^{2\pi\mathrm{i}a_j v/m_j}$ with the origin, by Lemma 4.10. As $j \to +\infty$, the length of the interval $I_{m_j,n,v}$ tends to 0. Thus the curves $P_{m_j,n,v}$ accumulate to $\delta(2\pi\langle \frac{bv}{n} \rangle)$ as $j \to +\infty$. □

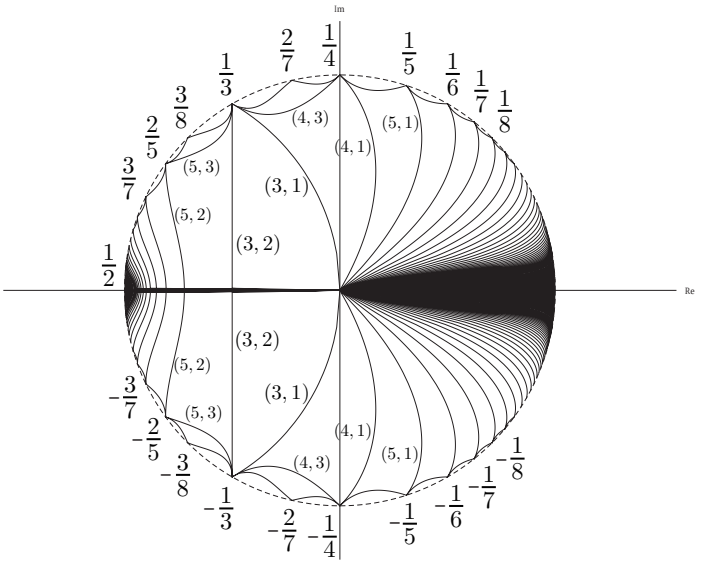

Figure 4.13: The set $P_1 \cup P_{-1}$ of generators for triangular spiral tilings with opposed parastichy pairs. The arcs $P_{m,n,1}$ and $P_{m,n,-1}$ are denoted by $\{m, n\}$. Compare this figure with a diagram on the topology of knot complements [23, Fig.4]. The arcs $P_{m,1,\pm 1}$ accumulate to the interval $[0, 1]$ on the real axis as $m \to \infty$. The arcs $P_{2k+1,2,\pm 1}$ tending to the boundary point -1 (marked $\frac{1}{2}$) as $k \to \infty$.

Figure 4.13 indicates that the arcs $P_{m,1,\pm 1}$ accumulate to the unit interval $[0, 1] = \delta(0)$ as $m \to \infty$.

4.3.4 Generators of triangular spiral multiple tilings with non-opposed parastichy pairs

Let $m, n > 0$ be relatively prime integers. In this section, we consider a set of generators of triangular spiral multiple tilings for each non-opposed parastichy pair $\{m, n\}$.

Theorem 4.13. *Let $m, n > 0$ be relatively prime integers. Let $v > 0$ be an integer. Then the followings are mutually equivalent.*

(i) There exists $\zeta \in \mathbb{D}\backslash\mathbb{R}$ such that

$$\mathcal{T} = \{T_j = \square(\zeta^j, \zeta^{j+m}, \zeta^{j+m+n}, \zeta^{j+n}) = \triangle(\zeta^j, \zeta^{j+m}, \zeta^{j+m+n})\}_{j\in\mathbb{Z}} \tag{4.3.6}$$

is a triangular spiral multiple tiling of multiplicity v with a non-opposed parastichy pair $\{m, n\}$, where

$$|\angle(\zeta^{j+m}, \zeta^{j+m+n}, \zeta^j)| = \alpha \text{ and } |\angle(\zeta^{j+m+n}, \zeta^j, \zeta^{j+m})| = \beta$$

for all $j \in \mathbb{Z}$.

(ii) $n\alpha - m\beta = 2\pi v$ and there exists $0 < r < 1$ such that

$$\sin\beta = r^m \sin(\alpha + \beta) - r^{m+n} \sin\alpha. \tag{4.3.7}$$

Proof. (i) $\Rightarrow$ (ii): By the assumption (i), the quadrilateral $\square(1, \zeta^m, \zeta^{m+n}, \zeta^n)$ is the triangle $\triangle(1, \zeta^m, \zeta^{m+n})$. So ζ^n lies on the line segment $\ell(1, \zeta^{m+n})$. Then we have $\zeta^n - 1 = t(\zeta^{m+n} - 1)$ for any $0 < t < 1$, and hence $0 < \phi_{m+n,n}(\zeta) < 1$. By Lemma 4.4, the four points 0, 1, ζ^m and

ζ^{m+n} lie on a same circle. Thus we have $|\angle(\zeta^m, \zeta^{m+n}, 1)| = \mathrm{Arg}(\zeta^m) = \alpha$ and $|\angle(\zeta^{m+n}, 1, \zeta^m)| = \mathrm{Arg}(\zeta^n) = \beta$ for any $j \in \mathbb{Z}$, and hence $n\alpha - m\beta = 2\pi v$. Since $0 < \phi_{m+n,n}(\zeta) < 1$, we have

$$\mathrm{Im}(\phi_{m+n,n}(\zeta)) = \frac{r^n(-r^{m+n}\sin m\theta - \sin n\theta + r^m \sin(m+n)\theta)}{|\zeta^{m+n} - 1|^2} = 0,$$

and hence we obtain the equation (4.3.7).
(ii) $\Rightarrow$ (i): Since $(\alpha, \beta) \in \iota_{m,n}(I)$, there exists a unique $\theta \in I$ such that $\iota_{m,n}(\theta) = (\alpha, \beta)$. Let $\zeta = re^{\mathrm{i}\theta}$. By Lemma 4.4, the four points 0, 1, ζ^m and ζ^{m+n} lie on a same circle, so we have $\phi_{m+n,n}(\zeta) \in \mathbb{R}$. $|\angle(\zeta^{j+m}, \zeta^{j+m+n}, \zeta^j)| = \mathrm{Arg}(\zeta^m) = \alpha$ and $|\angle(\zeta^{j+m+n}, \zeta^j, \zeta^{j+m})| = \mathrm{Arg}(\zeta^n) = \beta$. The three points $\mathrm{A}_{m+n}, \mathrm{A}_{2m+n}$ and A_m are collinear, so the three points $\mathrm{A}_n, \mathrm{A}_{m+n}$ and A_0 are also collinear. Since $\mathrm{Arg}(\zeta^m), \mathrm{Arg}(\zeta^n) > 0$, we have $\mathrm{Arg}(\zeta^{m+n}) > \mathrm{Arg}(\zeta^n) > 0$, so ζ^n lies on the line segment $\ell(1, \zeta^{m+n})$. Thus (4.3.6) is a triangular spiral multiple tiling with a non-opposed parastichy pair $\{m, n\}$. □

Lemma 4.14. *Let $m, n > 0$ be relatively prime integers. Let $\zeta \in \mathbb{D} \setminus \mathbb{R}$. Then the followings are mutually equivalent.*

(i) $\mathcal{T} = \{T_j = \square(\zeta^j, \zeta^{j+m}, \zeta^{j+m+n}, \zeta^{j+n}) = \triangle(\zeta^j, \zeta^{j+m}, \zeta^{j+m+n})\}_{j\in\mathbb{Z}}$ *is a triangular spiral multiple tiling with a non-opposed parastichy pair $\{m, n\}$.*

(ii) $\zeta \in Q_{m,n}$, *where* $Q_{m,n} := \{\zeta \in \mathbb{D} \setminus \mathbb{R} : 0 < \phi_{m+n,n}(\zeta) < 1\}$.

(iii) $0 < \phi_{m+n,m}(1/\zeta) < 1$.

Proof. (i) $\Rightarrow$ (ii): By the assumption (i), the quadrilateral $\square(1, \zeta^m, \zeta^{m+n}, \zeta^n)$ is the triangle $\triangle(1, \zeta^m, \zeta^{m+n})$. So ζ^n lies on the line segment $\ell(1, \zeta^{m+n})$, that is, we have $\zeta^n = t\zeta^{m+n} + 1 - t$ for some $0 < t < 1$, so we obtain $0 < \phi_{m+n,n}(\zeta) < 1$.
(ii) $\Rightarrow$ (i): If $0 < \phi_{m+n,n}(\zeta) < 1$, then $(\zeta^n - 1) = t(\zeta^{m+n} - 1)$ for some $0 < t < 1$. This implies that ζ^n lies on the line segment $\ell(1, \zeta^{m+n})$. Thus the quadrilateral $\square(1, \zeta^m, \zeta^{m+n}, \zeta^n)$ is the triangle $\triangle(1, \zeta^m, \zeta^{m+n})$. Since the angular region $\angle(\zeta^n, 0, 1)$ is contained in the angular region $\angle(\zeta^{m+n}, 0, 1)$, we obtain $\mathrm{Arg}(\zeta^m)\mathrm{Arg}(\zeta^n) > 0$.
(ii) $\Leftrightarrow$ (iii): This follows from $\phi_{m+n,n}(\zeta) + \phi_{m+n,m}(1/\zeta) = 1$. □

We have $Q_{m,n} = \bigcup_{0<|v|<n/2} Q_{m,n,v}$, where

$$Q_{m,n,v} := \{\zeta \in Q_{m,n} :\ n\mathrm{Arg}(\zeta^m) - m\mathrm{Arg}(\zeta^n) = 2\pi v\}.$$

We will give a parameterization of each arc $Q_{m,n,v}$ by r. Let $\Delta' = \Delta'_+ \cup \Delta'_-$,

$$\Delta'_+ = \{(\theta_1, \theta_2) \in I^2 :\ \theta_1, \theta_2 > 0, \theta_1 + \theta_2 < \pi\},$$
$$\Delta'_- = \{(\theta_1, \theta_2) \in I^2 :\ \theta_1, \theta_2 < 0,\ \theta_1 + \theta_2 > -\pi\}.$$

Let

$$\ell'_{m,n,v} = \{(\theta_1, \theta_2) \in \Delta' :\ n\theta_1 - m\theta_2 = 2\pi v\}$$

for $0 < |v| < n/2$. Let $a, b > 0$ be integers such that $mb - na = 1$, $0 < \frac{a}{m} < \frac{b}{n} < 1$. Then the interval $I'_{m,n,v} := \iota^{-1}_{m,n}(\ell'_{m,n,v})$ is written as $I'_{m,n,v} = (2\pi\langle\frac{bv}{n}\rangle, 2\pi\langle\frac{(a+b)v+\frac{1}{2}}{m+n}\rangle)$ for $0 < v < \frac{n}{2}$; $I'_{m,n,v} = (2\pi\langle\frac{(a+b)v-\frac{1}{2}}{m+n}\rangle, 2\pi\langle\frac{bv}{n}\rangle)$ for $-\frac{n}{2} < v < 0$.

Theorem 4.15. *For each $v \in \mathbb{Z}$ with $0 < |v| < \frac{n}{2}$, there exists a real analytic function $\theta_{m,n,v} : (0,1) \to I'_{m,n,v}$ such that the function $\zeta(r) = r\exp(\mathrm{i}\theta_{m,n,v}(r))$ is a homeomorphism of the unit interval $(0,1)$ onto $Q_{m,n,v}$. Moreover, we have*

$$\lim_{r\to 0}\theta_{m,n,v}(r) = \lim_{r\to 1}\theta_{m,n,v}(r) = 2\pi\langle\frac{bv}{n}\rangle. \tag{4.3.8}$$

Proof. Suppose that $v > 0$ without loss of generality. For each $v \in \mathbb{Z}$ with $0 < v < n/2$, we have the interval $I'_{m,n,v} = (2\pi\langle\frac{bv}{n}\rangle, 2\pi\langle\frac{(a+b)v+\frac{1}{2}}{m+n}\rangle)$. Fix $0 < r < 1$. For $\theta = 2\pi\langle\frac{bv}{n}\rangle$, we have

$$\begin{aligned}\mathrm{Arg}(\phi_{m+n,n}(\zeta)) &= \mathrm{Arg}(r^n - 1) - \mathrm{Arg}(\zeta^{m+n} - 1)\\ &= \pi - \mathrm{Arg}(\zeta^{m+n} - 1)\\ &= \pi - \pi - \mathrm{Arg}(1 - \zeta^{m+n})\\ &= -\mathrm{Arg}(1 - \zeta^{m+n}) > 0;\end{aligned}$$

For $\theta = 2\pi\langle\frac{(a+b)v+\frac{1}{2}}{m+n}\rangle$, we have

$$\begin{aligned}\mathrm{Arg}(\phi_{m+n,n}(\zeta)) &= \mathrm{Arg}(\zeta^n - 1) - \mathrm{Arg}(-r^{m+n} - 1)\\ &= \mathrm{Arg}(\zeta^n - 1) - \pi - \mathrm{Arg}(r^{m+n} + 1)\\ &= \pi + \mathrm{Arg}(1 - \zeta^n) - \pi\\ &= \mathrm{Arg}(1 - \zeta^n) < 0.\end{aligned}$$

The Intermediate Value Theorem implies that for each $0 < r < 1$, there exists $\zeta = r\mathrm{e}^{\mathrm{i}\theta}$, $\theta \in I'_{m,n,v}$ such that $\mathrm{Arg}(\phi_{m+n,n}(\zeta)) = 0$, and hence $\phi_{m+n,n}(\zeta) \in \mathbb{R}$. Since $\mathrm{Arg}(\zeta^{m+n}) > \mathrm{Arg}(\zeta^n) > 0$, we have $|\zeta^n - 1| < |\zeta^{m+n} - 1|$, $0 < \phi_{m+n,n}(\zeta) < 1$, and hence $\zeta \in Q_{m,n,v}$.

The uniqueness of $\theta \in I'_{m,n,v}$ shall follow if we show that

$$\frac{\partial}{\partial\theta}\mathrm{Arg}(\phi_{m+n,n}(\zeta)) < 0 \text{ for } \zeta \in Q_{m,n,v},$$

or equivalently,

$$\frac{\partial}{\partial\theta}\mathrm{Im}(\phi_{m+n,n}(\zeta)) < 0 \text{ for } \zeta \in Q_{m,n,v}.$$

For $z = \hat{r}\mathrm{e}^{\mathrm{i}\hat{\theta}} \in \mathbb{D}$, let

$$\hat{\rho}(\hat{r}, \hat{\theta}) := \frac{\hat{r}\sin\hat{\theta}}{1 - \hat{r}\cos\hat{\theta}} = \tan\angle\mathrm{ZA_0O},$$

where Z denotes the point with the complex coordinate z. Then we have

$$\frac{|1 - \zeta^{m+n}|^2}{\mathrm{Re}(1 - \zeta^n)\mathrm{Re}(1 - \zeta^{m+n})}\mathrm{Im}(\phi_{m+n,n}(\zeta)) = \hat{\rho}(r^{m+n}, (m+n)\theta) - \hat{\rho}(r^n, n\theta).$$

Let $E = \{z \in \mathbb{D} : |z - \frac{1}{2}| < \frac{1}{2}\} = \{z = \hat{r}\mathrm{e}^{\mathrm{i}\hat{\theta}} : \hat{r} < \cos\hat{\theta}\}$ be a disk consisting of the points Z such that $\cos\angle\mathrm{OZA_0} < 0$.

Lemma 4.16. *$\zeta^n \in E$ if $\zeta \in Q_{m,n,v}$.*

Proof. It is easy to see that for $z \in \mathbb{C}$, there exists $\lambda > 1$ such that $|\lambda(z-1)+1| < |z|$, if and only if $z \in E$.

Let $\lambda = (\zeta^{m+n} - 1)/(\zeta^n - 1)$. Then we have $\lambda > 1$ and $|\zeta^{m+n}| = |\lambda(\zeta^n - 1) + 1| < |\zeta^n|$. Thus we obtain $\zeta^n \in E$. □

Lemma 4.17. *$\frac{\partial}{\partial\theta}\mathrm{Im}(\phi_{m+n,n}(\zeta)) < 0$, if $\zeta = r\mathrm{e}^{\mathrm{i}\theta} \in Q_{m,n,v}$ and $\zeta^{m+n} \notin E$.*

Proof. For $z = \hat{r}\mathrm{e}^{\mathrm{i}\hat{\theta}}$, we have $\frac{\partial\hat{\rho}}{\partial\hat{\theta}}(\hat{r}, \hat{\theta}) = \frac{\hat{r}(\cos\hat{\theta} - \hat{r})}{(1 - \hat{r}\cos\hat{\theta})^2}$, so $z \in E \Leftrightarrow \frac{\partial\hat{\rho}}{\partial\hat{\theta}} > 0$. Thus, if $\zeta = r\mathrm{e}^{\mathrm{i}\theta} \in Q_{m,n,v}$ and $\zeta^{m+n} \notin E$, we obtain

$$\frac{\partial\hat{\rho}}{\partial\hat{\theta}}(r^{m+n}, (m+n)\theta) \le 0 < \frac{\partial\hat{\rho}}{\partial\hat{\theta}}(r^n, n\theta),$$

and hence $\frac{\partial}{\partial\theta}\mathrm{Im}(\phi_{m,n}(\zeta)) < 0$. □

Now suppose that $\zeta \in Q_{m,n,v}$ and $\zeta^{m+n} \in E$. For $z = \hat{r}\mathrm{e}^{\mathrm{i}\hat{\theta}} \in E$, consider two coordinate systems as follows.

$$\varphi_1 : E \to \mathbb{R}^2, \quad \varphi_1(z) = (\hat{r}, \hat{\theta}) = (|z|, \arg z),$$
$$\varphi_2 : E \to \mathbb{R}^2, \quad \varphi_2(z) = (\hat{r}, \hat{\rho}) = (\hat{r}, \frac{\hat{r}\sin\hat{\theta}}{1 - \hat{r}\cos\hat{\theta}}), \quad \text{where } (\hat{r}, \hat{\theta}) = \varphi_1(z).$$

The derivative of the coordinate changes are written as

$$\begin{pmatrix} \frac{\partial\hat{r}}{\partial\hat{r}} & \frac{\partial\hat{r}}{\partial\hat{\theta}} \\ \frac{\partial\hat{\rho}}{\partial\hat{r}} & \frac{\partial\hat{\rho}}{\partial\hat{\theta}} \end{pmatrix} = \begin{pmatrix} 1 & 0 \\ \frac{\sin\hat{\theta}}{(1-\hat{r}\cos\hat{\theta})^2} & \frac{\hat{r}(\cos\hat{\theta} - \hat{r})}{(1-\hat{r}\cos\hat{\theta})^2} \end{pmatrix},$$
$$\begin{pmatrix} \frac{\partial\hat{r}}{\partial\hat{r}} & \frac{\partial\hat{r}}{\partial\hat{\rho}} \\ \frac{\partial\hat{\theta}}{\partial\hat{r}} & \frac{\partial\hat{\theta}}{\partial\hat{\rho}} \end{pmatrix} = \begin{pmatrix} 1 & 0 \\ \frac{-\sin\hat{\theta}}{\hat{r}(\cos\hat{\theta} - \hat{r})} & \frac{(1-\hat{r}\cos\hat{\theta})^2}{\hat{r}(\cos\hat{\theta} - \hat{r})} \end{pmatrix}.$$

Lemma 4.18. *Let $0 < r_1 < r_2 < 1$, $0 < \rho_1 < \rho_2$ and suppose that $(r_i, \rho_j) \in \varphi_2(E)$, $i, j = 1, 2$. Then*

$$\frac{\partial\hat{\theta}}{\partial\hat{\rho}}(r_2, \rho_2)\frac{\partial\hat{\theta}}{\partial\hat{\rho}}(r_1, \rho_1) < \frac{\partial\hat{\theta}}{\partial\hat{\rho}}(r_2, \rho_1)\frac{\partial\hat{\theta}}{\partial\hat{\rho}}(r_1, \rho_2).$$

Proof. The ratio $\frac{\partial\hat{\theta}}{\partial\hat{\rho}}(r_2, \rho)/\frac{\partial\hat{\theta}}{\partial\hat{\rho}}(r_1, \rho)$ is a strictly decreasing function of ρ, since

$$\begin{aligned} &\frac{\partial}{\partial\hat{\rho}}(\log\frac{\partial\hat{\theta}}{\partial\hat{\rho}}(r_2, \hat{\rho}) - \log\frac{\partial\hat{\theta}}{\partial\hat{\rho}}(r_1, \hat{\rho})) \\ &= \int_{r_1}^{r_2} \frac{\partial^2}{\partial\hat{\rho}\partial\hat{r}} \log\frac{\partial\hat{\theta}}{\partial\hat{\rho}}(\hat{r}, \hat{\rho})\, d\hat{r} \\ &= \int_{r_1}^{r_2} \frac{(1-\hat{r}\cos\hat{\theta})^2(-2 + \hat{r}\cos\hat{\theta} + \hat{r}^2)\sin\hat{\theta}}{\hat{r}^2(\hat{r} - \cos\hat{\theta})^4}\, d\hat{r} < 0. \end{aligned}$$

□

Fix $0 < r < 1$. Let $\rho_{m+n}(\theta) := \hat{\rho}(r^{m+n}, (m+n)\theta)$, $\rho_n(\theta) := \hat{\rho}(r^n, n\theta)$ for $\theta \in I'_{m,n,v}$, and consider their inverse functions $\theta_{m+n}(\rho)$, $\theta_n(\rho)$ respectively. Note that

$$\frac{d}{d\hat{\rho}}\theta_{m+n}(\hat{\rho}) = \frac{1}{m+n}\frac{\partial\hat{\theta}}{\partial\hat{\rho}}(r^{m+n}, \hat{\rho}), \quad \frac{d}{d\hat{\rho}}\theta_n(\hat{\rho}) = \frac{1}{n}\frac{\partial\hat{\theta}}{\partial\hat{\rho}}(r^m, \hat{\rho}). \tag{4.3.9}$$

Lemma 4.19. *$\frac{\partial}{\partial\theta}\mathrm{Im}(\phi_{m+n,n}(\zeta)) < 0$, if $\zeta = r_0\mathrm{e}^{\mathrm{i}\theta_0} \in Q_{m,n,v}$, $\theta_0 \in I'_{m,n,v}$ and $\zeta^{m+n} \in E$.*

Proof. Denote by $\hat{\rho}_0 := \hat{\rho}_{m+n}(\theta_0) = \hat{\rho}_n(\theta_0)$. Suppose that $\frac{\partial}{\partial\theta}\mathrm{Im}(\phi_{m+n,n}(\zeta)) \geq 0$ by contradiction. This implies that $\frac{d}{d\theta}\hat{\rho}_{m+n}(\theta_0) \geq \frac{d}{d\theta}\hat{\rho}_n(\theta_0)$. By considering their inverse functions, we have $\frac{d}{d\hat{\rho}}\theta_{m+n}(\hat{\rho}_0) \leq \frac{d}{d\hat{\rho}}\theta_n(\hat{\rho}_0)$. Lemma 4.18 and (4.3.9) imply that

$$\frac{d}{d\hat{\rho}}\theta_{m+n}(\hat{\rho}) < \frac{d}{d\hat{\rho}}\theta_n(\hat{\rho}), \qquad 0 < \hat{\rho} < \hat{\rho}_0.$$

The mean value theorem implies that $|\theta_{m+n}(\hat{\rho}_0) - \theta_{m+n}(\hat{\rho})| < |\theta_n(\hat{\rho}_0) - \theta_n(\hat{\rho})|$, $0 \leq \hat{\rho} < \hat{\rho}_0$ and hence

$$\theta_{m+n}(\hat{\rho}) > \theta_n(\hat{\rho}), \quad 0 \leq \hat{\rho} < \hat{\rho}_0.$$

However, we have $\theta_{m+n}(0) = 2\pi\langle\frac{(a+b)v}{m+n}\rangle < \theta_n(0) = 2\pi\langle\frac{bv}{n}\rangle$, a contradiction. This completes the proof. □

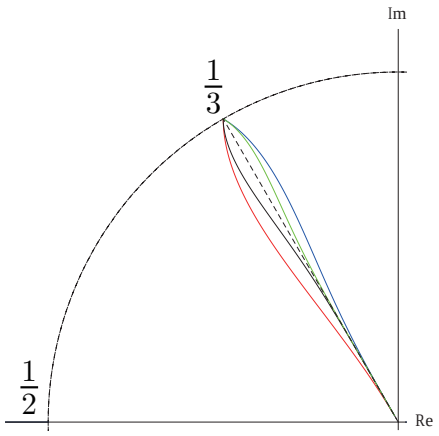

Figure 4.14: Two arcs $Q_{1,3,1}$, $Q_{4,3,1}$, the radial line segment $\delta(2\pi/3)$, and two arcs $Q_{5,3,-1}$ and $Q_{2,3,-1}$, from left to right, all connecting the origin with the point $\mathrm{e}^{2\pi\mathrm{i}/3}$ (marked $\frac{1}{3}$).

Consequently, the function $\theta_{m,n,v} : (0,1) \to I'_{m,n,v}$ is well-defined. Finally we will show (4.3.8). When $\sin n\theta = r^m$, we have

$$\begin{aligned}
&\hat{\rho}(r^{m+n}, (m+n)\theta) - \hat{\rho}(r^n, n\theta) \\
&= \frac{r^{m+n}(\sin(m+n)\theta - r^{-m}\sin n\theta - r^n \sin m\theta)}{(1 - r^{m+n}\cos(m+n)\theta)(1 - r^n \cos n\theta)} \\
&= \frac{r^{m+n}(\sin(m+n)\theta - 1 - r^n \sin m\theta)}{(1 - r^{m+n}\cos(m+n)\theta)(1 - r^n \cos n\theta)} < 0.
\end{aligned}$$

The Intermediate Value Theorem implies that $0 < \sin n\theta < r^m$ for $\theta = \theta_{m,n,v}(r)$, so

$$\lim_{r\to 0} \theta_{m,n,v}(r) = 2\pi\langle \frac{bv}{n} \rangle.$$

This completes the proof of Theorem 4.15. □

Theorem 4.20. *For each $v \neq 0$, $Q_v = \bigcup_{(m,n)\in R} Q_{m,n,v}$ is a dense subset of $\mathbb{D}$.*

Proof. We may suppose that $v > 0$. It is shown that the closure of Q_v contains any radial line segments $\delta(2\pi bv/n)$ for $n > 2v$, $0 < b < n$, such that n, b are relatively prime.

Let $m > a > 0$ be integers such that $a/m < b/n$ and $mb - na = 1$. The curve $Q_{m+jn,n,v}$, for each $j > 0$, connects the origin with the n-th root of unity $\mathrm{e}^{2\pi\mathrm{i}bv/n}$. Since the length of the interval $I'_{m+jn,n,v}$ tends to 0 as $j \to \infty$, the curves $Q_{m+jn,n,v}$ accumulate to $\delta(2\pi bv/n)$. This completes the proof. □

Figure 4.14 shows four arcs $Q_{1,3,1}$, $Q_{4,3,1}$, $Q_{5,3,-1}$ and $Q_{2,3,-1}$ from left to right, together with the radial line segment $\delta(2\pi/3)$, all connecting the origin with the point $\mathrm{e}^{2\pi\mathrm{i}/3}$ (marked $\frac{1}{3}$). This indicates that the arcs $Q_{1+3j,3,1}$ accumulate to $\delta(2\pi/3)$ as $j \to \infty$ monotonically from left, while the arcs $Q_{2+3j,3,-1}$ accumulate to $\delta(2\pi/3)$ as $j \to \infty$ monotonically from right.

4.3.5 Triangles which admit spiral multiple tilings with non-opposed parastichy pairs

In this section, we consider shapes of triangular spiral multiple tilings with non-opposed parastichy pairs.

Let

$$\begin{aligned}
\Delta''_+ &= \{(\theta_1, \theta_2) \in I^2 : \ \theta_1, \theta_2 > 0, \ \theta_1 + 2\theta_2 < \pi\} \subset \Delta'_+, \\
\Delta''_- &= \{(\theta_1, \theta_2) \in I^2 : \ \theta_1, \theta_2 < 0, \ \theta_1 + 2\theta_2 > -\pi\} \subset \Delta'_-,
\end{aligned}$$

and consider the mapping

$$\mathrm{Arg}_{m,n} : \mathbb{D} \setminus \mathbb{R} \to I^2, \quad \mathrm{Arg}_{m,n}(\zeta) = (\mathrm{Arg}(\zeta^m), \mathrm{Arg}(\zeta^n))$$

where $m, n > 0$ are relatively prime integers. Theorem 4.13 and Lemma 4.14 imply that $\mathrm{Arg}_{m,n}(Q_{m,n,v})$ denotes the set of shapes of the triangles that admit spiral multiple tilings (4.3.6) of multiplicity v with the non-opposed parastichy pair $\{m, n\}$.

Theorem 4.21. *For each $v > 0$, $L'_v := \bigcup_{(m,n)\in R} \mathrm{Arg}_{m,n}(Q_{m,n,v})$ is a nowhere dense subset of Δ''_+.*

Proof. Let $\zeta \in Q_{m,n,v}$. By Lemma 4.4, we have $\sin n\theta = r^m \sin(m+n)\theta - r^{m+n} \sin m\theta$, which implies that $|\mathrm{A}_m\mathrm{A}_{m+n}| = r^m|\mathrm{A}_0\mathrm{A}_{m+n}| - r^{m+n}|\mathrm{A}_0\mathrm{A}_m|$ by the Law of Sines. Thus we obtain $|\mathrm{A}_m\mathrm{A}_{m+n}| < |\mathrm{A}_0\mathrm{A}_{m+n}|$, i.e., $\sin n\theta < \sin(\pi - (m+n)\theta)$, and hence $2\pi\langle\frac{n\theta}{2\pi}\rangle < \pi - 2\pi\langle\frac{(m+n)\theta}{2\pi}\rangle$, so $\mathrm{Arg}_{m,n}(\zeta) \in \Delta''_+$.

Fix $v > 0$ and let $K \subset \Delta''_+$ be a compact set. We shall show that K intersects $\mathrm{Arg}_{m,n}(Q_{m,n,v}) \subset \ell'_{m,n,v}$ for only finitely many pairs (m, n). If $(\theta_1, \theta_2) \in K \cap \mathrm{Arg}_{m,n}(Q_{m,n,v})$, then we have $n\theta_1 - m\theta_2 = 2\pi v$ and there exists $0 < r < 1$ such that

$$\sin(\theta_1 + \theta_2) = r^n \sin\theta_1 + r^{-m} \sin\theta_2. \tag{4.3.10}$$

However, consider the function

$$f(\theta_1, \theta_2, m) = \inf_{0<r<1}(r^{(m\theta_2+2\pi v)/\theta_1} \sin\theta_1 + r^{-m} \sin\theta_2). \tag{4.3.11}$$

The minimum of the right hand side of (4.3.11) is attained at

$$r = \left(\frac{m\theta_1 \sin\theta_2}{(m\theta_2 + 2\pi v)\sin\theta_1}\right)^{\frac{\theta_1}{m(\theta_1+\theta_2)+2\pi v}}.$$

By taking the limit as $m \to \infty$, we have

$$\begin{aligned}\lim_{m\to\infty} f(\theta_1, \theta_2, m) &= (\sin\theta_1)^{\frac{\theta_1}{\theta_1+\theta_2}} (\sin\theta_2)^{\frac{\theta_2}{\theta_1+\theta_2}} \left(\left(\frac{\theta_2}{\theta_1}\right)^{\frac{\theta_1}{\theta_1+\theta_2}} + \left(\frac{\theta_1}{\theta_2}\right)^{\frac{\theta_2}{\theta_1+\theta_2}}\right) \\ &> \sin(\theta_1 + \theta_2),\end{aligned}$$

on $(\theta_1, \theta_2) \in \Delta''_+$. Since K is compact, we have $f(\theta_1, \theta_2, m) > \sin(\theta_1 + \theta_2)$, $(\theta_1, \theta_2) \in K$, for a sufficiently large $m > 0$. Thus (4.3.10) hold for only finitely many $m > 0$.

If m is fixed, K intersects the line segment $\ell'_{m,n,v}$ for only finitely many $n > 0$, because $\ell'_{m,n,v}$ tend to the θ_2-axis as $n \to \infty$. This completes the proof. □

Theorem 4.22. *The union $L' := \bigcup_{v>0} L'_v = \bigcup_{v>0,\ (m,n)\in R} \mathrm{Arg}_{m,n}(Q_{m,n,v})$ is a dense subset of Δ''_+.*

Proof. We shall show that L' contains any rational point $(\theta_1, \theta_2) \in \Delta''_+$ such that $\theta_1, \theta_2 \in 2\pi\mathbb{Q}$. First we observe that

$$\sin(\pi - \theta_1 - \theta_2) > \sin\theta_2$$

since $(\theta_1, \theta_2) \in \Delta''_+$. Let $m, n > 0$ be relatively prime integers such that $v = (n\theta_1 - m\theta_2)/2\pi$ is an integer. Let $0 < r < 1$ be sufficiently close to 1 such that

$$\sin(\pi - \theta_1 - \theta_2) > r^{-m} \sin\theta_2.$$

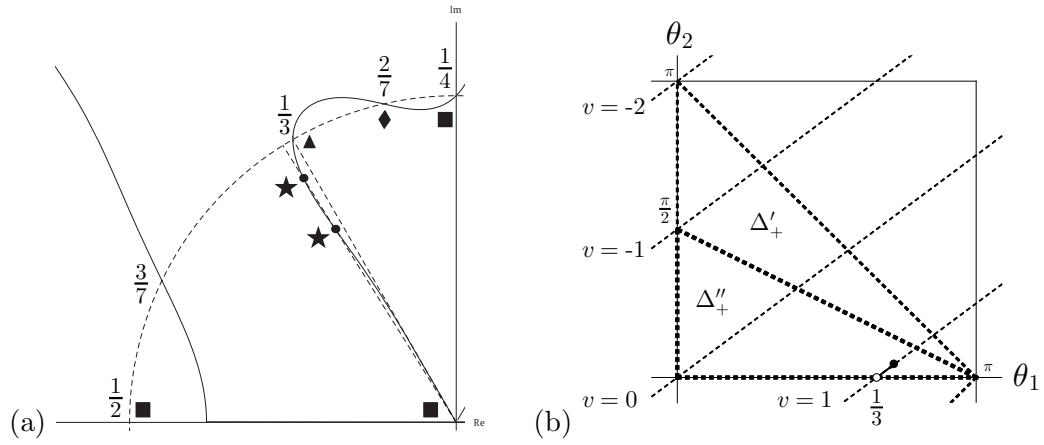

Figure 4.15: (a) The curve $\mathrm{Im}(\phi_{7,3}(\zeta)) = 0$ in Figure 4.12 (b) redrawn. The arc $Q_{4,3,1}$ connects the point $\mathrm{e}^{2\pi\mathrm{i}/3}$ with the origin. Two marks ★ denote the generators $\zeta = (0.8822\cdots)\mathrm{e}^{2\pi\mathrm{i}(0.339)}$ and $\zeta = (0.6984\cdots)\mathrm{e}^{2\pi\mathrm{i}(0.339)}$ for the tilings in figure 4.16. (b) The solid line $\arg_{4,3}(Q_{4,3,1})$ in the stripe $\iota_{4,3}(I) \cap \Delta''_+$ has an endpoint • in the interior of Δ''_+.

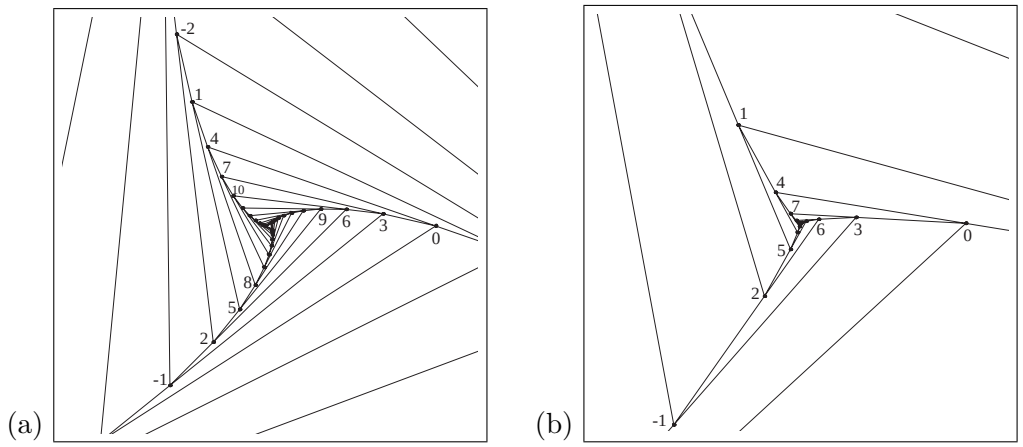

Figure 4.16: Spiral tilings with the non-opposed parastichy pair $\{4, 3\}$ consisting of triangles of the same shape. (a) $\zeta = (0.8822\cdots)\mathrm{e}^{2\pi\mathrm{i}(0.339)}$. (b) $\zeta = (0.6984\cdots)\mathrm{e}^{2\pi\mathrm{i}(0.339)}$.

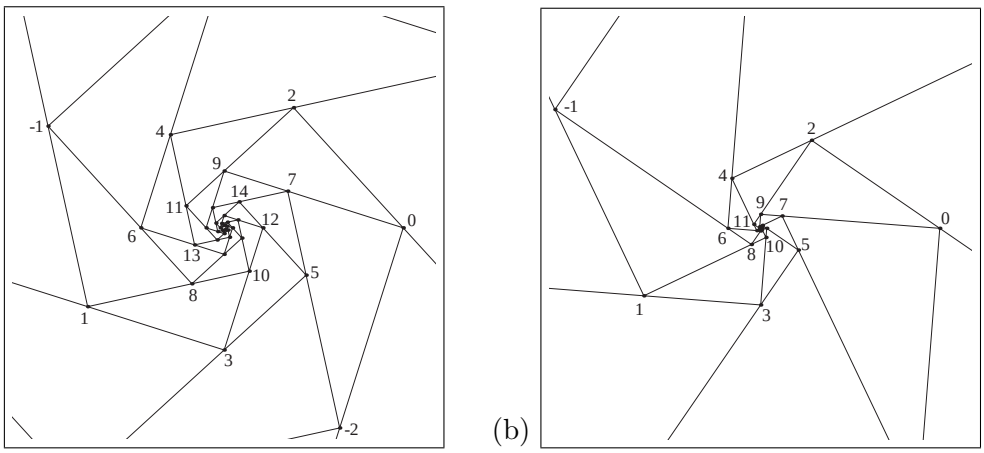

Figure 4.17: Spiral tilings by the right triangles with angles 30°, 60°, 90°, with a non-opposed parastichy pair $\{2, 7\}$. The divergence angle is $\theta = 7\pi/6$. These two tilings are topologically equivalent to each other. (a) $r = 0.8803\cdots$. (b) $r = 0.7535\cdots$.

Take $k > 0$ sufficiently large that

$$\sin(\pi - \theta_1 - \theta_2) > r^{n+mk} \sin\theta_1 + r^{-m} \sin\theta_2,$$

and that $\tilde{v} = ((n + mk)\theta_1 - m\theta_2)/2\pi$ is still an integer. Since $\sin(\pi - \theta_1 - \theta_2) < \sin\theta_1 + \sin\theta_2$, the Intermediate Value Theorem implies that we can re-choose $r < \tilde{r} < 1$ such that

$$\sin(\pi - \theta_1 - \theta_2) = \tilde{r}^{n+mk} \sin\theta_1 + \tilde{r}^{-m} \sin\theta_2.$$

Hence $(\theta_1, \theta_2) \in \mathrm{Arg}_{m,n+mk}(Q_{m,n+mk,\tilde{v}})$, which completes the proof. □

Figure 4.12 (b) and Figure 4.15 (a) show $Q_{4,3,1}$ as an arc connecting the origin and $\mathrm{e}^{2\pi\mathrm{i}/3}$. Its complex conjugate is $Q_{4,3,-1}$. Two marks ★ on $Q_{4,3,1}$ in Figure 4.15 (a) denote the generators of spiral tilings with the non-opposed parastichy pair $\{4, 3\}$ consisting of triangles of the same shape, figure 4.16. Figure 4.15(b) shows the line segment $\arg_{4,3}(Q_{4,3,1})$ in the stripe $\iota_{4,3}(I) \cap \Delta''_+$. This indicates that the mapping $Q_{4,3,1} \to \arg_{4,3}(Q_{4,3,1})$ is 2 to 1, with a turning point • in this figure.

4.3.6 Examples of triangles which admit spiral multiple tilings with opposed parastichy pairs

By Theorem 4.13, we obtain the following example of triangular spiral multiple tilings with non-opposed parastichy pairs.

(i) Spiral tilings by right triangles with angles 30°, 60° and 90°: The right triangle with angles 30° and 60° has a spiral tilings with a non-opposed parastichy pair $\{2, 7\}$, since $7 \cdot \frac{\pi}{3} - 2 \cdot \frac{\pi}{6} = 2\pi$. See Figure 4.17. The divergence angle $\theta = 7\pi/6$ is determined by the equations $\arg(\zeta^2) = \pi/3$ and $\arg(\zeta^7) = \pi/6$. The equation $\sqrt{3}r^9 - 2r^2 + 1 = 0$ has two positive roots $r = 0.8803\cdots$ and $0.7535\cdots$.

(ii) Spiral tilings by right triangles with angles 45°, 45° and 90°: The right triangle with angles 45° and 45° has a spiral tilings with a non-opposed parastichy pair $\{1, 9\}$, since $9 \cdot \frac{\pi}{4} - \cdot \frac{\pi}{4} = 2\pi$. See Figure 4.18. The divergence angle $\theta = \pi/4$ is determined by the equations $\arg(\zeta^1) = \pi/4$ and $\arg(\zeta^9) = \pi/4$. The equation $r^{10} - \sqrt{2}r + 1 = 0$ has two positive roots $r = 0.8553\cdots$ and $0.7437\cdots$.

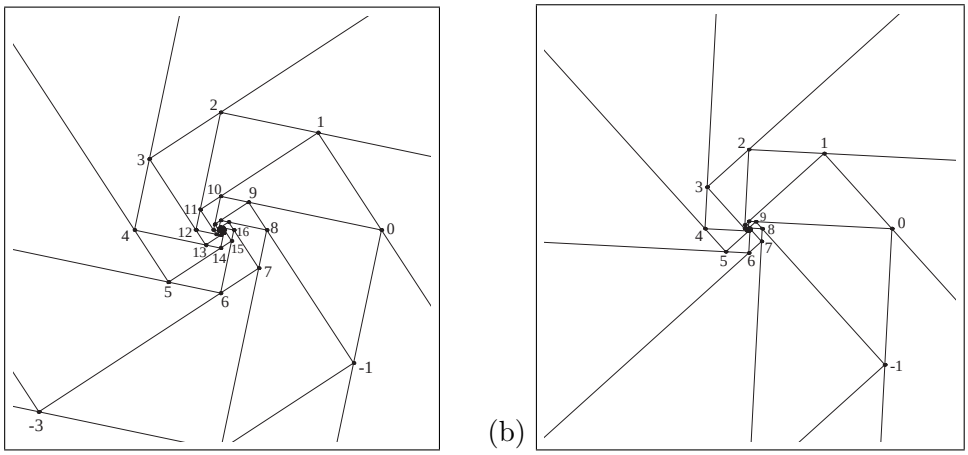

Figure 4.18: Spiral tilings by the right triangles with angles 45°, 45°, 90°, with a non-opposed parastichy pair $\{1, 9\}$. The divergence angle is $\theta = \pi/8$. These two tilings are topologically equivalent to each other. (a) $r = 0.8553\cdots$. (b) $r = 0.7437\cdots$.

4.4 Shape limit of triangular spiral multiple tilings with opposed parastichy pairs

Let $v > 0$, $\theta \in (-\pi v, \pi v]$. In this section we suppose that $\theta/2\pi v$ is a fixed irrational number. In the continued fraction expansion of $x = \theta/2\pi v$, we defined the sequences q_j and $q_{j,k}$, $j > 0$, $0 < k \le a_{j+1}$, in Section 2.3. For each $j > 0$ and $0 < k \le a_{j+1}$, denote by $a_{j,k}/m_{j,k} < b_{j,k}/n_{j,k}$ a pair of convergents of $x = \theta/2\pi v$ such that $\{m_{j,k}, n_{j,k}\} = \{q_j, q_{j,k}\}$. Suppose that j is sufficiently large that $(2\pi\langle\frac{m_{j,k}\theta}{2\pi}\rangle, 2\pi\langle\frac{n_{j,k}\theta}{2\pi}\rangle) \in \Delta_+$. Let $0 < r = r_{j,k} < 1$ be the root of the equation $f_{m,n,\theta}(r) = 0$, and $\zeta_{j,k} = r_{j,k}\mathrm{e}^{\mathrm{i}\theta}$. Then we obtain a triangular spiral (multiple) tiling with an opposed parastichy pair $\{m, n\} = \{m_{j,k}, n_{j,k}\}$.

Lemma 4.23. $\mathrm{Arg}(\zeta_{j,k}^{q_{j,k}}) \to 0$ *as* $j \to \infty$.

Proof. It is known that

$$\left|\frac{\theta}{2\pi v} - \frac{p_j}{q_j}\right| \le \frac{C}{q_j^2}$$

where the constant $C > 0$ is independent of j. Hence

$$|\mathrm{Arg}(\zeta_{j,k}^{q_{j,k}})| \le |\mathrm{Arg}(\zeta_{j,k}^{q_j})| = 2\pi|\langle\frac{q_j\theta}{2\pi}\rangle| = 2\pi|\frac{q_j\theta}{2\pi} - p_j v| \le \frac{2\pi C v}{q_j} \to 0$$

as $j \to \infty$. □

Lemma 4.24. *Let $v > 0$, $\theta \in (-\pi, \pi]$, and suppose that $\theta/2\pi v$ is an irrational number. Then the angles $\angle(1, \zeta_{j,k}^{m_{j,k}}, \zeta_{j,k}^{n_{j,k}})$ and $\angle(\zeta_{j,k}^{m_{j,k}}, \zeta_{j,k}^{n_{j,k}}, 1)$ tend to 0 as $j \to \infty$.*

Proof. Since (4.1.2) generated by $\zeta_{j,k}$ is a triangular spiral multiple tiling of multiplicity v with an opposed parastichy pair $\{m_{j,k}, n_{j,k}\}$, the four points $\zeta_{j,k}^{m_{j,k}}$, 0, $\zeta_{j,k}^{n_{j,k}}$, 1 lie on a same circle. Thus we have

$$\angle(1, \zeta_{j,k}^{m_{j,k}}, \zeta_{j,k}^{n_{j,k}}) = \angle(1, 0, \zeta_{j,k}^{n_{j,k}}) = \mathrm{Arg}(\zeta_{j,k}^{n_{j,k}}) \to 0,$$

$$\angle(\zeta_{j,k}^{m_{j,k}}, \zeta_{j,k}^{n_{j,k}}, 1) = \angle(\zeta_{j,k}^{m_{j,k}}, 0, 1) = \mathrm{Arg}(\zeta_{j,k}^{m_{j,k}}) \to 0$$

as $j \to \infty$. □

Suppose that $\theta/2\pi v$ is a quadratic irrational number.

Lemma 4.25. *Suppose that $\theta/2\pi v$ is a quadratic irrational number. Then we have*

$$0 < 1 - r_{j,k} \leq \frac{C}{m_{j,k}^3},$$

where $C > 0$ is a constant independent of j, k.

Proof. Since $\theta/2\pi v$ is a fixed quadratic irrational number, the coefficients a_j are bounded, and hence the ratios $n_{j,k}/m_{j,k}$ are also bounded. Moreover, there exist constants $C_1, C_2 > 0$, independent of $j > 0$, $0 < k \leq a_{j+1}$, such that

$$\frac{C_1}{q_{j,k}^2} < \left| \frac{\theta}{2\pi v} - \frac{p_{j,k}}{q_{j,k}} \right| < \frac{C_2}{q_{j,k}^2}.$$

This implies that

$$\frac{C_1 v}{m_{j,k}} < \left| \langle \frac{m_{j,k}\theta}{2\pi} \rangle \right| < \frac{C_2 v}{m_{j,k}}. \tag{4.4.1}$$

We adopt a notation $\varphi = O(m^{-s})$ when there exists a constant C independent of j, k such that $|\varphi| \leq C/m_{j,k}^s$. Then we have

$$\sin m_{j,k}\theta = 2\pi \langle \frac{m_{j,k}\theta}{2\pi} \rangle - \frac{(2\pi)^3}{6} \langle \frac{m_{j,k}\theta}{2\pi} \rangle^3 + O(m_{j,k}^{-5}) = O(m_{j,k}^{-1}),$$

$$\cos m_{j,k}\theta = 1 - \frac{(2\pi)^2}{2} \langle \frac{m_{j,k}\theta}{2\pi} \rangle^2 + \frac{(2\pi)^4}{24} \langle \frac{m_{j,k}\theta}{2\pi} \rangle^4 + O(m_{j,k}^{-6}) = 1 + O(m_{j,k}^{-2}).$$

By the equation $f_{m_{j,k},n_{j,k}}(r, \theta) = 0$, we have

$$(r_{j,k}^m - \cos m_{j,k}\theta) \sin n_{j,k}\theta - (r_{j,k}^n - \cos n_{j,k}\theta) \sin m_{j,k}\theta = 0,$$

and so we have

$$(r_{j,k}^m - 1 - O(m_{j,k}^{-2}))O(m_{j,k}^{-1}) - (r_{j,k}^n - 1 - O(m_{j,k}^{-2}))O(m_{j,k}^{-1}) = 0$$

Thus we obtain

$$1 - r = \frac{O(m_{j,k}^{-2})}{\sum_{s=0}^{m_{j,k}-1} r_{j,k}^s + \sum_{s=0}^{n_{j,k}-1} r_{j,k}^s}.$$

Since we have $1 - r_{j,k} \leq C/m_{j,k}^2$, that is, this implies that

$$\sum_{s=0}^{m_{j,k}-1} r^s \geq \sum_{s=0}^{m_{j,k}-1} (1 - \frac{C}{m_{j,k}^2})^s = \frac{m_{j,k}}{C}(1 - (1 - \frac{C}{m_{j,k}^2})_{j,k}^m) \geq C' m_{j,k}$$

with $C' > 0$. Hence we obtain $1 - r_{j,k} = O(m_{j,k}^{-3})$. Let $t_{j,k} = 1 - r_{j,k}$. Then we have

$$r_{j,k}^{m_{j,k}} = 1 + O(m_{j,k}^{-2}),\ r_{j,k}^{n_{j,k}} = 1 + O(m_{j,k}^{-2}).$$

That is, $\lim_{j\to\infty} r_{j,k}^{m_{j,k}} = \lim_{j\to\infty} r_{j,k}^{n_{j,k}} = 1$.

□

Let $R(\theta, v)$ be the set of ratios $(\zeta_{j,k}^{n_{j,k}} - 1)/(\zeta_{j,k}^{m_{j,k}} - 1)$ for $j > 0$ and $0 < k \leq a_j$. Let

$$\Omega(\theta, v) := \Omega(R(\theta, v))$$

be the limit set, i.e., the set of the accumulation points, of $R(\theta, v)$.

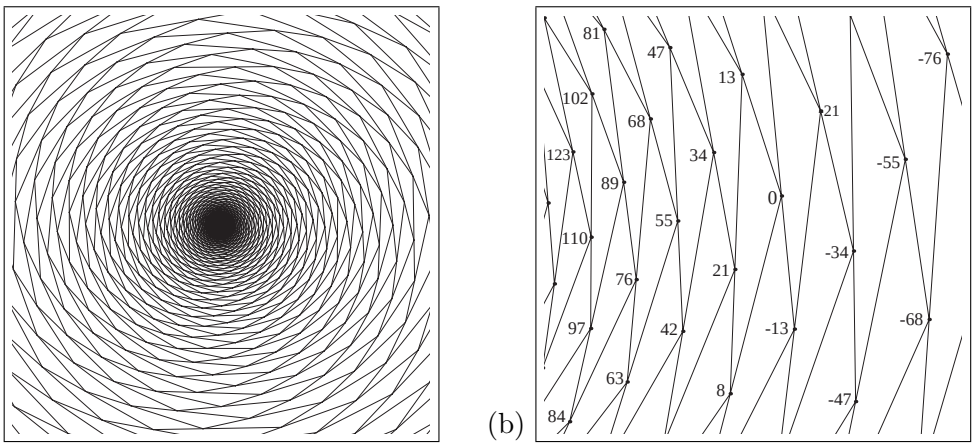

Figure 4.19: A triangular spiral tiling with the divergence angle $\theta = 2\pi\tau$. (a) $r = 0.9965\cdots$ and the opposed parastichy pair is $\{13, 8\}$. (b) Local view around the tile T_0.

Theorem 4.26. *Suppose that $\theta/2\pi v$ is a quadratic irrational number. Then we have*

$$\Omega(\theta, v) = \{(\omega_{s+1} - k)^{(-1)^s} : 1 \le s \le d, 0 < k \le b_{s+1}\}. \tag{4.4.2}$$

In particular, it is a finite set.

Proof. Since $\theta/2\pi v$ is a quadratic irrational number, we have (4.4.1). So we have

$$\begin{aligned}
\frac{\zeta_{j,k}^{n_{j,k}} - 1}{\zeta_{j,k}^{m_{j,k}} - 1} &= \frac{-1 + r^n \cos n\theta + \mathrm{i} r^n \sin n\theta}{-1 + r^m \cos m\theta + \mathrm{i} r^m \sin m\theta} \\
&= \frac{-1 + 1 + O(m^{-2}) + \mathrm{i}(2\pi\langle\frac{n\theta}{2\pi}\rangle + O(m^{-2}))}{-1 + 1 + O(m^{-2}) + \mathrm{i}(2\pi\langle\frac{m\theta}{2\pi}\rangle + O(m^{-2}))} \\
&= \frac{2\pi\mathrm{i}\langle\frac{n\theta}{2\pi}\rangle + O(m^{-2})}{2\pi\mathrm{i}\langle\frac{m\theta}{2\pi}\rangle + O(m^{-2})} \\
&= \frac{2\pi\mathrm{i}\langle\frac{n\theta}{2\pi}\rangle(1 + O(m^{-1}))}{2\pi\mathrm{i}\langle\frac{m\theta}{2\pi}\rangle(1 + O(m^{-1}))} \\
&= \frac{\langle\frac{n\theta}{2\pi}\rangle}{\langle\frac{m\theta}{2\pi}\rangle}(1 + O(m^{-1})),
\end{aligned}$$

where we denote by $m = m_{j,k}$, $n = n_{j,k}$. Thus it is written as

$$\frac{\zeta_{j,k}^{n_{j,k}} - 1}{\zeta_{j,k}^{m_{j,k}} - 1} = \left(\frac{\langle\frac{q_{j,k}\theta}{2\pi v}\rangle}{\langle\frac{q_j\theta}{2\pi v}\rangle}\right)^{(-1)^j} (1 + O(q^{-1})).$$

By using the continued fractions, we have

$$\begin{aligned}
\langle\frac{q_{j,k}\theta}{2\pi v}\rangle / \langle\frac{q_j\theta}{2\pi v}\rangle &= -[a_{j+1} - k, a_{j+2}, a_{j+3}, \dots] \\
&= -[b_{s+1} - k, b_{s+2}, b_{s+3}, \dots] \\
&= -(\omega_{s+1} - k)
\end{aligned}$$

for j sufficiently large, and $0 < k \le b_{s+1}$. Thus we obtain (4.4.2). □

Corollary 4.27. *If the coefficients $a_j = 1$ of the continued fraction expansion of $\theta/2\pi v$ for sufficiently large j, then $\Omega(\theta, v) = \{-\tau, -1/\tau\}$.*

Proof. Since the golden section has a purely periodic continued fraction expansion $\tau = [1, 1, \dots] = [1, \overline{1, 1}]$, we have

$$\langle \frac{q_{j,1}\theta}{2\pi v} \rangle / \langle \frac{q_j \theta}{2\pi v} \rangle = -[1 - 1, 1, 1, \dots] = -\frac{1}{\tau}$$

for sufficiently large j. □

Figure 4.19 shows a triangular spiral tiling generated by $z = r\mathrm{e}^{2\pi \mathrm{i}\tau}$, $r = 0.9965$, $\tau = (1+\sqrt{5})/2$, with an opposed parastichy pair $\{8, 13\}$, and the ratio $(z^8 - 1)/(z^{13} - 1) = -1.348 + 0.857\mathrm{i}$. If we fix the divergence angle $2\pi\tau$, and consider larger the Fibonacci numbers as an opposed parastichy pair, for example $\{55, 89\}$, then we have $r = 0.999989$, and so the ratio $(z^{55} - 1)/(z^{89} - 1) = -1.61208 + 0.13355\mathrm{i}$ gets closer to $-\tau = -1.618$. By Corollary 4.27, the limit of these ratios is $-\tau$.

Chapter 5

Concluding remarks

In Part I, Part II and Part III, we could give theoretical frameworks about the helical Voronoi tilings on the cylinder, the Voronoi spiral tilings and the triangular spiral tilings. As prospects of the thesis, we have the following two studies: A mathematical description of flat-foldable for triangular spiral multiple tilings as the rigid origami and a mathematical application of the theoretical framework of the spiral tilings for geometrical phyllotactic Voronoi tilings based on the Vogel model.

One of the prospects is to consider the following question about origami developments for the triangular spiral multiple tilings. *Can we fold a triangular spiral multiple tiling as the rigid origami ?* Computational simulations of triangular spiral multiple tilings show that the Fibonacci tornado is flat-foldable (See Figure 5.1). Moreover, for the rigid origami of the triangular spiral multiple tilings, we have the following questions. *How flexible are rigid origami sheets of triangular spiral multiple tilings ? Which rigid origami sheets for the triangular spiral multiple tilings are flat-foldable ?* In other words, we need a necessary and sufficient condition for flat-foldable of the triangular spiral multiple tilings by the rigid origami sheets.

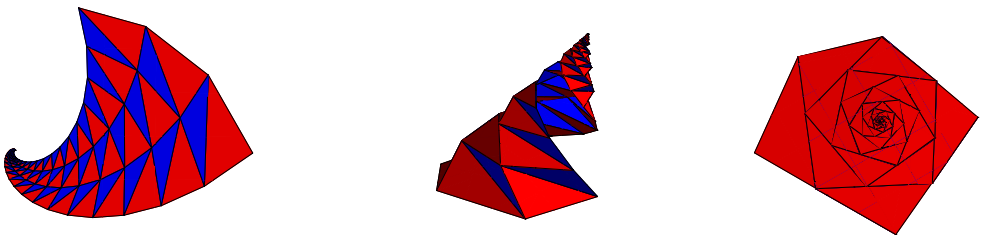

(a) (b) (c)

Figure 5.1: A computational simulation for the Fibonacci tornado in Figure 4.5. (a) A rigid origami sheet. (b) Side view from right, before squash. (c) Top-down view, after squashed.

Another of the prospects is to explain the combinatorial structures of geometrical phyllotactic Voronoi tilings based on the Vogel model. The theoretical frameworks of the helical Voronoi tilings on the cylinder and the Voronoi spiral tilings can be applied to this study.

Acknowledgements

I studied basic theories of mathematics and informatics in the Department of Applied Mathematics and Informatics of Ryukoku University between April 2005 and March 2009. In the Graduate School of Science and Technology of Ryukoku University, I have studied the topology and geometry of the spiral tilings throughout discussions with Professor Yoshikazu Yamagishi and Professor Akio Hizume since April 2009.

I would like to thank Professor Yoshimasa Nakamura of Kyoto University, Professor Masashi Iwasaki of Kyoto Prefectural University, Professor Masayo Fujimura of National Defense Academy of Japan, Professor Kinji Kimura of Kyoto University, Professor Tatsuyoshi Hamada of Fukuoka University, Professor Kokichi Sugihara of Meiji University, Professor Ichiro Hagiwara of Meiji University and Professor Akiyasu Tomoeda of Meiji University for giving me the opportunities to talk in the workshops and helpful comments. Moreover, I would like to thank Ph.D student Yoshitaro Tanaka of Meiji University for helpful comments about mathematical models of phyllotaxis by considering biological backgrounds.

Finally, I would like to thank Professor Hiroe Oka, Professor Junta Matsukidaira, Professor Shoji Yotsutani, Professor Yoshihisa Morita, Professor Waichiro Matsumoto and Professor Yoshikazu Yamagishi for refining the thesis.

Bibliography

[1] I. Adler, D. Barabe and R. V. Jean, A History of the Study of Phyllotaxis, Annals of Botany 80 (1997) 231-244.

[2] I. Adler, Solving the riddle of phyllotaxis: Why the Fibonacci numbers and the golden ratio occur on plants (2012) World Scientific.

[3] P. Atela, C. Gole and S. Hotton, A dynamical system for plant pattern formation: A rigorous analysis, J. Nonlinear Sci. 12 (2002) 641-676.

[4] S. Hotton, V. Johnson, J. Wilbarger, K. cmieniecki, P. Atela, C. Gole and J. Dumais, The Possible and the Actual in Phyllotaxis: Bridging the Gap between Empirical Observations and Iterative Models, J. Plant Growth Regulation 25(4) (2006) 313-323.

[5] P. Atela, The geometric and dynamic essence of phyllotaxis, Math. Model. Nat. Phenom. 6 (2011) 173-186.

[6] F. Aurenhammer, Voronoi diagrams: A survey of a fundamental geometric data structure, ACM Comput. Surv. 23 (1991) 345-405.

[7] K. Bainbridge, S. Guyomarc'h, E. Bayer, et al., Auxin influx carriers stabilize phyllotactic patterning, Genes Dev. 22 (2008) 810-823.

[8] K. van. Berkel, R. J. Boer, B. Scheres and K. ten Tusscher, Polar auxin transport: models and mechanism, Development 140 (2013) 2253-2268.

[9] A. I. Bobenko and Y. B. Suris, Discrete differential geometry: integrable structure, Graduate Studies in Mathematics 98, AMS (2009).

[10] H. S. M. Coxeter, The role of intermediate convergents in tait's explanation for phyllotaxis, Journal of algebra 20 (1972) 167-175.

[11] H. S. M. Coxeter, Introduction to geometry, second edition (1989) Wiley Classics Library Edition.

[12] J. E. Dale and F. L. Milthorpe, The growth and functioning of leaves, Cambridge University Press (1983).

[13] R. Dixon, Spiral phyllotaxis, Computers Math. Applic, 17 (1989) 535-538.

[14] S. Douady and Y. Couder, Phyllotaxis as a dynamical self organizing process Part I: The spiral modes resulting from time-periodic iterations, J. Theor. Biol. 178 (1996) 255-274.

[15] S. Douady and Y. Couder, Phyllotaxis as a dynamical self organizing process Part II: The spontaneous formation of a periodicity and the coexistence of spiral and whorled patterns, J. Theor. Biol. 178 (1996) 275-294.

[16] S. Douady and Y. Couder, Phyllotaxis as a dynamical self organizing process Part III: The simulation of the transient regimes of ontogeny, J. Theor. Biol. 178 (1996) 295-312.

[17] 布施 知子「ねじれ多重塔」MANIFOLD 5 (2002) 8-11.

[18] 布施 知子「続 · ねじれ多重塔」MANIFOLD 12 (2006) 2-27.

[19] E. Galois, Analyse algébrique. Démonstration d'un théorème sur les fractions continues périodiques, *Annales de Mathématiques Pures et Appliquées*, 19 (1828-1829) 294-301.

[20] E. I. Galyarskii and A. M. Zamorzaev, Similarity symmetric and antisymmetric groups, Soviet physics - crystallography, 8(5) (1964) 553-558.

[21] B. Grunbaum and G. C. Shephard, Tilings and patterns (San Francisco, CA: Freeman) (1987).

[22] G. H. Hardy and E. M. Wright, An introduction to the theory of numbers, sixth edition (2008) Oxford University Press.

[23] A. Hatcher and W. Thurston, Incompressible surfaces in 2-bridge knot complements, Inventiones math 79 (1985) 225-246.

[24] Akio Hizume, Sunflower tower, MANIFOLD 7 (2003) 4-7.

[25] Akio Hizume, Fibonacci Tornado, MANIFOLD 11 (2005) 6-8.

[26] Akio Hizume, Origami Fibonacci Tornado, MANIFOLD 11 (2005) 9-10.

[27] 日詰 明男「音楽の建築 フィボナッチ, ペンローズ, 黄金比をめぐる幾何学の冒険」トム出版 (2006).

[28] Akio Hizume, Fibonacci Tornado, Proceeding. 11th bridges conference (2008) 485-486.

[29] Akio Hizume, Real Tornado, MANIFOLD 17 (2008) 8-11.

[30] Akio Hizume and Yoshikazu Yamagishi, Real Tornado, MANIFOLD 19 (2009).

[31] Akio Hizume and Yoshikazu Yamagishi, Real Tornado, Bridges Proceeding (2009).

[32] A. Hizume and Y. Yamagishi, Stripes on Penrose tilings, J. Phys. A: Math. Theor. 44 (2011) 015202.

[33] 石田 祥子, 野島 武敏, 亀井 岳行, 萩原 一郎「等角写像とその円錐殻折紙構造物設計への応用」日本応用数理学会論文誌, 22(4) (2012) 301-318.

[34] 石田 祥子, 野島 武敏, 萩原 一郎「等角写像の折紙への応用」日本機械学会論文集 (C 編) 79 巻 801 号 (2013) 336-344.

[35] R. V. Jean, Phyllotaxis, A systemic study in plant morphogenesis, Cambridge University Press (1994).

[36] R. Rutishauser, R. V. Jean and Barab'e D eds, Symmetry in Plants, World Scientific, Singapore (1998) 171—212

[37] 来嶋 大二「数学かんどころ 8 ひまわりの螺旋」共立出版 (2012).

[38] V. Mirabet, F. Besnard, T. Vernoux and A. Boudaoud, Noise and Robustness in Phyllotaxis, PLos Comput Biol 8 (2012) e1002389.

[39] K. Miura, Proposition of Pseudo-Cylindrical Concave Polyhedral Shells, ISAS report/Institute of Space and Aeronautical Science, University of Tokyo, 34(9) (1969) 141-163.

[40] M. Pennybacker and A. C. Newell, Phyllotaxis, Pushed Pattern-Forming Fronts and Optimal Packing, Phys. Rev. Lett. 110 (2013) 248104.

[41] 野島 武敏「折りたたみ可能な円錐殻の創製」日本機械学会論文集 (C 編) 66 (2000) 349-355.

[42] 野島 武敏「生物に見る螺旋模様とその工学への応用」日本機械学会 (No.02-35) 第 15 回バイオエンジニアリング講演会 講演論文集 (2003) 59-60.

[43] 野島 武敏, 萩原一郎「折紙の数理とその応用」共立出版 (2012).

[44] D. Reinhardt, E. R. Pesce, T. Mandel, K. Balyensperger, M. Bennett, J. Traas, J. Friml and C. Kuhlemeier, Regulation of phyllotaxis by polar auxin transport, NATURE, 426 (2003) 255-260.

[45] N. Rivier, R. Occelli, J. Pantaloni and A. Lissowski, Structure of Benard convection cells, phyllotaxis and crystallography in cylindrical symmetry, J. Physique 45 (1984) 49-63.

[46] N. Rivier, A Botanical quasicrystal, J. Physique 47 (1986) 299-309.

[47] J. F. Sadoc, N. Rivier and J. Charvolin, Phyllotaxis: a non conventional crystalline solution to packing efficiency in situations with radial symmetry, Acta Cryst. A. 68 (2012) 470-483.

[48] J. F. Sadoc, J. Charvolin and N. Rivier, Phyllotaxis on surfaces of constant Gaussian curvature, J. Phys. A: Math. Gen. 46 (2013), 295202.

[49] F. Rothen and A. J. Koch, Phyllotaxis, or the properties of spiral lattice. I. shape invariance under compression, J. Phys. France (1989) 633-657.

[50] F. Rothen and A. J. Koch, Phyllotaxis, or the properties of spiral lattice. II. Packing of circles along logarithmic spirals, J. Phys. France (1989) 1603-1621.

[51] J. Rutzky and C. K. Palmer, Shadowfolds: Surprisingly Easy-to-Make Geometric Designs in Fabric (2011) Kodansha International.

[52] R. S. Smith, C. Kuhlemeier and P. Prusinliewicz, Inhibition fields for phyllotactic pattern formation: a simulation study, Can. J. Bot 84 (2006) 1635-1649.

[53] R. S. Smith, S. Guyomarc'h, T. Mandel, D. Reinhardt, C. Kuhlemeier and P. Prusinkiewicz, A plausible model of phyllotaxis, Proc. Nat. Acad. Sci. 103(5) (2006) 1301-1306.

[54] I. Stewart, Mathematics: Some assembly needed, Nature 448(7152) (2007) 419.

[55] I. Stewart, Mathematics of life unlocking the secrets of existence (2011) Joat Enterprises.

[56] 杉原 厚吉「なわばりの数理モデル ボロノイ図からの数理工学入門」共立出版 (2009).

[57] 須志田 隆道「葉序的および非葉序的な三角形の相似タイリングと折り紙」修士論文 龍谷大学大学院理工学研究科修士課程数理情報学専攻 (2010)

[58] 須志田 隆道「Fibonacci Tornado の折り紙展開図」MANIFOLD 19 (2009) 10-20.

[59] T. Sushida, A. Hizume and Y. Yamagishi, Triangular spiral tilings, J. Phys. A: Math. Theor. 45(23) (2012) 235203.

[60] 須志田 隆道「三角形螺旋タイリングと折り紙」平成 24 年度 数学 · 数理科学と諸科学 · 産業との連携ワークショップ「折紙工学の深化と適用拡大に貢献する数理科学」講演資料集 (2012) 77-107.

[61] 須志田 隆道, 日詰 明男, 山岸 義和「三角形螺旋タイリングと折り紙」数式処理 Bulletin of JSSAC 20(1) (2013) 31-40.

[62] T. Sushida, A. Hizume and Y. Yamagishi, Shape limit in triangular spiral tilings, to appear in Acta Physica Polonia A.

[63] T. Sushida, A. Hizume and Y. Yamagishi, Voronoi spiral tilings, submitted.

[64] T. Sushida, A. Hizume and Y. Yamagishi, Helical Voronoi tilings on the cylinder, submitted.

[65] A. V. Shubnikov, Symmetry of similarity, Comput. Math. Applic. 16(5-8) (1988) 365-371.

[66] T. Tachi, Origamizing Polyhedral Surfaces, Journal of the International Association for Shell and Spatial Structures (IASS), 50(3) (2009) 173—179.

[67] T. Tachi, Generalization of Rigid-Foldable Quadrilateral-Mesh Origami, IEEE Transactions on Visualization and Computer Graphics, 16(2) (2010) 298-311.

[68] 高木貞治「初等整数論講義」共立出版 (1931).

[69] Y. Tanaka, A reaction-diffusion model study of formation of inflorescence (in Japanese), Master Thesis, Meiji University (2011).

[70] J. H. M. Thornley, Phyllotaxis. I. A mechanistic model, Ann. Bot. 39 (1975) 491-507.

[71] H. Veen and A. Lindenmayer, Diffusion Mechanism for Phyllotaxis, Plant Physiol, 60 (1977) 127-139.

[72] H. Vogel, A better way to construct the sunflower head, Mathematical Biosciences 44 (1979) 179-189.

[73] R. F. Williams, The shoot apex and leaf growth (1975), Cambridge University Press.

[74] D. A. Young, On the diffusion theory of phyllotaxis, J. Theor. Biol, 71 (1978) 421-432.